Approximate Riemann solvers for viscous flows

Master's thesis

Part II

Sander Rhebergen

University of Twente
Department of Applied Mathematics
Numerical analysis and Computational Mechanics Group

January - August, 2005

ir. C.M. Klaij
prof.dr.ir. J.J.W. van der Vegt
prof.dr.ir. B.J. Geurts
dr.ir. O. Bokhove

Abstract

In this Report we present an approximate Riemann solver based on travelling waves. It is the discontinuous Galerkin finite element (DG-FEM) analogue of the travelling wave (TW) scheme introduced by Weekes [Wee98]. We present the scheme for the viscous Burgers equation and for the 1D Navier-Stokes equations.

Some steps in Weekes' TW scheme for the Burgers equation are replaced by numerical approximations simplifying and reducing the cost of the scheme while maintaining the accuracy. A comparison of the travelling wave schemes with standard methods for the viscous Burgers equation showed no significant difference in accuracy. The TW scheme is both cheaper and easier to implement than the method of Bassi and Rebay, and does not separate the viscous part from the inviscid part of the equations.

We attempted to extend the DG-TW scheme to the 1D Navier-Stokes equations, but we have not yet succeeded in doing so due to a large number of non-linear equations that have to be solved. To avoid this problem, a first step is made in simplifying these equations, but no tests have been done so far.

Acknowledgments

I would like to thank Jaap and Bernard for their weekly advice during this project. A special thank you goes out to Chris for our almost daily discussions. We wouldn't have come this far without his help.

Contents

List of Figures

Nomenclature

List of the main symbols used in this thesis:

a	speed of sound
c_p	specific heat at constant pressure
c_v	specific heat at constant volume
CFL	CFL number
DN	diffusion number
e	internal energy
E	total energy
F^e	inviscid flux vector
F^v	viscous flux vector
h	enthalpy
K_k	element k
M	Mach number
n	outward normal
p	pressure
Pr	Prandtl number
R	specific gas constant
$\mathcal{R}(f)$	global lifting operator
$\mathcal{R}^S(f)$	local lifting operator
Re	Reynolds number
s	wave speed, shock speed
S^i	internal face
S^b	boundary face
t^n	the nth time level, $n\Delta t$, with $n \in \mathbb{N}$, $n \geq 0$
T	temperature
Δt	temporal mesh width
u	flow speed
v	flow speed relative to a shock
x_k	the kth vertex, $x_1 + (k-1)\Delta x$, with $k \in \mathbb{N}$, $k \geq 1$
Δx	spatial mesh width

1   Introduction

Many applications in fluid dynamics require the solution of the compressible Navier-Stokes equations. For almost all applications, finding analytical solutions is impossible, but with the aid of computers, one can numerically approximate the exact solution. This field of numerically approximating fluid dynamics solutions is called Computational Fluid Dynamics (CFD).

One numerical technique for computing solutions of PDE's is the finite element method. In this thesis we consider the discontinuous Galerkin finite element method (DG-FEM). In this method the domain is partitioned by a finite number of non-intersecting elements. On each element the exact solution is approximated by polynomials which are discontinuous across element faces. In the present study we consider only linear polynomial basis-functions.
Some well known benefits of the DG-FEM method are: optimal flexibility for local mesh refinement, adjustment of the polynomial order in each element (*hp*-adaptation) and excellent performance on parallel computers. These benefits are the result of the very compact stencil of DG methods.
DG was developed for first order hyperbolic equations and it was possible to compute solutions for inviscid compressible flows. Viscous compressible flow equations described by the compressible Navier-Stokes equations are not hyperbolic and new techniques had to be developed to discretize the diffusion operator. Bassi and Rebay [BR97] and Oden et al. [BO99] provide such techniques, extending the DG formulation for hyperbolic equations developed by Cockburn and Shu [CS01] to incompletely parabolic equations. In [BRM+], improvements to the formulation in [BR97], which showed a weak instability, have been made. These improvements were analyzed by Brezzi et.al. in [ABCM02, BMM+00]. A different technique to deal with the diffusion operator has been proposed by Cockburn and Shu [CS98] with the local discontinuous Galerkin method.
Other recent work in DG-FEM on compressible flows was the extension of DG-FEM to space-time by van der Vegt and van der Ven [vdVvdV02a, vdVvdV02b] and Klaij, van der Vegt and van der Ven [KvdVvdV].

All presently available DG methods split the viscous contribution of the flux from the inviscid part and deal with them seperately in the numerical discretization.As mentioned above, in DG-FEM the domain is partitioned by a finite number of non-intersecting elements and on each element the exact solution of the equation to be solved is approximated by a polynomial. Due to the discontinuous nature of the polynomial representation in each element the flux at a face is not uniquely defined. To overcome this problem a numerical flux depending on the left and right traces is introduced. At each face, a viscous Riemann problem must be solved:

$$U_t + F^e(U)_x = F^v(U, U_x)_x,$$

$$U(x,0) = \begin{cases} U_L, & \text{if } x < 0, \\ U_R, & \text{if } x > 0, \end{cases}$$

with U a column vector of conserved variables, $F^e(U)$ the inviscid flux, $F^v(U, U_x)$ the viscous

flux and U_L and U_R the left and right traces at the face. In this Report we assume that $U_t + F^e(U)_x = 0$ is hyperbolic.

For certain equations (e.g. the Euler equations where $F^v(U, U_x)_x = 0$) it is possible to find an exact solution to this problem. However, in practical computations this problem needs to be solved many times, making the Riemann problem one of the most computationally demanding parts in the numerical method. Therefore, instead of solving this problem exactly, one approximates the numerical flux.

Much work has been done on approximating the numerical flux for inviscid problems. Some examples are the HLL and HLLC Riemann solvers which are discussed in [Rhe05]. Less is known about approximating the numerical flux for viscous problems. Instead, methods have been developed splitting the flux at element faces into an inviscid and a viscous contribution. In DG-FEM the method of Bassi and Rebay is a well known method for handling the viscous contributions of the flux, while inviscid Riemann solvers are used for the inviscid contributions. A drawback of this scheme is that a penalty term needs to be introduced for stability reasons, penalizing the discontinuity at the element faces without making a distinction if it originates from the physics or from the use of discontinuous polynomials. Furthermore, this is a costly method based on mathematical properties rather than on the physics of the problem.
These drawbacks motivate the development of an approximate viscous Riemann solver. Travelling waves will be introduced as approximate solutions to shocks. Travelling wave solutions to viscous conservation laws are similarity solutions of the form $U(x, t) = \varphi(\omega)$, with $\omega = x - st$, which are constant along lines with the slope $dx/dt = s$. Using these approximations it is possible to obtain a flux which does not separate the viscous part from the inviscid part of the flux.

This Report is the second part of my Master's thesis. Part I was a literature report. In this Report we present an approximate Riemann solver based on travelling waves. The outline of this Report is as follows: in Section 2 we consider the viscous Burgers equation. We show how to solve this equation using the DG-FEM method of Bassi and Rebay and we will introduce a new scheme for this equation based on travelling waves, the DG-TW scheme. The DG-TW scheme is a travelling wave scheme based on the schemes introduced by Harabetian [Har90] for finite difference methods and by Weekes [Wee98] for finite volume methods. In Section 3 the DG-TW scheme is extended to the 1D Navier-Stokes equations based on the analysis done in [Wee98]. In the Appendix an approximate viscous Riemann solver is presented based on the HLL and HLLC Riemann solvers.

2   The viscous Burgers equation

In this chapter, we start by showing how to solve the viscous Burgers equation numerically using the DG-FEM method of Bassi and Rebay (Section 2.1). Afterwards, in Section 2.2, we consider two travelling wave schemes: by Harabetian [Har90] for finite difference methods and by Weekes [Wee98] for finite volume methods. The travelling wave solution to a viscous conservation law is a similarity solution of the form $u(x,t) = \varphi(\omega)$, where $\omega = x - st$. The advantage of the travelling wave approach is that it does not separate the viscous part from the hyperbolic part of the equation. Finally, in Section 2.3 we introduce an alternative DG-FEM method based on travelling wave theory.

In this chapter we focus on the following situation:

$$u_t + f(u)_x = \mu u_{xx}, \quad f(u) = \tfrac{1}{2}u^2, \quad \text{with } x \in \mathbb{R},\, t \in \mathbb{R}^+, \tag{2.1}$$

where μ is the viscosity coefficient. Boundary conditions are given by:

$$\lim_{x \to -\infty} u(x,t) = 2, \quad \lim_{x \to +\infty} u(x,t) = 0, \quad \forall t \in \mathbb{R}^+, \tag{2.2}$$

and the initial condition is:

$$u(x,0) = \frac{2}{1 + \exp(x/\mu)}. \tag{2.3}$$

The exact solution of this problem is given by [Har90]:

$$u(x,t) = \frac{2}{1 + \exp((x-t)/\mu)}.$$

2.1   Classic DG-FEM approach

2.1.1   Introduction

We consider the viscous Burgers problem as given by Eqs. (2.1) and (2.2) with initial condition given by Eq. (2.3).

To discretize the Burgers equation, we define the tessellation $\mathcal{T}_h$ of N elements K_k in the open spatial domain $\Omega \in \mathbb{R}$ as:

$$\mathcal{T}_h = \{K_k : \cup_{k=1}^{N} K_k = \Omega_h \quad \text{and} \quad K_k \cap K_{k'} = \emptyset \quad \text{if} \quad k \neq k', 1 \leq k, k' \leq N\}.$$

The approximations u_h and v_h of the variable $u(x,t)$ and test function $v(x)$ belong to the space V_h:

$$V_h = \{v \in L^2(\Omega_h) : v|_{K_k} \in P^1(K_k), k = 1, ..., N\}, \tag{2.4}$$

in which $P^1(K_k)$ denotes the space of linear polynomials, and $L^2(\Omega_h)$ the space of Lebesque square integrable functions. DG was developed for first order hyperbolic equations so second order derivatives cannot be treated directly. Therefore we apply the method by Bassi and Rebay and start by introducing the necessary definitions and propositions [Kla04].
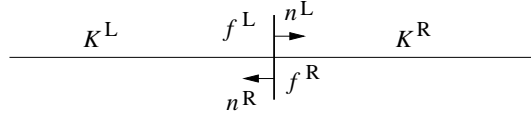
Figure 1: The face between the elements K^L and K^R with outward normal vectors n^L and n^R (in one dimension). The trace of a function f from K^L is denoted f^L, the trace from K^R is denoted f^R

The definitions and propositions given in this section are needed to deal with discontinuities on element faces in which a function f is double-valued. This is the result of the discontinuous functions approximation. For clarity and brevity $f(x,t)$ is written as f.

At the internal faces $S^i = \bar{K}^L \cap \bar{K}^R$ (see Fig. 1), the traces of a function f are defined as $f^L = \lim_{\varepsilon \downarrow 0} f(x - \varepsilon n^L)$ with n^L the outward normal vector. At boundary faces $S^b = \bar{K}^L \cap \partial\Omega$, the traces of a function f are just the value of f on the boundary.

Averages of a function f across an internal face are defined as $\{\!\{f\}\!\} = \frac{1}{2}(f^L + f^R)$. Across a boundary face the average of a function f is the value of f on the boundary.

The jump $[\![f]\!]$ of the function f across an internal face is defined by $[\![f]\!] = f^L n^L + f^R n^R$ and on a boundary face $[\![f]\!] = f^L n^L$. Since n^L is the outward normal vector to K^L and n^R the outward normal vector to K^R, by definition $n^L = -n^R$.

The jump and average are used to link the element boundary integrals with face integrals, as stated in the next proposition:

Proposition 2.1. *The following relation holds for arbitrary functions f and g:*

$$\sum_k \int_{\partial K_k} g^L f^L n^L \, d(\partial K_k) = \int_\Gamma \{\!\{g\}\!\} [\![f]\!] \, dS + \int_{\Gamma^i} [\![g]\!] \{\!\{f\}\!\} \, dS,$$

where $\Gamma = \{S^i\} \cup \{S^b\}$ is the set of all faces and $\Gamma^i = \{S^i\}$ the set of internal faces.

Besides jumps and averages across faces, we also define lifting operators which are used to extend face data to the element:

Definition 2.1. (Lifting operators). The global lifting operator working on a function f is defined in the weak sense as:

$$\int_\Omega g \mathcal{R}(f) \, d\Omega := \int_\Gamma \{\!\{g\}\!\} f \, d\Gamma, \quad \forall g \in V_h$$

and the local lifting operator as:

$$\int_\Omega g \mathcal{R}^S(f) \, d\Omega := \int_S \{\!\{g\}\!\} f \, dS, \quad \forall S \in \Gamma,$$

for all test functions $g \in V_h$. The difference between the local and global lifting operator is that the local lifting operator is 0 everywhere except on the cells adjacent to the face under consideration.

2.1.2   The weak formulation

We follow the report of [Kla04] to apply the method of Bassi and Rebay to Eq. (2.1). The method of Bassi and Rebay introduces an auxiliary variable σ and Eq. (2.1) is written as a system of first order equations:

$$u_t + (f(u) - \sigma)_x = 0 \quad \text{in } \Omega,$$
$$\sigma - \mu u_x = 0 \quad \text{in } \Omega.$$

The auxiliary variable σ will be eliminated from these equations later on. Because of the discontinuous function approximation, a function f is double-valued on the element faces. The definitions and propositions given in the previous section are used to deal with these discontinuities.

The equation for the auxiliary variable is: $\mu u_x = \sigma$. Multiplying by a test function v and partially integrating twice in space over an element K_k results in:

$$\int_{K_k} v\sigma \, dx = \int_{K_k} v\mu u_x \, dx,$$
$$= -\int_{K_k} v_x \mu u \, dx + \int_{\partial K_k} v\mu \hat{u} n \, ds,$$
$$= \int_{K_k} v\mu u_x \, dx + \int_{\partial K_k} v\mu(\hat{u} - u)n \, ds,$$

with n the component of the outward normal vector to ∂K_k. Summing over all elements of the tessellation $\mathcal{T}_h$ gives:

$$\int_{\Omega_h} v\sigma \, dx = \int_{\Omega_h} v\mu u_x \, dx + \sum_k \int_{\partial K_k} v\mu(\hat{u} - u)n \, ds.$$

The integral over the element boundaries can be transformed into an integral over the faces using Prop. 2.1:

$$\int_{\Omega_h} v\sigma \, dx = \int_{\Omega_h} v\mu u_x \, dx + \int_{\Gamma} \mu \{\!\{v\}\!\} [\![\hat{u} - u]\!] \, ds + \int_{\Gamma^i} \mu [\![v]\!] \{\!\{\hat{u} - u\}\!\} \, ds. \tag{2.5}$$

To find an expression for the auxiliary variable σ we introduce the numerical flux $\hat{u} = \{\!\{u\}\!\}$ and we find from Eq. (2.5) and the definition of the global lifting operators:

$$\sigma = \mu u_x - \mathcal{R}([\![u]\!]). \tag{2.6}$$

Now we consider the equation $u_t + (f - \sigma)_x = 0$. This equation is multiplied by a test function w and integrated by parts over an element K_k to get:

$$\int_{K_k} \left(wu_t - w_x(f - \sigma) \right) dx + \int_{\partial K} w(\hat{f} - \hat{\sigma})n \, ds = 0.$$

Summing over all elements of the tessellation $\mathcal{T}_h$ gives:

$$\int_{\Omega_h} \left(wu_t - w_x(f - \sigma) \right) dx + \sum_k \int_{\partial K} w(\hat{f} - \hat{\sigma})n \, ds = 0.$$

Using Prop. 2.1 to transform the integral over the element boundaries into an integral over the faces, we find:

$$\int_{\Omega_h} \left(wu_t - w_x(f - \sigma) \right) dx + \int_{\Gamma} \{\!\{w\}\!\} [\![\hat{f} - \hat{\sigma}]\!] \, ds + \int_{\Gamma^i} [\![w]\!] \{\!\{\hat{f} - \hat{\sigma}\}\!\} \, ds = 0.$$

Using expression Eq. (2.6) for the auxiliary variable gives:

$$\int_{\Omega_h} \left(wu_t - w_x(f - \mu u_x + \mathcal{R}([\![u]\!])) \right) dx + \int_{\Gamma} \{\!\{w\}\!\} [\![\hat{f} - \hat{\sigma}]\!] \, ds + \int_{\Gamma^i} [\![w]\!] \{\!\{\hat{f} - \hat{\sigma}\}\!\} \, ds = 0,$$

which is called the primal form as it is written in terms of the primary unknown u and the generic numerical fluxes $\hat{f}$ and $\hat{\sigma}$.

We obtain the following weak formulation: *Find a $u \in V_h$ such that $B(u, w) = 0, \forall w \in V_h$ with:*

$$B(u, w) = \int_{\Omega_h} \left(wu_t - w_x \big(f - \mu u_x + \mathcal{R}([\![u]\!]) \big) \right) dx$$
$$+ \int_{\Gamma} \{\!\{w\}\!\} [\![\hat{f} - \hat{\sigma}]\!] \, ds + \int_{\Gamma^i} [\![w]\!] \{\!\{\hat{f} - \hat{\sigma}\}\!\} \, ds.$$

2.1.3   The numerical fluxes

As seen in the previous section, we require three numerical fluxes $\hat{f}$, $\hat{u}$ and $\hat{\sigma}$. We already defined the numerical flux of u as the average of u of the face, $\hat{u} = \{\!\{u\}\!\}$, and we now define the numerical fluxes for σ and f.

As seen in the previous section, we derived the following expression for σ:

$$\sigma = \mu u_x - \mathcal{R}\big([\![u]\!]\big).$$

We choose the numerical flux $\hat{\sigma}$ as:

$$\hat{\sigma} = \{\!\{\mu u_x - \eta \mathcal{R}^S\big([\![u]\!]\big)\}\!\},$$

where the global lifting operator $\mathcal{R}$ was approximated by the local lifting operator $\mathcal{R}^S$ with weight η to ensure locality of the scheme. The weight η should be strictly larger than the number of faces per element.

The numerical flux $\hat{f}$ is based on the exact solution of the Riemann problem for the inviscid Burgers equation [Tor97]. The Riemann problem for the inviscid Burgers equation is:

$$\begin{cases} u_t + f(u)_x = 0 \quad \text{with } f(u) = \frac{1}{2}u^2, \\ u(x, 0) = \begin{cases} u_L & \text{if } x < 0, \\ u_R & \text{if } x > 0. \end{cases} \end{cases}$$

The complete solution of this problem depends on the following cases:

- If $u_L > u_R$:

$$u(x, t) = \begin{cases} u_L & \text{if } \frac{x}{t} < s, \\ u_R & \text{if } \frac{x}{t} > s, \end{cases} \tag{2.7}$$

where $s = \frac{1}{2}(u_L + u_R)$ and where u_L is the velocity immediately to the left and u_R the velocity immediately to the right of an element face.

- If $u_L \leq u_R$:

$$
u(x,t) = \begin{cases} u_L & \text{if } \frac{x}{t} \leq u_L, \\ 0 & \text{if } u_L < \frac{x}{t} < u_R, \\ u_R & \text{if } \frac{x}{t} \geq u_R. \end{cases}
\tag{2.8}
$$

We are interested in the flux on the face between neighboring elements. This is the case where $x = 0$. The flux is defined as $f(u) = \frac{1}{2}u^2$. Using these facts combined with Eq. (2.7) and Eq. (2.8), the following numerical flux can be derived:

$$
\mathrm{h}(u_L, u_R) = \begin{cases} \frac{1}{2}u_L^2 & \text{if } 0 \leq s_L, \\ 0 & \text{if } s_L < 0 < s_R, \\ \frac{1}{2}u_R^2 & \text{if } 0 \geq s_R, \end{cases}
$$

where s_L and s_R are defined as:

$$
s_L = \min\left(\tfrac{1}{2}(u_L + u_R), u_L\right), \qquad s_R = \max\left(\tfrac{1}{2}(u_L + u_R), u_R\right).
$$

Note that by taking periodic boundary conditions, we can omit all boundary integrals.

2.1.4 Discretization

The domain $\Omega = [0,1] \subset \mathbb{R}$ is partitioned by $N+1$ grid points, $\mathcal{E} := \{x_k\}_{k=1}^N$, defining N elements. It is convenient to introduce a reference element, $\hat{K} = [-1,1]$, and the mapping $F_K : \mathbb{R} \to \mathbb{R}$ between the reference element $\hat{K}$ and element K_k as follows:

$$
x = F_{K_k}(\xi) = \sum_{m=1}^2 x_{k,m}\chi_m(\xi) = \hat{x}_k + \frac{|K_k|\xi}{2},
$$

where $K_k = (x_k, x_{k+1})$. The shape functions are $\chi_1(\xi) = (1 - \xi)/2, \chi_2(\xi) = (1 + \xi)/2$; $\hat{x}_k = \frac{1}{2}(x_k + x_{k+1})$, and $|K_k| = (x_{k+1} - x_k)$. In the reference element $\hat{K}$, we define basis functions $\hat{\varphi}_0$ and $\hat{\varphi}_1$ as:

$$
\hat{\varphi}_0(\xi) = 1, \quad \text{and} \quad \hat{\varphi}_1(\xi) = \xi.
$$

Finally, the local basis functions in $\hat{K}$ are related to the basis functions in K_k as follows:

$$
\hat{\varphi}_n(\xi) = \hat{\varphi}_n(F_{K_k}^{-1}(x)) = \varphi_n^k(x) \quad \text{for} \quad n = 0, 1.
$$

The variable u and test functions v are approximated in each element K_k by their approximations u_h and v_h given respectively by:

$$
u_h(x,t)|_{K_k} = \bar{u}(K_k,t)\varphi_0^k(x) + \hat{u}(K_k,t)\varphi_1^k(x) \quad \text{and} \quad v_h(x) = \bar{v}(K_k)\varphi_0^k(x) + \hat{v}(K_k)\varphi_1^k(x),
$$

where, since $\varphi_0^k(x) = 1$, $\bar{u}(K_k, t)$ represents the mean of $u(x, t)$ on $|K_k|$:

$$\bar{u}(K_k, t) = \frac{1}{|K_k|} \int_{K_k} u(x, t) dx,$$

and $\hat{u}(K_k, t)$ the slope of $u(x, t)$ on $|K_k|$. When discretizing the equations, a two points Gauss scheme is used for the volume integrals. Furthermore we use the limits $\varphi_1^k(x_k^-) = 1$ and $\varphi_1^k(x_k^+) = -1$, where $x_k^- = \lim_{\varepsilon \downarrow 0}(x_k - \varepsilon)$ and $x_k^+ = \lim_{\varepsilon \downarrow 0}(x_k + \varepsilon)$.

Time integration is done by using a total variation diminishing (TVD) third-order Runge-Kutta discretization. The dynamical system $\frac{du}{dt} = R(u)$, is solved as follows:

$$u^{(1)} = u^n + \Delta t R(u^n)$$
$$u^{(2)} = \tfrac{1}{4}\big(3u^n + u^{(1)} + \Delta t R(u^{(1)})\big)$$
$$u^{n+1} = \tfrac{1}{3}\big(u^n + 2u^{(2)} + 2\Delta t R(u^{(2)})\big),$$

where $u^n = u(t)$ and $u^{n+1} = u(t + \Delta t)$. For stability, which requires a restriction on Δt, we make use of the CFL and diffusion number. The CFL number is:

$$\text{CFL} = \frac{\lambda \Delta t}{\Delta x},$$

and the diffusion number, DN:

$$\text{DN} = \frac{\mu \Delta t}{(\Delta x)^2},$$

where μ is the viscosity. We define Δx and λ as:

$$\Delta x = \min_k |K_k|, \quad \lambda = \max_k (s_{L_k}, s_{R_k}).$$

The value of Δt used when implementing is:

$$\Delta t = \min \left(\frac{CFL\Delta x}{\lambda}, \frac{DN(\Delta x)^2}{\mu} \right). \tag{2.9}$$

Note that in the inviscid case Eq. (2.9) reduces to $\Delta t = \frac{CFL\Delta x}{\lambda}$.

Numerical results for this method can be found in Section 2.3.

2.2   Travelling wave schemes

2.2.1   Introduction

In this section we will consider the schemes introduced by Harabetian [Har90] and Weekes [Wee98] for the numerical approximation of viscous perturbations of nonlinear hyperbolic conservation laws. We will solve the viscous Burgers problem as given by Eq. (2.1) and (2.2) with initial condition given by Eq. (2.3). For finite difference schemes, a standard approach for these types of equations is to approximate the viscous term with a centered difference approximation and a centered difference or an upwind difference approximation for the hyperbolic term.

In [Har90] a second order scheme is introduced using travelling wave solutions which does not split the viscous term from the hyperbolic term. A travelling wave solution to a viscous conservation law is a similarity solution of the form $u(x,t) = \varphi(\omega)$, where $\omega = x - st$. The key idea of this scheme is to interpolate a piece of a travelling wave (TW) between grid points and then let the exact solution operator to Eq. (2.1) act on it. Then, the flux $\mu u_x - f(u)$ at the cell boundaries is evaluated. This scheme only works in the case a travelling wave exists $(u_j^n > u_{j+1}^n)$. If not, a centered difference scheme is applied to the viscous and hyperbolic term.

The TW scheme introduced in [Wee98] is also second order accurate. The main difference between the scheme by Weekes and by Harabetian is that the latter only considers the situation of shocks, resorting to centered difference schemes in the case of rarefactions. The TW scheme by Weekes treats rarefactions as entropy-violating travelling waves maintaining the travelling wave approach. Another improvement of the scheme by Weekes is that a conservation requirement is imposed.

In Section 2.2.2 we derive Harabetian's TW scheme. Weekes' TW scheme is derived in Section 2.2.3. Both schemes are tested in Section 2.2.4, where we also compare results.

2.2.2 Harabetian's travelling wave scheme

Define the following (non dimensional) quantities:

$$
\begin{aligned}
\mathrm{Re} &= \frac{|f'| \cdot \Delta x}{\mu}, \quad \text{Cell Reynolds number,} \\
\lambda &= \frac{|f'| \cdot \Delta t}{\Delta x}, \quad \text{CFL Number,}
\end{aligned}
\tag{2.10}
$$

where $|f'| = \sup|f'(u)|$ and Δx and Δt are the spatial and temporal mesh widths of the discretization. As mentioned in the introduction, a travelling wave φ must be found such that $\varphi(\omega)$, where $\omega = x - st$, is a solution to Eq. (2.1) and $\varphi(x_j) = u_j, \varphi(x_{j+1}) = u_{j+1}$. Substituting the travelling wave into Eq. (2.1) we find the following equation:

$$
\mu \varphi'' = -s\varphi' + f(\varphi)', \quad \varphi(x_j) = u_j, \quad \varphi(x_{j+1}) = u_{j+1},
\tag{2.11}
$$

where the prime $'$ denotes differentiation with respect to ω. Since this is a second order ODE and the speed s is still undetermined, an extra boundary condition for φ' is prescribed, the choice being dictated by stability and accuracy considerations. In [Har90] it is proven that if $u_j > u_{j+1}$ and $\varphi'(x_j) = \varphi_j' < 0$, then there exists a unique s and $\varphi(x)$ that solve Eq. (2.11). The speed s is found by solving:

$$
\int_{u_j}^{u_{j+1}} \frac{\mu}{-s(z - u_j) + f(z) - f(u_j) + \mu\varphi_j'} \, dz = \Delta x,
\tag{2.12}
$$

so that $\varphi(x)$ can be determined from the following formula:

$$
\int_{u_j}^{\varphi(x)} \frac{\mu}{-s(z - u_j) + f(z) - f(u_j) + \mu\varphi_j'} \, dz = x - x_j.
\tag{2.13}
$$

CFL number λ:	0	0.25	0.5	0.6	0.65	0.75	0.8	1
Reynolds number $\mathrm{Re}_*(\lambda)$:	2	2.6	3.6	3.9	4.1	4.3	4.5	4.9

Table 2.1: The range of CFL and Reynolds numbers for which Harabetian's scheme is TVD.

Given u_j, u_{j+1} and φ'_j, the numerical flux for the travelling wave scheme as given in [Har90] is defined by:

$$H^{TW}_{j+1/2} = \mu\varphi'\left(x_{j+1/2} - \tfrac{1}{2}s\Delta t\right) - f\left(\varphi\left(x_{j+1/2} - \tfrac{1}{2}s\Delta t\right)\right),$$

and the travelling wave scheme is:

$$u_j^{n+1} = u_j^n - \frac{\Delta t}{\Delta x}(H^{TW}_{j+1/2} - H^{TW}_{j-1/2}).$$

Define:

$$\mathrm{Re}_*(\lambda) = \sup_{0 \le z \le 1} \frac{2}{(1 - \lambda z)(1 - z)} \log\left(\frac{1}{z}\right).$$

To avoid oscillatory solutions around discontinuities, one would like the scheme to be total variation diminishing (TVD). The travelling wave scheme is proven to be TVD in [Har90] if the following is satisfied:

$$\mathrm{Re} \le \mathrm{Re}_*(\lambda), \tag{2.14a}$$

$$\lambda\left(\frac{2}{\mathrm{Re}} + 1\right) \le 1. \tag{2.14b}$$

The upper limits of the Reynolds number as a function of λ are given in Table 2.1. From Eq. (2.14a) and (2.14b) it follows that $2\lambda(1 - \lambda) \le \mathrm{Re} \le \mathrm{Re}_*(\lambda)$. Since, according to Eq. (2.14b) $\lambda \le 1$, this means that the TW scheme by Harabetian is restricted to cases with $\mathrm{Re} \le 4.9$ when one is interested in obtaining non-oscillatory solutions.

Optimal stability in the TW scheme by Harabetian is obtained by taking $\varphi'_j = u_{j+1} - u_j$ in Eq. (2.12). Evaluating the integral in Eq. (2.12):

$$\frac{2\mu}{\sqrt{2\mu(u_{j+1} - u_j) - (s - u_j)^2}}\left(\arctan\left(\frac{u_{j+1} - s}{\sqrt{2\mu(u_{j+1} - u_j) - (s - u_j)^2}}\right)\right.$$
$$\left. - \arctan\left(\frac{u_j - s}{\sqrt{2\mu(u_{j+1} - u_j) - (s - u_j)^2}}\right)\right) = \Delta x, \quad (2.15)$$

where:

$$2\mu(u_{j+1} - u_j) - (s - u_j)^2 < 0.$$

To avoid having to work with complex numbers, we use the fact that $\arctan(ix) = i\operatorname{arctanh}(x)$ and write Eq. (2.15)as:

$$\frac{2\mu\left(\operatorname{arctanh}\big((s-u_{j+1})/\mathcal{A}\big) - \operatorname{arctanh}\big((s-u_j)/\mathcal{A}\big)\right)}{\mathcal{A}} - \Delta x = 0, \tag{2.16}$$

where:

$$\mathcal{A} = \sqrt{|2\mu(u_{j+1} - u_j) - (s-u_j)^2|}.$$

To find s a bisection method [vDDS$^+$01] is used with left initial condition $s_l = -10$ and right initial condition the asymptote of Eq. (2.16): $s_r = \frac{1}{2}(u_{j+1}^2 - u_j^2)/(u_{j+1} - u_j) + \mu$ (see also Eq. (2.12)). Analogously to deriving Eq. (2.16), we obtain from Eq. (2.13):

$$\frac{2\mu\left(\operatorname{arctanh}\big((s-\varphi(x))/\mathcal{A}\big) - \operatorname{arctanh}\big((s-u_j)/\mathcal{A}\big)\right)}{\mathcal{A}} - x + x_j = 0,$$

from which it follows that:

$$\varphi(x) = s - \mathcal{A}\tanh\left(\frac{2\mu\operatorname{arctanh}\big((s-u_j)/\mathcal{A}\big) + (x-x_j)\mathcal{A}}{2\mu}\right). \tag{2.17}$$

Differentiating the expression for $\varphi(x)$ in Eq. (2.17) we obtain:

$$\varphi'(x) = \frac{\mathcal{A}^2}{2\mu}\left(\tanh^2\left(\frac{2\mu\operatorname{arctanh}\big((s-u_j)/\mathcal{A}\big) + (x-x_j)\mathcal{A}}{2\mu}\right) - 1\right).$$

Besides using a bisection method to determine s as mentioned above, we also consider an s determined by using a 2-point Gauss method to evaluate the integral in Eq. (2.12) leading to a quadratic equation for s. First we define a mapping $F : \mathbb{R} \to \mathbb{R}$ between $[-1, 1]$ and $[u_j, u_{j+1}]$ as:

$$z = F(\xi) = \tfrac{1}{2}(u_j + u_{j+1}) + \frac{u_{j+1} - u_j}{2}\xi.$$

Using this mapping, Eq. (2.12) can be written as:

$$\tfrac{1}{2}(u_{j+1} - u_j)\int_{-1}^{1}\frac{\mu}{-s(F(\xi) - u_j) + f(F(\xi)) - f(u_j) + \mu\varphi_j'}\,d\xi = \Delta x. \tag{2.18}$$

Define $G(\xi)$ as:

$$G(\xi) = \frac{\mu}{-s(F(\xi) - u_j) + f(F(\xi)) - f(u_j) + \mu\varphi_j'}.$$

By applying the 2-point Gauss integration technique on Eq. (2.18) we obtain the following quadratic equation for s:

$$\tfrac{1}{2}(u_{j+1} - u_j)(G(-\sqrt{1/3}) + G(\sqrt{1/3})) = \Delta x.$$

Solving for s, the speed is given by the following expression:

$$s_\pm = \frac{-AD + h(CD + BE) - AB \pm F}{2hBD},$$

where:

$$A = \tfrac{1}{2}\mu(u_{j+1} - u_j),\ \ B = \varphi(-\sqrt{1/3}) - u_j,\ \ C = f(\varphi(-\sqrt{1/3})) - f(u_j) + \mu\varphi_j'$$

$$D = \varphi(\sqrt{1/3}) - u_j,\ \ E = f(\varphi(\sqrt{1/3})) - f(u_j) + \mu\varphi_j',$$

$$F = \big((AD)^2 - 2AD^2C\Delta x + 2ADBE\Delta x + 2A^2DB + (\Delta xCD)^2 - 2\Delta x^2CDBE$$

$$+2\Delta xCDAB + (\Delta xBE)^2 - 2\Delta xB^2EA + (AB)^2\big)^{\frac{1}{2}}$$

We take s such that the entropy condition for a shock is satisfied. For the Burgers equation: $u_j > s > u_{j+1}$ (see also [Rhe05] for details on the entropy condition for shock waves).

As stated before, the travelling wave scheme can only be used if $u_j^n > u_{j+1}^n$. If this is not the case a centered difference scheme to the viscous and hyperbolic terms is used. We use Richtmeyer's two-step procedure:

$$u_{j+1/2}^{n+1/2} = \frac{1}{2}\big(u_j^n + u_{j+1}^n\big) - \frac{\Delta t}{2\Delta x}\big(f(u_{j+1}^n) - f(u_j^n)\big) + \frac{\mu\Delta t}{2\Delta x^2}\big(u_{j+1}^n - 2u_{j+1/2}^n + u_j^n\big),$$

$$u_j^{n+1} = u_j^n - \frac{\Delta t}{\Delta x}\big(f\big(u_{j+1/2}^{n+1/2}\big) - f\big(u_{j-1/2}^{n+1/2}\big)\big).$$

As mentioned above, we take s such that the entropy condition for a shock is satisfied, but it is possible that both s_- and s_+ do not satisfy the entropy condition. This occurs when the difference between u_j and u_{j+1} is very small. To prevent this from happening we only use the travelling wave scheme if $u_j^n - u_{j+1}^n > 10^{-8}$. Furthermore, we do not use the travelling wave scheme if the previous point was calculated with Richtmeyer's procedure, for then no travelling wave flux term has been calculated at that point which is needed to join the two schemes together.

2.2.3   Weekes' travelling wave scheme

In [Wee98] a function $\Phi(x,t)$ is constructed to approximate the exact solution $u(x,t)$ of Eq. (2.1). This profile, $\Phi(x,t)$, consists of travelling waves $\varphi_{j+\frac{1}{2}}(\omega)$ that interpolate the data at $x = x_j$ and $x = x_{j+1}$ at time t_n. Defining $\omega = x - x_{j+1/2} - s_{j+1/2}(t - t_n)$, where $x_{j+1/2} = \frac{1}{2}(x_j + x_{j+1})$, the interpolation requirement for $\varphi_{j+\frac{1}{2}}$ is:

$$\varphi_{j+\frac{1}{2}}\big(-\tfrac{1}{2}\Delta x\big) = u_j^n, \qquad \varphi_{j+\frac{1}{2}}\big(\tfrac{1}{2}\Delta x\big) = u_{j+1}^n. \tag{2.19}$$

If $u_j^n < u_{j+1}^n$ there are no travelling wave solutions $u = \varphi$ to Eq. (2.1) and Eq. (2.19). Instead, $\varphi_{j+\frac{1}{2}}$ is taken to be a travelling wave solution to the modified PDE:

$$u_t + f(u)_x = \tilde{\mu}u_{xx}, \quad f(u) = \tfrac{1}{2}u^2,$$

where $\tilde{\mu} = \mu\,\mathrm{sgn}(u_j^n - u_{j+1}^n)$. The $\varphi_{j+\frac{1}{2}}$ are therefore solutions to the ODE:

$$-s\varphi' + f(\varphi)' = \tilde{\mu}\varphi''. \tag{2.20}$$

Since this is a second order ODE and the speed s is unknown, three constraints are needed to obtain a particular solution, $\varphi_{j+\frac{1}{2}}$. Two constraints are given by the interpolation requirement. As a third constraint, $\varphi_{j+\frac{1}{2}}$ has to satisfy the conservation requirement:

$$\int_{-\frac{1}{2}\Delta x}^{\frac{1}{2}\Delta x} \varphi_{j+\frac{1}{2}}\, d\omega = \frac{\Delta x}{2}(u_j^n + u_{j+1}^n). \tag{2.21}$$

Note the difference with the TW scheme of Harabetian. Harabetian did not have a conservation requirement, but instead prescribed φ', his choice being dictated by stability and accuracy considerations.

The motivation behind the conservation requirement is that as $\mu \to \infty$, the travelling wave profiles steepen and become step functions. The conservation requirement forces the discontinuities to occur at cell interfaces, $x_{j+1/2}$, at time t_n and so, in the limit, the constructed profile $\Phi(x, t_n)$ agrees with the piecewise constant profile of Godunov's method for the inviscid problem.

In [Wee98] it is proven that if $f(u)$ is convex, there exists an s and a $\varphi(\omega)$ that solve the problem given by Eq. (2.19), (2.20) and (2.21). From Eq. (2.20):

$$d\omega = \frac{\tilde{\mu}}{-s\varphi + f(\varphi) + c}d\varphi, \tag{2.22}$$

where c is a constant of integration. It follows that:

$$\omega + \tfrac{1}{2}\Delta x = \int_{u_j}^{\varphi(\omega)} \frac{\tilde{\mu}}{-s\varphi + f(\varphi) + c}\, d\varphi, \tag{2.23}$$

and, using Eq. (2.19), the interpolation requirement becomes:

$$\Delta x = \int_{u_j}^{u_{j+1}} \frac{\tilde{\mu}}{-s\varphi + f(\varphi) + c}\, d\varphi. \tag{2.24}$$

Multiplying Eq. (2.22) with φ we obtain:

$$\varphi d\omega = \frac{\tilde{\mu}\varphi}{-s\varphi + f(\varphi) + c}d\varphi.$$

Using Eq. (2.21), the conservation requirement becomes:

$$\tfrac{1}{2}\Delta x(u_j + u_{j+1}) = \int_{u_j}^{u_{j+1}} \frac{\tilde{\mu}\varphi}{-s\varphi + f(\varphi) + c}\, d\varphi. \tag{2.25}$$

The system consisting of Eq. (2.24) and (2.25) is solved simultaneously for the unknowns s and c and, along with Eq. (2.23), gives the solution for $\varphi(\omega)$.

In [Wee98] it is suggested to use Newton's method to solve this system, and for the cases where the Jacobian of the iteration matrix is large, to use asymptotic approximations for $\varphi_{j+\frac{1}{2}}$.

As initial condition for the Newton method we use a 2-points Gauss method to evaluate the integrals in Eq. (2.24) and Eq. (2.25). In Section 2.2.4 we show that using the s and c calculated only with the Gauss method results in approximately the same solution as when applying the Newton method. This is explained as follows:
An integral of the form:

$$I = \int_{u_j}^{u_{j+1}} f(u)\, du$$

can be approximated with $\widehat{I}$ using the 2-points Gauss method resulting in:

$$I = \widehat{I} + \mathcal{O}(|u_{j+1} - u_j|^3).$$

Since $|u_{j+1} - u_j|$ in our cases is small, $\mathcal{O}(|u_{j+1} - u_j|^3)$ is small and $\widehat{I}$ is a good approximation to I resulting in good approximations for s and c.
Using a Gauss integration technique (as was done in Section 2.2.2) we can solve Eq. (2.24) and Eq. (2.25) simultaneously to find the following initial expressions for s and c:

$$s = \frac{u_j + u_{j+1}}{2}, \quad c = \frac{\Delta x(u_j^2 + u_{j+1}^2) + 12\tilde{\mu}(u_{j+1} - u_j) + 4\Delta x u_j u_{j+1}}{12\Delta x}.$$

An expression for $\varphi(\omega)$ can be obtained by first evaluating the integral in Eq. (2.23) leading to:

$$\frac{2\mu}{\sqrt{s^2 - 2c}}\left(\operatorname{arctanh}\left(\frac{s - u_j}{\sqrt{s^2 - 2c}}\right) - \operatorname{arctanh}\left(\frac{\varphi - s}{\sqrt{s^2 - 2c}}\right)\right) = \omega + \tfrac{1}{2}\Delta x.$$

This equation can be solved for $\varphi(\omega)$ leading to:

$$\varphi(\omega) = s + A \tanh\left(\frac{4\tilde{\mu}\operatorname{arctanh}\big((u_j - s)/A\big) - (2\omega + \Delta x)A}{4\tilde{\mu}}\right),$$

where:

$$A = \sqrt{s^2 - 2c}. \tag{2.26}$$

It follows that:

$$\varphi'(\omega) = \frac{A^2\left(\tanh^2\left(\frac{4\tilde{\mu}\operatorname{arctanh}((u_j - s)/A) - (2\omega + \Delta x)A}{4\tilde{\mu}}\right) - 1\right)}{2\tilde{\mu}}.$$

The numerical scheme for the viscous problem Eq. (2.1) is derived by integrating the equation over the jth cell from time t_n to time t_{n+1},

$$\int_{x_{j-\frac{1}{2}}}^{x_{j+\frac{1}{2}}} u(x, t_{n+1})\, dx = \int_{x_{j-\frac{1}{2}}}^{x_{j+\frac{1}{2}}} u(x, t_n)\, dx - \int_{t_n}^{t_{n+1}} (f(u) - \mu u_x)(x_{j+\frac{1}{2}}, t)\, dt$$

$$+ \int_{t_n}^{t_{n+1}} (f(u) - \mu u_x)(x_{j-\frac{1}{2}}, t)\, dt.$$

In [Wee98] three versions of a travelling wave scheme are given. We only consider the first scheme since the other two schemes are simple extensions of the first scheme. Approximating u_j with the cell average of u:

$$\bar{u} = \frac{1}{\Delta x} \int_{x_{j-\frac{1}{2}}}^{x_{j+\frac{1}{2}}} u(x, t_n)\, dx,$$

the travelling wave scheme is given by:

$$u_j^{n+1} = u_j^n - \frac{\Delta t}{\Delta x}(H^{TW}(u_j, u_{j+1}) - H^{TW}(u_{j-1}, u_j)),$$

where:

$$
\begin{aligned}
H^{TW}(u_j, u_{j+1}) &= \frac{1}{\Delta t} \int_{t_n}^{t_{n+1}} (f(\Phi) - \mu\Phi_x)(x_{j+\frac{1}{2}}, t)\, dt \\
&= \frac{-1}{s\Delta t} \int_0^{-s\Delta t} \left(f(\varphi_{j+\frac{1}{2}}) - \mu\varphi'_{j+\frac{1}{2}} \right)(\omega)\, d\omega,
\end{aligned}
\tag{2.27}
$$

which, for fixed μ is second-order accurate on smooth solutions. The stability condition is satisfied if Δt is of order Δx^2.

As mentioned in the introduction, when $u_j < u_{j+1}$, viscous rarefaction fans are replaced by entropy-violating travelling waves. Numerically, this poses a danger only when the rarefaction is sonic, that is, if the characteristic speeds, $f'(u_j)$ and $f'(u_{j+1})$, are of opposite signs. When this occurs, a sonic entropy fix may have to be employed. The sonic point $\omega = \hat{\omega}$ is found by solving $f'(\varphi(\hat{\omega})) = 0$:

$$\hat{\omega} = \frac{4\mu\operatorname{arctanh}(s/A) - 4\mu\operatorname{arctanh}\big((s - u_j)/A\big) - \Delta x A}{2A},$$

with A given by Eq. (2.26). If $\hat{\omega}$ is beyond the region between 0 and $-s\Delta t$, no entropy fix is needed and H^{TW} remains as in Eq. (2.27), where the total quantity of $f(\varphi) - \mu\varphi'$ that passes through the interface $x_{j+\frac{1}{2}}$ from time t_n to t_{n+1} as the travelling wave moves with its speed s, is calculated. Otherwise, if $\hat{\omega}$ is between 0 and $-s\Delta t$, H^{TW} is computed as:

$$H^{TW} = \frac{-1}{s\Delta t} \int_0^{\hat{\omega}} (f(\varphi) - \mu\varphi')(\omega)\, d\omega + (-s\Delta t - \hat{\omega})\frac{-1}{s\Delta t}(f(\varphi) - \mu\varphi')(\hat{\omega}).$$

The travelling wave starts moving through the interface with speed s. When the sonic point is encountered, the profile is kept stationary and the flux is calculated as if the wave speed were zero. In the implementation the integral term is computed using the 2-points Gauss integration method. In [Wee98] it is shown that with this entropy fix, the resulting flux is the Godunov flux $f(\varphi(0))$, plus an additional nonpositive term. Furthermore, with this entropy fix, the TW scheme for $\mu \to 0$ is first-order accurate and generates TVD, entropy satisfying solutions.
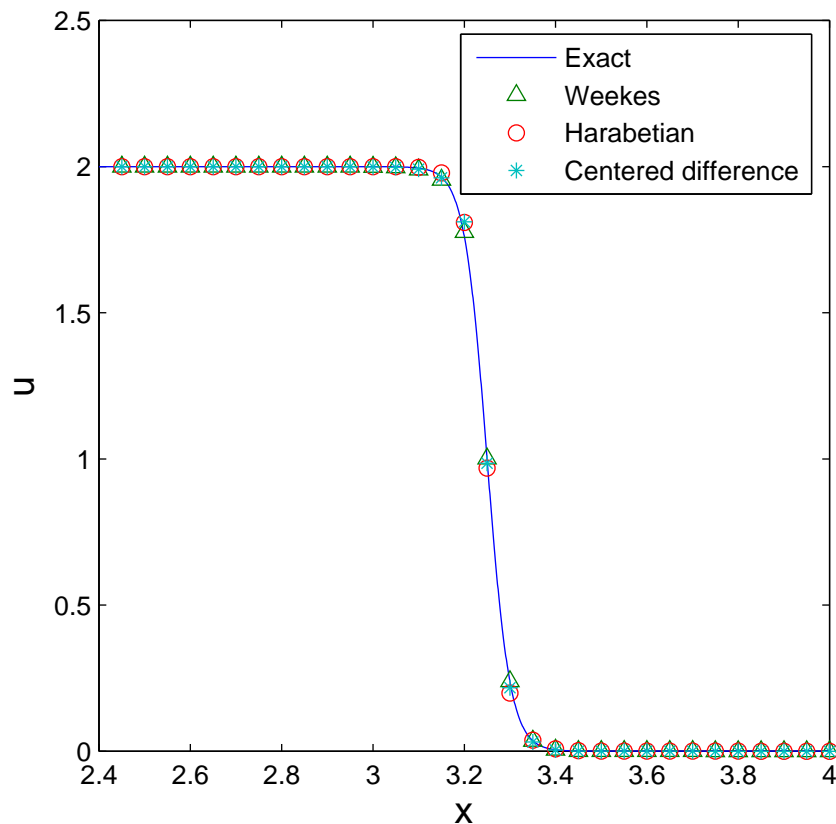
Figure 2: The solution for $u(x,t)$ calculated using the TW schemes by Harabetian and Weekes and a centered difference scheme. In this case: $\lambda = 0.65$, Re = 4.0, $\Delta t = 0.01625$, $\Delta x = 0.05$ and 200 time steps. These parameters correspond to a viscosity coefficient of $\mu = 0.025$ and a final time of $t = 3.25$.

2.2.4   Numerical results

As mentioned in the introduction, we consider the travelling wave scheme for the viscous Burgers equations given in Section 2.2.1.

Test case 1

For this test case we used the following parameters: $\lambda = 0.65$, Re = 4, $\Delta t / \Delta x = 0.325$, $\Delta x = 0.05$ and we did a total of 200 time steps. This situation corresponds to a viscosity coefficient of $\mu = 0.025$, see Eq. (2.10). This is the same test case as was done in [Har90]. In Figure 2 the solution for $u(x,t)$ is depicted using the different schemes. In Section 2.2.2, we mentioned that we consider calculating the speed s from Eq. (2.12) using a bisection method or using a Gauss method. In Figure 3a we depict the pointwise error $|u_h - u|$ of the TW scheme by Harabetian for both ways of calculating s.

	Harabetian		Weekes		Centered difference
	Gauss	Bisection	Gauss	Newton	
$\|u_h - u\|_2$	0.041	0.016	0.0043	0.0042	0.0126

Table 2.2: L^2-norm of the error in the TW-schemes at $t = 3.25$.

Similarly, for the TW scheme by Weekes, we considered calculating s and c using a Gauss method or applying a Newton method. The pointwise errors $|u_h - u|$ are depicted in Figure 3b. The reason for the different behavior of the pointwise error for Weekes' TW scheme when using a Newton method as shown in Figure 3b for $x \in [2.4, 3]$ is because in this region $|u_j - u_{j+1}|$ is small. As mentioned in the previous section, in these regions Weekes [Wee98] uses asymptotic approximations since the Newton method has difficulties obtaining a solution when $|u_j - u_{j+1}|$ is small. We did not implement these asymptotic approximations.

From Figure 3 we see that the error in Weekes' scheme is one order smaller than in Harabetian's scheme. Furthermore, we see that in Harabetian's scheme using the Gauss method results in larger errors than when using a bisection method. For Weekes' scheme the difference between Gauss' integration and the Newton method is minimal. This can also be seen by looking at the L^2 error in Table 2.2.

Test case 2

In this test case we use the following parameters: $\Delta x = 0.2$, $\mu = 0.5$, a diffusion number of DN $= 0.05$ (found by trial and error) and 2000 time steps. The time step Δt satisfies:

$$\Delta t \leq \frac{\text{DN} \cdot \Delta x^2}{\mu}, \tag{2.28}$$

where DN is the diffusion number. We use $\Delta t = 0.004$. We only consider the TW scheme by Weekes, because Harabetian's method is not stable for these parameters. In [Wee98] no stability or TVD analysis is given for the TW scheme we implemented, but we did not run into any problems doing this test case. The solution of $u(x, t)$ is depicted in Figure 4a. In Figure 4b the pointwise error $|u_h - u|$ in the travelling wave scheme using a Gauss method or a Newton method is depicted. As in the previous test case, the difference between Gauss' integration and Newton's method is minimal. This can also be seen by looking at the L^2 error: for both methods $\|u_h - u\|_2 = 0.0058$.
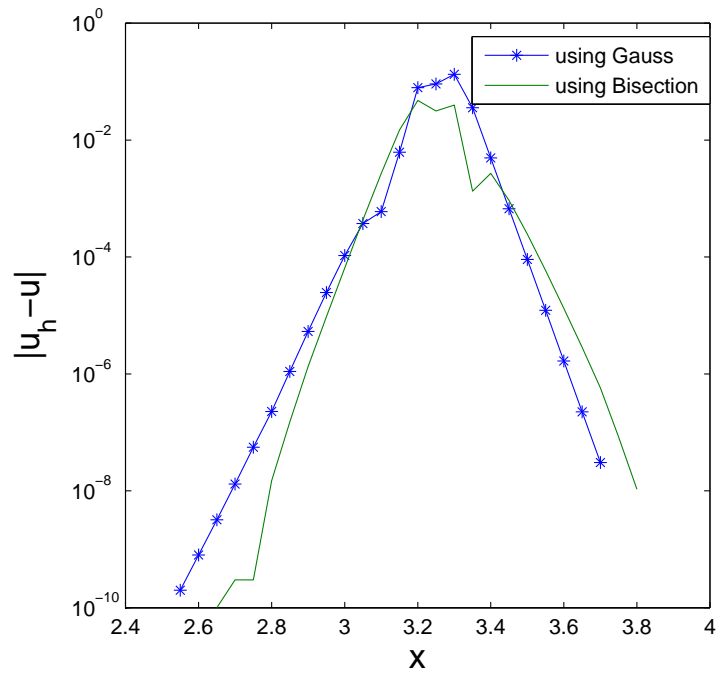
(a) Harabetian's TW scheme.
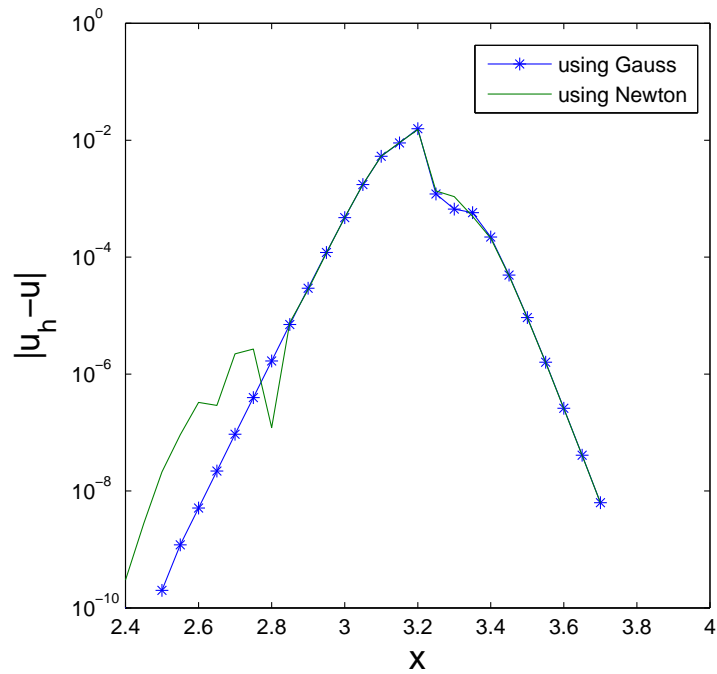
(b) Weekes' TW scheme.

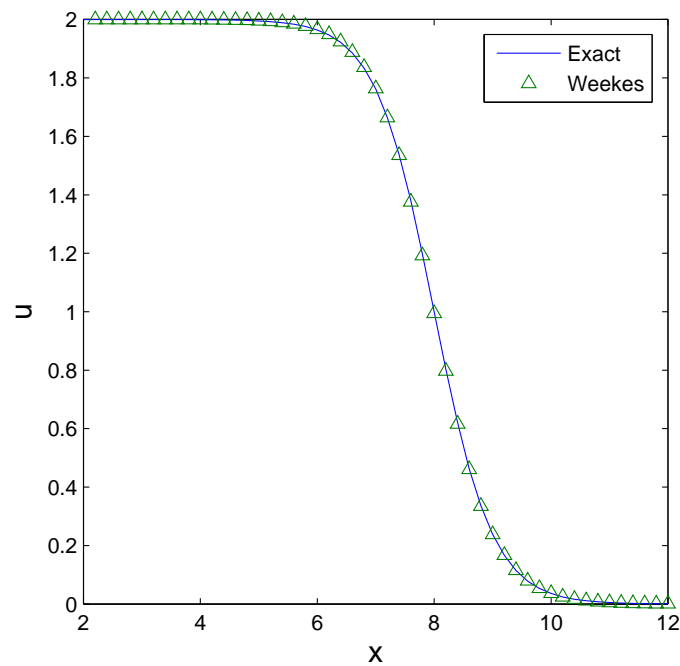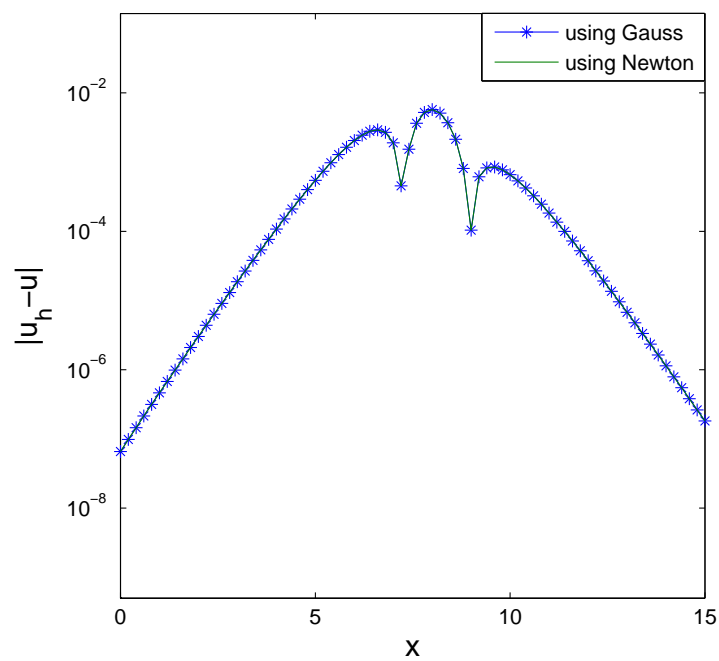Figure 3: The pointwise error $|u_h - u|$ in the travelling wave schemes at $t = 3.25$.

(a) The solution for $u(x, t)$.

(b) The pointwise error $|u_h - u|$.

Figure 4: In this case: $\Delta x = 0.2$, $\mu = 0.5$, diffusion number $= 0.05$, number of time steps $= 2000$, $\Delta t = 0.004$, with the TW scheme by Weekes. The final time is $t = 8$.
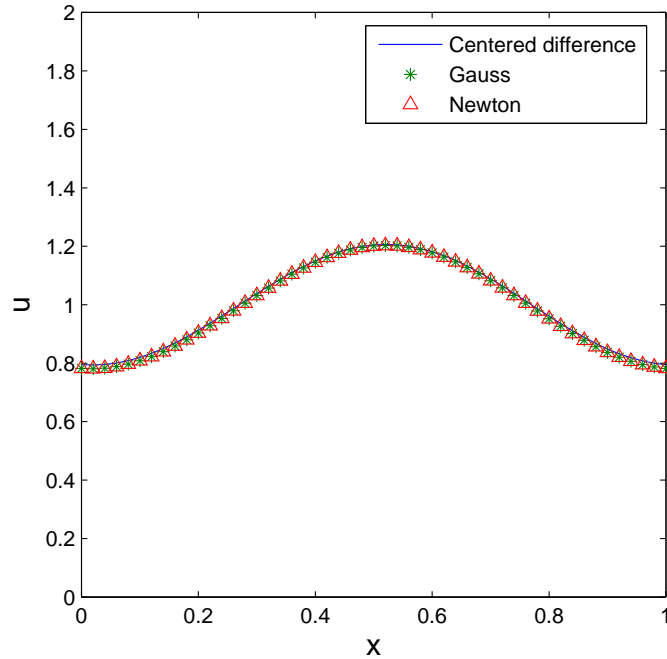
Figure 5: The solution for $u(x,t)$ calculated using the TW scheme and a centered difference scheme. The solution is depicted at $t = 0.02$. A viscosity coefficient of $\mu = 2.0$ and a spatial mesh width of $\Delta x = 0.02$ was used.

Test case 3

In our last test case we consider the viscous Burgers equations with periodic boundary conditions:

$$u_t + f(u)_x = \mu u_{xx}, \quad f(u) = \tfrac{1}{2}u^2, \quad \text{with } x \in [0,1], \, t \in \mathbb{R}^+,$$

with initial condition given by:

$$u(x,0) = \sin(2\pi x - \tfrac{\pi}{2}) + 1.$$

We use the following parameters: $\Delta x = 0.02$, $\mu = 2.0$, a diffusion number of 0.05 and 2000 time steps. Our time step is $\Delta t = 1.0 \cdot 10^{-5}$ which satisfies Eq. (2.28). The solution $u(x,t)$ is depicted in Figure 5. The solution of the TW scheme calculated with the Gauss method is exactly the same as the solution calculated with the Newton method and approximately the same as the solution determined with the centered difference scheme.

2.2.5   Conclusions

We saw in the previous section that the error in Weekes' scheme is much smaller than in Harabetian's scheme for the given test case. Furthermore, we saw that for Harabetian's

scheme to be TVD, the restrictions in Eq. (2.14a) and (2.14b) have to be satisfied where as for the TW scheme by Weekes, we only need Δt to be of order Δx^2 for stability. Therefore we continue with Weekes' scheme. Another reason to use the TW scheme by Weekes is that we do not have to use a different scheme for the case where a travelling wave solution does not exist.

We also tested the TW scheme using the s and c calculated using only the 2-points Gauss method for the integrals in Eq. (2.24) and Eq. (2.25) and using the Newton method and saw no significant differences, meaning we can use the cheaper Gauss method instead of Newton. In the next section we will modify the TW scheme by Weekes slightly so that we can apply the TW scheme to DG-FEM.

2.3 The travelling wave scheme in DG-FEM

2.3.1 Introduction

In this section we will modify the travelling wave scheme by Weekes such that we can apply it to DG-FEM. We consider the viscous Burgers problem as given by Eq. (2.1) and (2.2) with initial condition given by Eq. (2.3).

We will compare the results obtained with the DG-FEM travelling wave (DG-TW) scheme to the results obtained with the method of Bassi and Rebay.

2.3.2 The DG-TW scheme

As in [Wee98], we construct a function $\Phi(x,t)$ to approximate the exact solution $u(x,t)$ of Eq. (2.1). This profile, $\Phi(x,t)$, consists of travelling waves $\varphi_j(\omega)$ that interpolate the data at $x = x_{j-\frac{1}{2}}$ and $x = x_{j+\frac{1}{2}}$ at time t_n. Defining $\omega = x - x_j - s_j(t - t_n)$, the interpolation requirement for φ_j is:

$$\varphi_j(-\tfrac{1}{2}\Delta x) = \bar{u}_{j-1}^n, \qquad \varphi_j(\tfrac{1}{2}\Delta x) = \bar{u}_j^n, \tag{2.29}$$

where Δx is the spatial mesh width and $\bar{u}_{j-1}^n$ and $\bar{u}_j^n$ are the mean values of u on cell $j-1$ and j, respectively, at time $t = t_n$. If $\bar{u}_{j-1}^n < \bar{u}_j^n$ there are no travelling wave solutions $u = \varphi$ to Eq. (2.1) and (2.29). Instead, φ_j is taken to be a travelling wave solution to the modified PDE:

$$u_t + f(u)_x = \tilde{\mu} u_{xx}, \quad f(u) = \tfrac{1}{2}u^2,$$

where $\tilde{\mu} = \mu \operatorname{sgn}(\bar{u}_{j-1}^n - \bar{u}_j^n)$. The φ_j are therefore solutions to the ODE:

$$-s\varphi' + f(\varphi)' = \tilde{\mu}\varphi''. \tag{2.30}$$

Since this is a second order ODE and the speed s is unknown, three constraints are needed to obtain a particular solution, φ_j. Two constraints are given by the interpolation requirement. A third requirement that φ_j has to satisfy is the conservation requirement:

$$\int_{-\frac{1}{2}\Delta x}^{\frac{1}{2}\Delta x} \varphi_j \, d\omega = \frac{\Delta x}{2}(\bar{u}_{j-1}^n + \bar{u}_j^n). \tag{2.31}$$

Note that, unlike for inviscid numerical fluxes, we use the mean data of u in the $(j-1)^{\text{th}}$ and j^{th} element (which are second order approximations to u_{j-1} and u_j respectively) instead of the left and right trace of u on the jth face. The motivation behind this is the following: Let $u_h(x,t)|_{K_j} = \bar{u}_j + \hat{u}_k \psi_j(x)$ be the approximation of $u(x,t)$ on the jth cell, then:

$$
\begin{aligned}
\int_{K_{j-1} \cup K_j} u(x,t)\, dx &= \int_{K_{j-1}} u_h(x,t)|_{K_{j-1}}\, dx + \int_{K_j} u_h(x,t)|_{K_j}\, dx \\
&= \int_{K_{j-1}} \bar{u}_{j-1}\, dx + \int_{K_j} \bar{u}_j\, dx \\
&= \Delta x (\bar{u}_{j-1} + \bar{u}_j),
\end{aligned}
\tag{2.32}
$$

and so the conservation integral of $u(x,t)$ over both cells adjacent to face j equals the integral of the means of $u(x,t)$ on both cells adjacent to face j. Therefore, if we halve the cell size we should obtain:

$$
\int_{-\frac{1}{2}\Delta x}^{\frac{1}{2}\Delta x} u(x,t)\, dx \approx \tfrac{\Delta x}{2}(\bar{u}_{j-1}^n + \bar{u}_j^n),
$$

from which Eq. (2.31) follows. If we were to take the traces of u on the jth face, we would not satisfy the conservation constraint, Eq. (2.32). Note that we do not take:

$$
\int_{-\Delta x}^{\Delta x} u(x,t)\, dx = \int_{-\Delta x}^{\Delta x} \varphi_j\, d\omega = \Delta x (\bar{u}_{j-1}^n + \bar{u}_j^n),
\tag{2.33}
$$

as conservation requirement, even though this is an exact expression. The reason for this will become clear soon.

In [Wee98] it is proven that if $f(u)$ is convex, there exist an s and a $\varphi(\omega)$ that solve the problem given by Eq. (2.29), (2.30) and (2.31). From Eq. (2.30):

$$
\omega + \tfrac{1}{2}\Delta x = \int_{\bar{u}_{j-1}}^{\varphi(\omega)} \frac{\tilde{\mu}}{-s\varphi + f(\varphi) + c}\, d\varphi,
\tag{2.34}
$$

where c is a constant of integration. The interpolation requirement, Eq. (2.29), becomes:

$$
\Delta x = \int_{\bar{u}_{j-1}}^{\bar{u}_j} \frac{\tilde{\mu}}{-s\varphi + f(\varphi) + c}\, d\varphi,
\tag{2.35}
$$

and the conservation requirement, Eq. (2.31), becomes:

$$
\tfrac{\Delta x}{2}(\bar{u}_{j-1} + \bar{u}_j) = \int_{\bar{u}_{j-1}}^{\bar{u}_j} \frac{\tilde{\mu}\varphi}{-s\varphi + f(\varphi) + c}\, d\varphi.
\tag{2.36}
$$

If we had taken the conservation requirement satisfying Eq. (2.33) we would not have been able to obtain Eq. (2.34), (2.35) and (2.36) since $\varphi(-\Delta x)$ and $\varphi(\Delta x)$ are unknown.

The system consisting of Eq. (2.35) and (2.36) is solved simultaneously for the unknowns s and c and, along with Eq. (2.34), gives the particular solution for $\varphi(\omega)$.

As stated in Section 2.2.3, one could use a Newton method to solve this system or we could use a 2-points Gauss method. By applying the Gauss integration method (see Section 2.2.2 for more details on how to do this) on the integrals in Eq. (2.35) and (2.36) we obtain a simple system which can be solved simultaneously for s and c:

$$s = \frac{\bar{u}_{j-1} + \bar{u}_j}{2}, \quad c = \frac{\Delta x(\bar{u}_{j-1}^2 + \bar{u}_j^2) + 12\tilde{\mu}(\bar{u}_j - \bar{u}_{j-1}) + 4\Delta x \bar{u}_{j-1}\bar{u}_j}{12\Delta x}.$$

An expression for $\varphi(\omega)$ can be obtained from Eq. (2.34):

$$\varphi_j(\omega) = s + A\tanh\left(\frac{4\tilde{\mu}\operatorname{arctanh}\big((\bar{u}_{j-1} - s)/A\big) - (2\omega + \Delta x)A}{4\tilde{\mu}}\right),$$

where:

$$A = \sqrt{s^2 - 2c}.$$

It follows that:

$$\varphi_j'(\omega) = \frac{A^2\left(\tanh^2\left(\frac{4\tilde{\mu}\operatorname{arctanh}((\bar{u}_{j-1}-s)/A)-(2\omega+\Delta x)A}{4\tilde{\mu}}\right) - 1\right)}{2\tilde{\mu}}.$$

If $\bar{u}_j > \bar{u}_{j+1}$ we introduce the following numerical flux:

$$H^{DG-TW}(\bar{u}_{j-1}, \bar{u}_j) = f(\varphi_j(0)) - \mu\varphi_j'(0), \tag{2.37}$$

where $\omega = 0$ is the position of the discontinuity at time $t = t_n$.

As in the previous section, if $\bar{u}_j < \bar{u}_{j+1}$, we determine the sonic point $\omega = \hat{\omega}$, where $f'(\varphi(\hat{\omega})) = 0$. If $\hat{\omega} \geq 0$ or $\hat{\omega} < -s\Delta t$ no entropy fix is needed and H^{DG-TW} remains as in Eq. (2.37). Otherwise, if $\hat{\omega}$ is between 0 and $-s\Delta t$, H^{DG-TW} is computed as:

$$H^{DG-TW}(\bar{u}_{j-1}, \bar{u}_j) = f(\varphi_j(\hat{\omega})) - \mu\varphi_j'(\hat{\omega}).$$

Multiplying Eq. (2.1) by a test function v in each element K_k, integrating over each element K_k and summing the local weak formulation over all elements, we obtain the following global weak formulation for the viscous Burgers equation:

Find a $u \in V_h$ such that $B(u, w) = 0$, $\forall w \in V_h$ with:

$$B(u, w) = \int_{\Omega_h} w\, u_t\, dx - \int_{\Omega_h} w_x f\, dx + \mu \int_{\Omega_h} w_x u_x\, dx + \sum_{k=1}^{N} \int_{\partial K_k} w\, H^{DG-TW}(\bar{u}_{j-1}, \bar{u}_j)\, ds,$$

where V_h is defined in Section 2.1.1.

2.3.3 Testing the DG-TW scheme

In this section we will test the DG-TW scheme against the method of Bassi and Rebay.
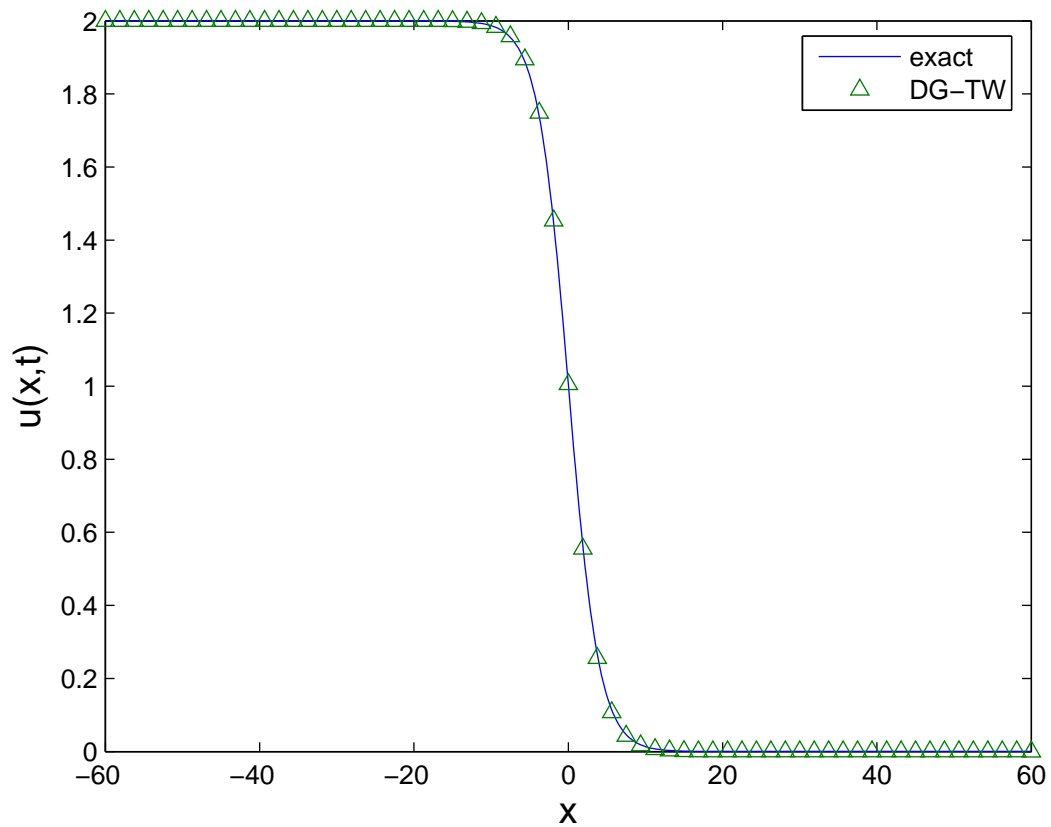
Figure 6: The solution for $u(x,t)$ calculated using the DG-TW scheme. The solution is depicted at $t = 0.02$. A viscosity coefficient of $\mu = 2.0$ and a spatial mesh width of $\Delta x = L/64$ was used.

Test case 1

We will determine the solution of Eq. (2.1) and (2.2) with initial condition given by Eq. (2.3) at time $t = 0.02$ using a viscosity coefficient of $\mu = 2.0$. We consider a spatial domain of length $L = 120$ with $\Omega = [-60, 60]$. See Figure 6 for the solution. The solutions of the DG-TW scheme are compared to solutions calculated with the method of Bassi and Rebay. We determine the L^2- and L^∞-norms of the errors as follows:

$$\|u^k - u\|_\infty := \max\{|u_i^k - u_i| : 1 \leq i \leq n\},$$

$$\|u^k - u\|_2 := \left(\Delta x \sum_{i=1}^n \left(u_i^k - u_i \right)^2 \right)^{\frac{1}{2}},$$

where k is the number of cells in the grid, $\Delta x = 1/k$ the cell width on the coarsest grid and x_i is the ith grid point on the grid with k cells.

The results of the order behavior are depicted in Figure (7). We see that there is no significant difference in the solution when using the DG-TW scheme or the method of Bassi and Rebay. Both schemes show second order behavior. We also see that determining the solution by using Gauss or Newton makes no difference. These can also be seen in Table (2.3).

To determine how much the viscosity plays a part in the scheme, we determine the ratio viscous/inviscid contributions in the method of Bassi and Rebay and of the DG-TW scheme. This ratio was determined in the calculation of the means as well as in the calculation for the slopes. In Figure 8 these ratios are depicted along the x-axis. We see that in the shock region, $x \in [0, 20]$, the viscous contributions certainly play a major part in the solution. We also see that the ratio in the calculation of the means are similar for the Bassi and Rebay method and the DG-TW scheme, but the peaks of the ratios in the calculation of the slopes between both methods are slightly apart.

Remark. In the calculation of the ratio viscous-/inviscid contributions, we set the ratio equal to 0 if the inviscid contributions were 0.

Test case 2

To show that the DG-TW scheme also works for other problems, we considered the viscous Burgers equation with periodic boundary conditions:

$$u_t + f(u)_x = \mu u_{xx}, \quad f(u) = \tfrac{1}{2}u^2, \quad \text{with } x \in [0, 1], \, t \in \mathbb{R}^+,$$

and initial condition given by:

$$u(x, 0) = \sin(2\pi x - \tfrac{\pi}{2}) + 1.$$

Figure 9 depicts the solution using the DG-TW scheme and the method of Bassi and Rebay at $t = 0.02$ calculated on a grid using 64 cells, a viscosity of 2.0 and a diffusion number of 0.05. The difference between the DG-TW solution and the Bassi and Rebay solution is depicted in Figure 10. We see that the DG-TW scheme and the method of Bassi and Rebay agree very well with each other. We do not test this any further for a scalar equation.

Remark. Doing these test cases, no situations occurred in which the entropy fix had to be applied.
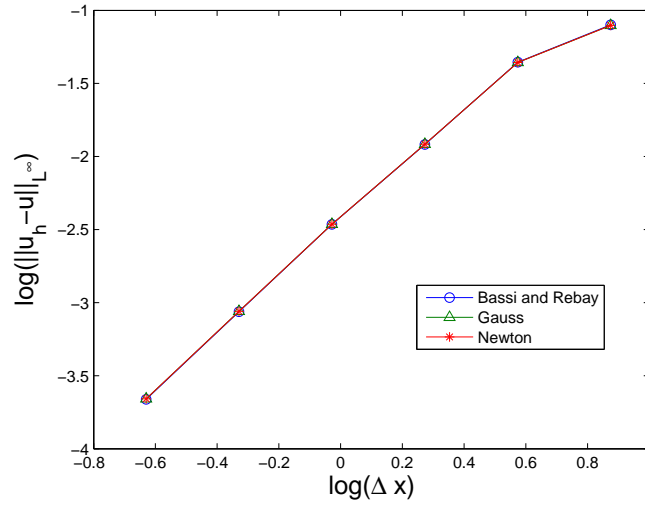
(a) Order behavior using the L^∞-norm.
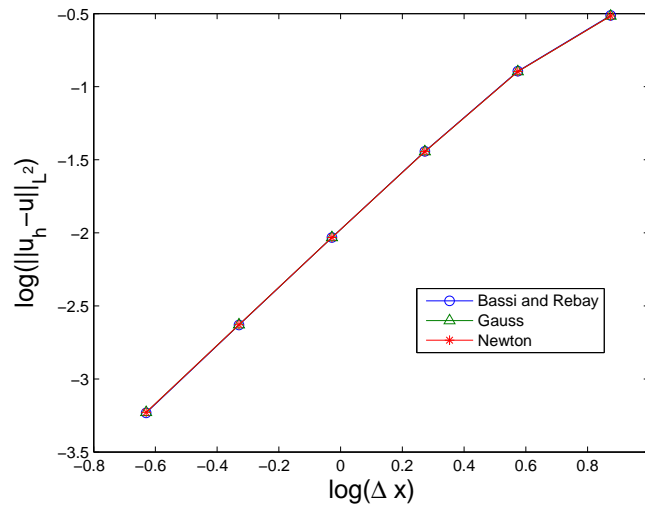
(b) Order behavior using the L^2-norm.

Figure 7: Comparing the order behavior of the DG-TW scheme against the order behavior using the method of Bassi and Rebay. In this case: $\mu = 2.0$, diffusion number DN $= 0.05$, time $t = 0.02$.
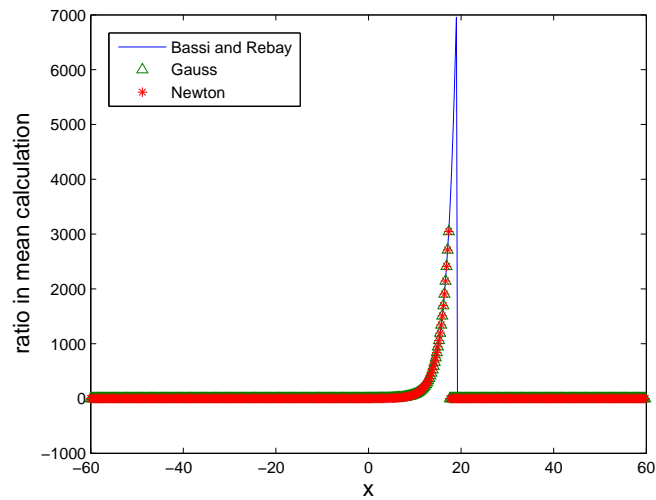
(a) Viscous-/inviscid ratio's in the calculation of the means.
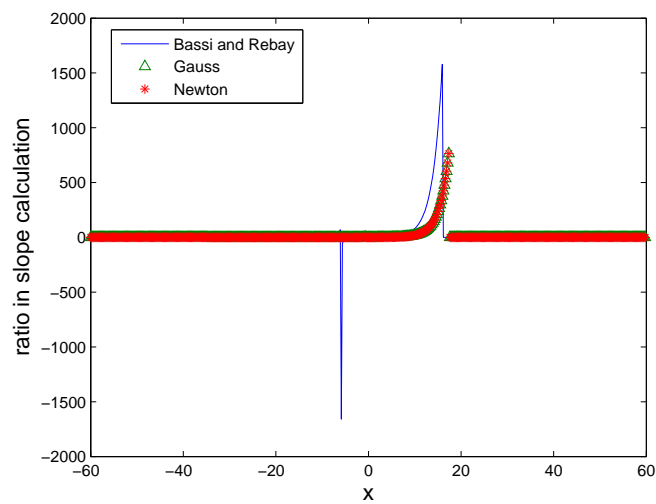
(b) Viscous-/inviscid ratio's in the calculation of the slopes.

Figure 8: Comparing the ratio viscous/inviscid contributions, in the calculations of the means and slopes, in the method of Bassi and Rebay and in the DG-TW scheme. In this case: $\mu = 2.0$, diffusion number DN $= 0.05$, time $t = 0.02$ and $\Delta x = L/512$ with $L = 120$.

Δx	Bassi and Rebay				DG-TW Gauss/Newton			
	$\|u_h - u\|_\infty$	p	$\|u_h - u\|_2$	p	$\|u_h - u\|_\infty$	p	$\|u_h - u\|_2$	p
$L/16$	0.0796	-	0.307	-	0.0789	-	0.305	-
$L/32$	0.0442	0.8	0.128	1.3	0.0440	0.8	0.127	1.3
$L/64$	0.0121	1.9	0.0361	1.8	0.0121	1.9	0.0359	1.8
$L/128$	0.00343	1.8	0.00929	2.0	0.00344	1.8	0.00929	2.0
$L/256$	0.000867	2.0	0.00234	2.0	0.000872	2.0	0.00235	2.0
$L/512$	0.000218	2.0	0.000586	2.0	0.000220	2.0	0.000591	2.0

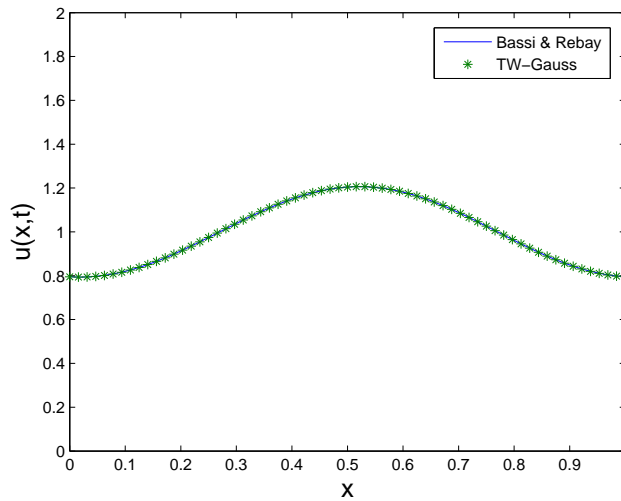Table 2.3: Norms of the method of Bassi and Rebay and the DG-TW scheme. The order is denoted as p.

Figure 9: The solution for $u(x,t)$ calculated using the DG-TW scheme and the method of Bassi and Rebay. The solution is depicted at $t = 0.02$. A viscosity coefficient of $\mu = 2.0$ and a spatial mesh width of $\Delta x = 1/64$ was used.
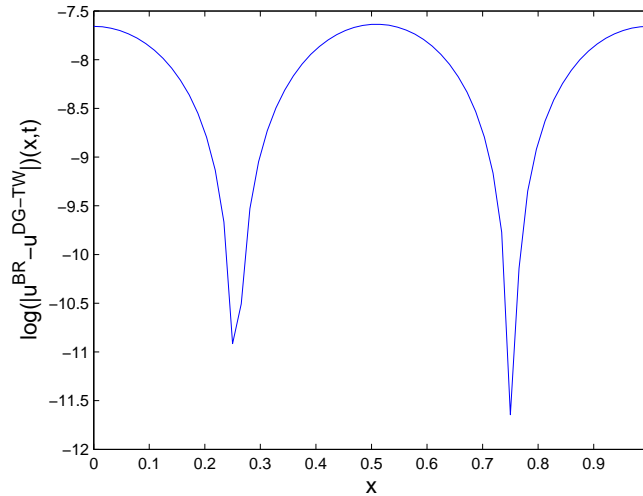
Figure 10: The difference between the DG-TW solution and the Bassi and Rebay solution for $u(x,t)$. This difference is depicted at $t = 0.02$. A viscosity coefficient of $\mu = 2.0$ and a spatial mesh width of $\Delta x = 1/64$ was used.

2.4   Conclusions

In this section we considered travelling wave schemes introduced in [Har90] and [Wee98]. It turned out that the TW scheme introduced by Weekes is more suitable to use than the TW scheme introduced by Harabetian. We also considered two ways of finding roots of the non-linear equations. In [Wee98] it is suggested to use a Newton method to find these roots. We, however, found that using a Gauss method gave the same results at much lower cost.

We modified Weekes' TW scheme in Section 2.3 so that it could be applied to DG-FEM. This resulted in the DG-TW scheme. The DG-TW scheme was compared to the method of Bassi and Rebay, the standard way of treating second order derivatives in a DG method, in a test case of which we verified that the viscous contributions in the algorithm play an important part in the solution. We see that there was no significant difference in the solution when using the DG-TW scheme or the method of Bassi and Rebay and that both schemes show second order behavior. We also see that using Gauss or Newton in the DG-TW scheme gives the same results.

Furthermore, the DG-TW scheme is easier to implement than the Bassi and Rebay method, since, once the inviscid Burgers equation is implemented, one needs only to modify the flux function and add a viscous volume term. It is therefore also cheaper than the Bassi and Rebay method: the costly lifting operators and viscous contributions are not needed.

The DG-TW scheme is a scheme evolving from the physics of the system. Inviscid and viscous contributions are not split. The method of Bassi and Rebay, on the other hand, is a scheme separating the flux at element faces into an inviscid and a viscous contribution. A penalty term is introduced for stability reasons, penalizing the discontinuity at the element faces

without making a distinction if it originates from the physics or from the use of discontinuous polynomials. So, besides being easier to implement and less costly, the DG-TW method is also based on the physics rather than only the mathematical properties.

3 1D Navier-Stokes equations

In this chapter we analyze the TW-scheme introduced in [Wee98] for the 1D Navier-Stokes equations. Afterwards we will adapt this scheme so that it can be applied to DG as was done in the previous chapter for Burgers. We start this chapter by deriving a dimensionless form of the 1D Navier-Stokes equations (see [Kla04]).

3.1 Dimensionless form

Consider the Navier-Stokes equations in dimensional form:

$$U_t + F^e(U)_x = F^v(U, U_x)_x,$$

where:

$$U = \begin{bmatrix} \rho \\ \rho u \\ \rho E \end{bmatrix}, \quad F^e(U) = \begin{bmatrix} \rho u \\ \rho u^2 + p \\ u(\rho E + p) \end{bmatrix}, \quad F^v(U, U_x) = \begin{bmatrix} 0 \\ \frac{4}{3}\mu u_x \\ \frac{4}{3}\mu u u_x + \kappa T_x \end{bmatrix},$$

Here ρ is the density, u the velocity, p the pressure, $E = e + \frac{1}{2}u^2$ the total energy, e the internal energy, T the temperature, μ the dynamic viscosity coefficient and κ the thermal conductivity coefficient.

Assuming a calorically perfect gas, the pressure p and internal energy e are given by the equations of state:

$$p = \rho R T,$$
$$e = c_v T,$$

where c_p and c_v are the specific heats respectively at constant pressure and constant volume and $R = c_p - c_v$ is the specific gas constant.

The magnitudes of the dimensional quantities involved in the Navier-Stokes equations are given in terms of the four fundamental magnitudes mass $[M]$, length $[L]$, time $[T]$ and temperature $[\theta]$. Our non dimensionalization is based on the recurrent set of reference values $\{\rho_\infty, a_\infty, T_\infty, L\}$ with a_∞ the free-stream speed of sound defined as:

$$a_\infty = \sqrt{\frac{\gamma p_\infty}{\rho_\infty}},$$

and L a characteristic length scale. The dimensionless form of the Navier-Stokes equations [Kla04] is given by:

$$C\big(\tilde{U}_{\tilde{t}} + F^e(\tilde{U})_{\tilde{x}} - F^v(\tilde{U}, \tilde{U}_{\tilde{x}})_{\tilde{x}}\big) = 0,$$

where:

$$\tilde{U} = \begin{bmatrix} \tilde{\rho} \\ \tilde{\rho}\tilde{u} \\ \tilde{\rho}\tilde{E} \end{bmatrix}, \quad F^e(\tilde{U}) = \begin{bmatrix} \tilde{\rho}\tilde{u} \\ \tilde{\rho}\tilde{u}^2 + \tilde{p} \\ \tilde{u}(\tilde{\rho}\tilde{E} + \tilde{p}) \end{bmatrix}, \quad F^v(\tilde{U}, \tilde{U}_x) = \begin{bmatrix} 0 \\ \frac{4}{3}\tilde{\mu}\tilde{u}_{\tilde{x}} \\ \frac{4}{3}\tilde{\mu}\tilde{u}\tilde{u}_{\tilde{x}} + \tilde{\kappa}\tilde{T}_{\tilde{x}} \end{bmatrix},$$

and:

$$C = \begin{bmatrix} \rho_\infty a_\infty/L & 0 & 0 \\ 0 & \rho_\infty a_\infty^2/L & 0 \\ 0 & 0 & \rho_\infty a_\infty^3/L \end{bmatrix}.$$

Since the form of the dimensionless equations is identical to the dimensional equations, the tilde notation is ommited from now on. We consider flow problems defined by the following eight parameters:

- the characteristic length L,

- the free-stream density ρ_∞, velocity u_∞ and temperature T_∞,

- the gas constant R and the specific heat at constant pressure c_p,

- the free-stream dynamic viscosity μ_∞ and thermal conductivity κ_∞,

Since the equations contain four fundamental magnitudes, according to the Buckingham's Pi theorem, four dimensionless Pi groups can be formed:

- the free-stream Mach number $\mathrm{M}_\infty = u_\infty/a_\infty$,

- the ratio of specific heats $\gamma = c_p/c_v$,

- the free-stream Reynolds number $\mathrm{Re}_\infty = \rho_\infty u_\infty L/\mu_\infty$,

- the Prandtl number $\mathrm{Pr} = c_p\mu_\infty/\kappa_\infty$,

The flow parameters can now be expressed in terms of the dimensionless Pi groups and the recurrent set $\{\rho_\infty, a_\infty, T_\infty, L\}$:

$$R = \frac{p_\infty}{\rho_\infty T_\infty}, \ c_p = \frac{\gamma}{\gamma - 1}R, \ \mu_\infty = \frac{\rho_\infty u_\infty L}{\mathrm{Re}_\infty}, \ \kappa_\infty = \frac{c_p\mu_\infty}{\mathrm{Pr}}.$$

By definition $\rho_\infty = 1$, $a_\infty = 1$, $T_\infty = 1$ and $L = 1$ so that all values can be calculated once M_∞, Re_∞ and Pr are given:

$$\mathrm{R} = \frac{1}{\gamma}, \quad c_p = \frac{1}{\gamma - 1}, \quad \mu_\infty = \frac{\mathrm{M}_\infty}{\mathrm{Re}_\infty}, \quad \kappa_\infty = \frac{\mathrm{M}_\infty}{\mathrm{Re}_\infty \mathrm{Pr}} c_p.$$

Using these expressions we can write the dimensionless Navier-Stokes equations as:

$$U_t + F^e(U)_x = F^v(U, U_x)_x,$$

where:

$$U = \begin{bmatrix} \rho \\ \rho u \\ \rho E \end{bmatrix}, \quad F^e(U) = \begin{bmatrix} \rho u \\ \rho u^2 + p \\ u(\rho E + p) \end{bmatrix}, \quad F^v(U, U_x) = \begin{bmatrix} 0 \\ \frac{4}{3}\mu u_x \\ \frac{4}{3}\mu u u_x + \kappa T_x \end{bmatrix},$$

with:

$$\mu = \frac{\mathrm{M}_\infty}{\mathrm{Re}_\infty}, \quad \kappa = \frac{c_p \mu}{\mathrm{Pr}}.$$

In [Wee98] a Prandtl number of $\mathrm{Pr} = 0.75$ is assumed resulting in $\kappa/c_p = \frac{4}{3}\mu$. For a calorically perfect gas, the enthalpy is given by:

$$h = c_p T.$$

Using these assumptions, and using $e = h - p/\rho$, the Navier-Stokes equations are given as:

$$U_t + F^e(U)_x = F^v(U, U_x)_x, \tag{3.1}$$

where:

$$U = \begin{bmatrix} \rho \\ \rho u \\ \rho E \end{bmatrix}, \quad F^e(U) = \begin{bmatrix} \rho u \\ \rho u^2 + p \\ \rho u(h + \frac{1}{2}u^2) \end{bmatrix}, \quad F^v(U, U_x) = \frac{4}{3}\mu \begin{bmatrix} 0 \\ u_x \\ (h + \frac{1}{2}u^2)_x \end{bmatrix}.$$

In [Wee98], the following form of the Navier-Stokes equations is used:

$$U_t + F(U)_x = \mu G(U)_{xx}, \tag{3.2}$$

where:

$$U = \begin{bmatrix} \rho \\ \rho u \\ \rho E \end{bmatrix}, \quad F(U) = \begin{bmatrix} \rho u \\ \rho u^2 + p \\ \rho u(h + \frac{1}{2}u^2) \end{bmatrix}, \quad G(U) = \frac{\gamma + 1}{2\gamma} \begin{bmatrix} 0 \\ u \\ h + \frac{1}{2}u^2 \end{bmatrix}. \tag{3.3}$$

For us it is unclear how the step is made from Eq. (3.1) to (3.2) since $(\gamma + 1)/2\gamma = 4/3$ results in a γ smaller than 1 which is physically not possible. However, we do continue with the dimensionless form given by Eq. (3.2).

3.2 Weekes' travelling wave scheme

The travelling wave scheme is based on assuming travelling wave solutions of the viscous Riemann problem. In [Wee98] a travelling wave scheme was developed for the one-dimensional, compressible Navier-Stokes equations. This scheme is different from other methods in that the viscous part is not split from the hyperbolic part of the equations. In this section a viscous Riemann solver is derived solving the local Riemann problem by interpolating each adjacent data pair via three waves.

A function Φ will be constructed to approximate the exact solution $U(x,t)$ of Eq. (3.2), which will interpolate the given data such that:

$$\Phi(x_j, t_n) = U(x_j, t_n), \ \forall j. \tag{3.4}$$

The Navier-Stokes equations admit three distinct eigenvalues, $\lambda^{(1)} < \lambda^{(2)} < \lambda^{(3)}$. Associated with $\lambda^{(1)}$ and $\lambda^{(3)}$ are genuinely nonlinear characteristic fields and associated with $\lambda^{(2)}$ is a
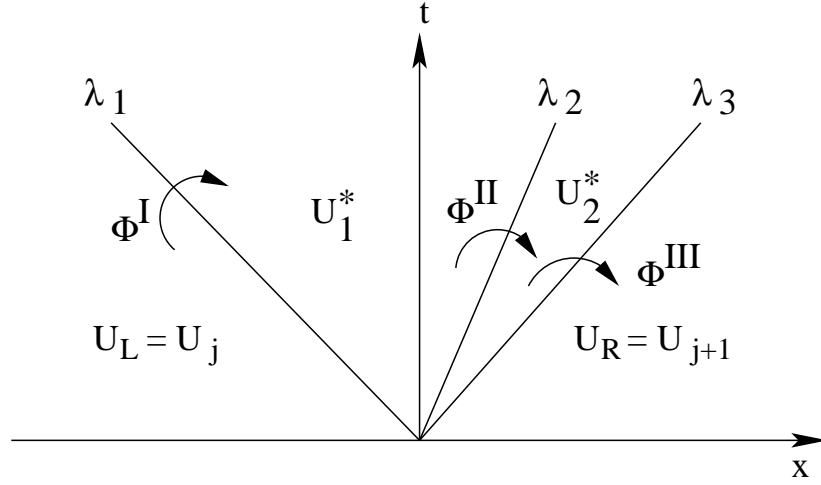
Figure 11: Structure of the solution for the viscous Riemann problem

linearly degenerate field. Within the genuinely nonlinear fields, shock waves or rarefaction waves are formed. Since we want to approximate the exact solution $U(x,t)$ of Eq. (3.2) with travelling waves, rarefaction waves are treated as entropy violating shocks. Consider the profile $\Phi = \Phi_{j+\frac{1}{2}}$ joining U_j to U_{j+1} as being made up of a I travelling wave $\Phi^I_{j+\frac{1}{2}}(x,t) = \varphi^I_{j+\frac{1}{2}}(\omega)$ with speed s_1 connecting U_j to a state U_1^*, followed by a diffusion wave $\Phi^{II}_{j+\frac{1}{2}}(x,t) = \varphi^{II}_{j+\frac{1}{2}}(\omega)$ connecting U_1^* to a state U_2^* in the second field, and $\Phi^{III}_{j+\frac{1}{2}}(x,t) = \varphi^{III}_{j+\frac{1}{2}}(\omega)$, a III travelling wave with speed s_3 connecting U_2^* to U_{j+1}. Here $\omega = x - x_{j+\frac{1}{2}} - s_{j+\frac{1}{2}}(t - t_n)$ and $x_{j+\frac{1}{2}} = \frac{1}{2}(x_j + x_{j+1})$. The profile Φ therefore can be described as:

$$\Phi_{j+\frac{1}{2}} - U_j = \left(\Phi^I_{j+\frac{1}{2}} - U_j\right) + \left(\Phi^{II}_{j+\frac{1}{2}} - U_1^*\right) + \left(\Phi^{III}_{j+\frac{1}{2}} - U_2^*\right). \tag{3.5}$$

See Figure 11 for the structure of the Riemann problem.
There is conservation of U in the sense that:

$$\int_{x_j}^{x_{j+1}} \Phi(x, t_n)\, dx = \tfrac{1}{2}\Delta x(U_j + U_{j+1}).$$

or equivalently:

$$0 = \left(\int_{-\frac{1}{2}\Delta x}^{\frac{1}{2}\Delta x} \varphi^I(\omega)\, d\omega - \tfrac{\Delta x}{2}(U_j + U_1^*)\right) + \left(\int_{-\frac{1}{2}\Delta x}^{\frac{1}{2}\Delta x} \varphi^{II}(\omega)\, d\omega - \tfrac{\Delta x}{2}(U_1^* + U_2^*)\right)$$
$$+ \left(\int_{-\frac{1}{2}\Delta x}^{\frac{1}{2}\Delta x} \varphi^{III}(\omega)\, d\omega - \tfrac{\Delta x}{2}(U_2^* + U_{j+1})\right).$$

The viscous Riemann solver which gives the φ^i and U_1^* and U_2^* is described in Section 3.2.2. Using the travelling wave scheme, Weekes introduces three numerical fluxes, H_0^{TW}, H_1^{TW} and

H_2^{TW}, which are calculated via a standard flux-difference splitting formulation:

$$
\begin{aligned}
H_k^{TW}(U_j, U_{j+1}) - F(U_j) &= [H_k^I(U_j, U_1^*) - F(U_j)] \\
&\quad + [H_k^{II}(U_1^*, U_2^*) - F(U_1^*)] + [H_k^{III}(U_2^*, U_{j+1}) - F(U_2^*)],
\end{aligned}
$$

where $k = 0, 1, 2$, and H_k^i the numerical flux corresponding to the Riemann problem in which only the i-th wave appears. In Section 3.2.4 we give the analysis for the H_0^{TW} flux, the other two fluxes are simple extensions of the H_0^{TW} flux and are not needed when deriving a DG version of the flux.

3.2.1   Travelling wave solutions of the Navier-Stokes equations

When the velocity on the right of a discontinuity is less than that on the left, there are no travelling wave solutions $U = \Phi$ for Eq. (3.2). We consider therefore, in the first and third wave fields, travelling wave solutions,

$$
U(x,t) = \varphi(\omega) = \begin{bmatrix} \rho \\ \rho u \\ \rho E \end{bmatrix}(\omega),
$$

of the modified Navier-Stokes equations:

$$
U_t + F(U)_x = \tilde{\mu} G(U)_{xx},
$$

where $\tilde{\mu} = -sgn(u'(\omega))\mu$. The tilde notation will be used for the modified Navier-Stokes equations. These tildes have no relation with the dimensionless form of the Navier-Stokes equations. As in the scalar case, if $u_j < u_{j+1}$, viscous rarefaction fans are replaced by entropy violating travelling waves.

In this section we derive an equation from which we can determine $\varphi(\omega)$.
We start by transforming the problem to a frame moving with the shock. Denote the shock speed by s, then the flow speed relative to the shock is $v = s - u$. The Rankine-Hugoniot conditions (derived in Appendix A.2) give:

$$
Q := \rho_L v_L = \rho_R v_R, \tag{3.6a}
$$

$$
P := \rho_L v_L^2 + p_L + \frac{\gamma+1}{2\gamma}\tilde{\mu}\left(\frac{dv}{d\omega}\right)_L = \rho_R v_R^2 + p_R + \frac{\gamma+1}{2\gamma}\tilde{\mu}\left(\frac{dv}{d\omega}\right)_R, \tag{3.6b}
$$

$$
\mathcal{E} := \left(h_L + \tfrac{1}{2}v_L^2\right)v_L\rho_L + \frac{\gamma+1}{2\gamma}\tilde{\mu}\left(\frac{d}{d\omega}\left(h+\tfrac{1}{2}v^2\right)\right)_L = \left(h_R + \tfrac{1}{2}v_R^2\right)v_R\rho_R + \frac{\gamma+1}{2\gamma}\tilde{\mu}\left(\frac{d}{d\omega}\left(h+\tfrac{1}{2}v^2\right)\right)_R, \tag{3.6c}
$$

and Q, P and $\mathcal{E}$ are constants. Note that v is measured positive in the negative ω direction. We can reduce the system to two equations for v and h, using $p = \rho h(\gamma - 1)/\gamma$:

$$
\frac{\gamma+1}{2\gamma}\tilde{\mu}\frac{dv}{d\omega} = P - Q\left(v + \frac{\gamma-1}{\gamma}\frac{h}{v}\right), \tag{3.7a}
$$

$$\frac{\gamma+1}{2\gamma}\tilde{\mu}\frac{d}{d\omega}\left(h+\tfrac{1}{2}v^2\right) = \mathcal{E} - Q\left(h+\tfrac{1}{2}v^2\right). \tag{3.7b}$$

Consider now the case that $\omega \to \infty$, then the flow tends to a uniform state. From Eq. (3.7b), since $d(\cdot)/d\omega = 0$, this results in $h_2 + \tfrac{1}{2}v_2^2 = \mathcal{E}/Q$, where $(\cdot)_2$ denotes the state at $\omega \to \infty$. Therefore, according to [Whi74], the only solution that is bounded as $\omega \to -\infty$ is:

$$h + \tfrac{1}{2}v^2 = H, \tag{3.8}$$

throughout, where $H = \mathcal{E}/Q$. It follows that $h + \tfrac{1}{2}v^2$ is the same on the two sides of the shock as well as throughout the shock. Using Eq. (3.8) we can write Eq. (3.6b) as:

$$\frac{\gamma+1}{2\gamma}\tilde{\mu}\frac{dv}{d\omega} = P - Q\left(\frac{\gamma+1}{2\gamma}v + \frac{\gamma-1}{\gamma}\frac{H}{v}\right). \tag{3.9}$$

The constants P, Q and $\mathcal{E}$ must be such that the right hand side vanishes for both $v = v_1$ and $v = v_2$ so:

$$\begin{aligned}
P &= Q\left(\frac{\gamma+1}{2\gamma}v_1 + \frac{\gamma-1}{\gamma}\frac{H}{v_1}\right) \\
&= Q\left(\frac{\gamma+1}{2\gamma}v_2 + \frac{\gamma-1}{\gamma}\frac{H}{v_2}\right).
\end{aligned}$$

It follows that H must be such that:

$$Q\left(\frac{\gamma+1}{2\gamma}v_1 + \frac{\gamma-1}{\gamma}\frac{H}{v_1}\right) - Q\left(\frac{\gamma+1}{2\gamma}v_2 + \frac{\gamma-1}{\gamma}\frac{H}{v_2}\right) = 0.$$

We find:

$$H = \frac{\gamma+1}{2(\gamma-1)}v_1 v_2,$$

and P follows as:

$$P = Q\frac{\gamma+1}{2\gamma}(v_1 + v_2).$$

Substituting these expressions into Eq. (3.9) we find:

$$Q\frac{(v_1 - v)(v - v_2)}{v} = \tilde{\mu}\frac{dv}{d\omega}, \tag{3.10}$$

with the relation:

$$v_1 v_2 = \frac{2(\gamma-1)}{\gamma+1}H. \tag{3.11}$$

Here $(\cdot)_1$ and $(\cdot)_2$ denote the states at $-\infty$ and $+\infty$. From Eq. (3.10), we see that in the limit $\mathrm{Re} \to \infty$, so $\mu \to 0$, we obtain $v = v_1$ and $v = v_2$ as the trivial solutions for v. From Eq. (3.10) it follows that:

$$-\frac{\tilde{\mu}}{Q}\frac{v}{(v - v_1)(v - v_2)}\,dv = d\omega, \tag{3.12}$$

leading to:

$$\int_{v_j}^{v} -\frac{\tilde{\mu}}{Q}\frac{v}{(v-v_1)(v-v_2)}\,dv = \int_{-\frac{1}{2}\Delta x}^{\omega} d\omega, \tag{3.13}$$

which results in the following equation for $v(\omega)$:

$$\frac{\tilde{\mu}}{Q(v_1-v_2)}\left(v_2\ln\left(\left|\frac{v(\omega)-v_2}{v_j-v_2}\right|\right) - v_1\ln\left(\left|\frac{v(\omega)-v_1}{v_j-v_1}\right|\right)\right) = \omega + \frac{1}{2}\Delta x. \tag{3.14}$$

Solving for $v(\omega)$ gives the travelling wave $\varphi(\omega) = s - v(\omega)$. In the next section we show how to determine u_1, u_2 and s where:

$$u_1 = s - v_1, \quad u_2 = s - v_2. \tag{3.15}$$

3.2.2   The viscous Riemann solver, I and III wave

The task of the viscous Riemann solver is to find the profiles $\varphi^i(\omega)$ for $i = I, II, III$ and the middle states U_1^* and U_2^*, given the states U_j and U_{j+1} at x_j and x_{j+1}. How the profiles and middle states are found is discussed in this and the following section.

Travelling wave solutions $\varphi^I(\omega)$ and $\varphi^{III}(\omega)$ are obtained by imposing requirements of interpolation and conservation. Given a middle velocity $u_* = u_1^* = u_2^*$, we interpolate a travelling wave solution, over wave I, such that:

$$\varphi^I\left(-\tfrac{1}{2}\Delta x\right) = U_j, \qquad u^I\left(\tfrac{1}{2}\Delta x\right) = u_*, \tag{3.16}$$

and require that the mass is conserved:

$$\int_{-\frac{1}{2}\Delta x}^{\frac{1}{2}\Delta x} \rho^I(\omega)\,d\omega = \tfrac{1}{2}\Delta x(\rho_j + \rho_1^*). \tag{3.17}$$

Similarly, over wave III, the interpolation requirement is:

$$\varphi^{III}\left(\tfrac{1}{2}\Delta x\right) = U_{j+1}, \qquad u^{III}\left(-\tfrac{1}{2}\Delta x\right) = u_*,$$

and the conservation requirement:

$$\int_{-\frac{1}{2}\Delta x}^{\frac{1}{2}\Delta x} \rho^{III}(\omega)\,d\omega = \tfrac{1}{2}\Delta x(\rho_2^* + \rho_{j+1}).$$

From Eq. (3.13) it follows that:

$$\int_{v_j}^{v_1^*} -\frac{\tilde{\mu}}{Q}\frac{v}{(v-v_1)(v-v_2)}\,dv = \int_{-\frac{1}{2}\Delta x}^{\frac{1}{2}\Delta x} d\omega,$$

which, by using Eq. (3.16), results in the interpolation equation for wave I:

$$\frac{\tilde{\mu}}{Q(v_1-v_2)}\left(v_2\ln\left(\left|\frac{v_1^*-v_2}{v_j-v_2}\right|\right) - v_1\ln\left(\left|\frac{v_1^*-v_1}{v_j-v_1}\right|\right)\right) = \Delta x. \tag{3.18}$$

Multiplying Eq. (3.12) by the density $\rho^I(\omega)$, and using $Q = \rho v$ from Eq. (3.6a) we obtain:

$$\frac{-\tilde{\mu}}{(v - v_1)(v - v_2)}\, dv = \rho(\omega)\, d\omega,$$

resulting in:

$$\int_{v_j}^{v_1^*} \frac{-\tilde{\mu}}{(v - v_1)(v - v_2)}\, dv = \int_{-\frac{1}{2}\Delta x}^{\frac{1}{2}\Delta x} \rho(\omega)\, d\omega.$$

From the mass conservation requirement, Eq. (3.17) we obtain:

$$\frac{\tilde{\mu}}{(v_1 - v_2)}\left(\ln\left(\left| \frac{v_1^* - v_2}{v_j - v_2} \right| \right) - \ln\left(\left| \frac{v_1^* - v_1}{v_j - v_1} \right| \right) \right) = \tfrac{1}{2}\Delta x(\rho_j + \rho_1^*). \tag{3.19}$$

Solving Eqs. (3.11), (3.15), (3.18) and (3.19) for u_1, u_2 and s would allow us to define φ^I completely. Similarly, the analogous equations over wave III can be solved to obtain φ^{III}. Where this inversion is to difficult, Weekes used asymptotic approximations to the viscous profiles [Wee98].

We guessed u_* to obtain solutions for u_1^k, u_2^k and s^k, $k = I, III$. To determine whether the guess is correct we need to determine the pressures in the intermediate states. The pressures p_1^* and p_2^* have to be equal since across a contact wave the pressure remains constant. If the pressures p_1^* and p_2^* are not equal a new u_* has to be determined and u_1^k, u_2^k and s^k, $k = I, III$ have to be calculated again.

We have u_*, s, ρ_1^*, E_j and u_j for the first intermediate state. We can now determine the pressure p_1^*. From Eq. (3.8) and $h = \gamma(E - \frac{1}{2}u^2)$ we obtain:

$$\begin{aligned}
H &= \gamma(E_j - \tfrac{1}{2}u_j^2) + \tfrac{1}{2}(s - u_j)^2, \\
&= \gamma(E_1^* - \tfrac{1}{2}u_*^2) + \tfrac{1}{2}(s - u_*)^2,
\end{aligned}$$

which is constant. It follows that:

$$E_1^* = \frac{1}{\gamma}\left(H - \tfrac{1}{2}(s - u_*^2) \right) + \tfrac{1}{2}u_*^2.$$

Knowing that $p = (E - \frac{1}{2}u^2)\rho(\gamma - 1)$ the pressure in the first intermediate state equals:

$$p_1^* = \left(E_1^* - \tfrac{1}{2}u_*^2 \right)\rho_1^*(\gamma - 1).$$

The pressure in the second intermediate state, p_2^*, is determined similarly. We need to determine the difference between the pressures p_1^* and p_2^*:

$$P(u_*) = p_1^* - p_2^*. \tag{3.20}$$

If $P(u_*) \neq 0$ then a new guess for u_* can be obtained by using a bisection method for $P(u_*)$ and the process of finding u_1^k, u_2^k and s^k, $k = I, III$, needs to be repeated.

If $u_* = u^I(\frac{1}{2}\Delta x) = u^{III}(-\frac{1}{2}\Delta x)$ is such that $p_1^* = p^I(\frac{1}{2}\Delta x)$ and $p_2^* = p^{III}(-\frac{1}{2}\Delta x)$ are equal, hence $P(u_*) = 0$, then we define:

$$U_1^* = \varphi^I\left(\tfrac{1}{2}\Delta x \right),$$

and:

$$U_2^* = \varphi^{III}\left(-\tfrac{1}{2}\Delta x \right).$$

Since $\rho u = s\rho - Q$, conservation of momentum over a travelling wave automatically follows from conservation of mass, but since:

$$\rho E = \rho\left(\frac{h}{\gamma} + \tfrac{1}{2}u^2 \right) = \left(\frac{H}{\gamma} + \tfrac{1}{2}s^2 \right)\rho + \left(\frac{\gamma - 1}{2\gamma}Q \right)v - sQ,$$

conservation of energy does not. Over the I wave an error $Err1$ is made:

$$\tfrac{1}{2}\Delta x\left(\frac{H}{\gamma}+\tfrac{1}{2}s^2 \right)(\rho_j+\rho_1^*)-\Delta x\,s\,Q+\left(\frac{\gamma-1}{2\gamma}Q \right)\int_{-\frac{1}{2}\Delta x}^{\frac{1}{2}\Delta x} v\,d\omega = \tfrac{1}{2}\Delta x\big(\rho_j E_j+\rho_1^* E_1^*\big)+Err1, \quad (3.21)$$

and similarly, over the III wave an error $Err3$ is made.

3.2.3   The viscous Riemann solver, II wave

As with a contact wave occurring in a solution to the Euler equations, the velocity is kept constant at $u_* = u_1^* = u_2^*$ across the II wave. A profile propagating with this contact speed will be looked for. On either side of a contact the densities ρ_1^* and ρ_2^* are not equal. These will be connected through a monotone diffusion wave convecting with speed u_*. The profile is taken to be a function of the similarity variable $\omega = x - x_{j+\frac{1}{2}} - u_*(t - t_n)$:

$$\rho^{II}(\omega) = \rho_a + \rho_b\mathrm{erf}\left(\frac{\omega}{\sqrt{\mu}} \right), \qquad\qquad\qquad\qquad (3.22)$$

where $\mathrm{erf}(x) = \frac{2}{\sqrt{\pi}}\int_0^x e^{-t^2}dt$. The values ρ_a and ρ_b are such that ρ^{II} interpolates ρ_1^* and ρ_2^*:

$$\rho^{II}\left(-\tfrac{1}{2}\Delta x \right) = \rho_1^*, \qquad \rho^{II}\left(\tfrac{1}{2}\Delta x \right) = \rho_2^*.$$

As $\mu \to 0$, the profile tends to a step function with states ρ_1^* and ρ_2^* on the left and the right, moving with speed u_* which is exactly the situation for an inviscid contact. In [Wee98] this profile choice is motivated by observing the form of the solution to the convection-diffusion problem $D_t + aD_x = \nu D_{xx}$ [Liu86]. By choosing the density profile Eq. (3.22), the density is symmetric about the line $\rho = \rho(0) = \tfrac{1}{2}(\rho_1^* + \rho_2^*)$, and conservation of mass,

$$\int_{-\frac{1}{2}\Delta x}^{\frac{1}{2}\Delta x} \rho^{II}(\omega)d\omega = \tfrac{1}{2}\Delta x(\rho_1^* + \rho_2^*),$$

holds automatically. Since u is constant over the profile, momentum conservation also follows. So far, conservation of mass and momentum hold over all three wave. A pressure profile $p^{II}(\omega)$ will be constructed to ensure energy conservation.

A similarity solution for the pressure $p^{II}(\omega)$ is assumed with a profile given by the diffusion wave:

$$p^{II}(\omega) = p_* + p_0\left(\exp\left(-\frac{\omega^2}{\mu} \right) - \exp\left(-\frac{\Delta x^2}{4\mu} \right) \right), \qquad\qquad (3.23)$$

such that:

$$p^{II}\left(-\tfrac{1}{2}\Delta x\right) = p_1^* = p_*, \qquad p^{II}\left(\tfrac{1}{2}\Delta x\right) = p_2^* = p_*.$$

The function for p^{II} given in Eq. (3.23) is symmetric with a centered bump with width and height diminishing with μ to give a constant pressure profile in the limit. This function is assumed so that energy conservation over the waves can be achieved by choosing the p_0 appropriately.

Since $\rho E = \frac{p}{\gamma-1} + \frac{1}{2}\rho u^2$:

$$\int_{-\frac{1}{2}\Delta x}^{\frac{1}{2}\Delta x} \rho E \, d\omega = \frac{1}{\gamma-1}\int_{-\frac{1}{2}\Delta x}^{\frac{1}{2}\Delta x} p^{II}(\omega) \, d\omega + \int_{-\frac{1}{2}\Delta x}^{\frac{1}{2}\Delta x} \tfrac{1}{2}u^2 \, d\omega, \tag{3.24}$$

has to hold. We know that in the intermediate states $u = u_*$ is constant. Furthermore, we know that mass and momentum are conserved. Using the definition $Q = \rho v$, from Eq. (3.24) we obtain that the following must hold:

$$\int_{-\frac{1}{2}\Delta x}^{\frac{1}{2}\Delta x} \rho E \, d\omega = \frac{1}{\gamma-1}\int_{-\frac{1}{2}\Delta x}^{\frac{1}{2}\Delta x} p^{II}(\omega) \, d\omega + \int_{-\frac{1}{2}\Delta x}^{\frac{1}{2}\Delta x} \left(\tfrac{1}{2}\rho u_*^2 - u_* Q\right) d\omega, \tag{3.25}$$

however, from Eq. (3.21) we know that an error $Err1$ is made as well as an error $Err3$. In Eq. (3.25) the last integral on the right is conserved. For energy to be conserved, p_0 is chosen such that:

$$\frac{1}{\gamma-1}\int_{-\frac{1}{2}\Delta x}^{\frac{1}{2}\Delta x} p^{II}(\omega) \, d\omega = \Delta x \frac{p_*}{\gamma-1} - (Err1 + Err3),$$

where p_* is the constant value of the pressure in the intermediate states and p_0 was introduced in the pressure function Eq. (3.23) to obtain energy conservation.

3.2.4 The numerical flux

Once the Riemann problem has been solved and $\Phi(x,t)$ has been defined, the numerical flux that defines the TW scheme in the finite volume context is given by:

$$H_0^i(U_j, U_{j+1}) = \frac{1}{\triangle t}\int_{t_n}^{t_{n+1}} (F(\Phi^i) - \mu G(\Phi^i)_x)(x_{j+\frac{1}{2}}, t)dt, \tag{3.26}$$

where $i = I, II, III$.

We will start computing H_0 in the first and third fields, where $\Phi^i(x,t) = \varphi^i(\omega)$ are travelling wave solutions to Eq. (3.2) with μ replaced by $\tilde{\mu}$. Substituting $\varphi^i(\omega)$ into Eq. (3.2) with μ replaced by $\tilde{\mu}$ and integrating, we obtain:

$$-s\varphi^i + F(\varphi^i) = \tilde{\mu}\frac{dG(\varphi^i)}{d\omega} + k,$$

where k is an integration constant which is determined by taking the limit $\omega \to -\infty$ for then $-s\varphi_1 + F(\varphi_1) = k$, where φ_1 is a constant state of the profile φ at $-\infty$. It then follows that:

$$F(\Phi^i) - \mu G(\Phi^i)_x = F(\varphi_1) + s(\varphi^i - \varphi_1) + (\tilde{\mu} - \mu)\frac{dG(\varphi^i)}{d\omega}. \tag{3.27}$$

Using Eq. (3.26):

$$H_0^i = \frac{1}{\Delta t} \int_{t_n}^{t_{n+1}} \left(F(\varphi_1) - s\varphi_1 \right) dt + \frac{1}{\Delta t} \int_{t_n}^{t_{n+1}} s\varphi^i + (\tilde{\mu} - \mu)\frac{dG}{d\omega}(\varphi^i)\, dt.$$

Use $\omega = -s(t - t_n)$ at $x = x_j$ to transform the second integral. We obtain:

$$H_0^i = \frac{1}{\Delta t} \int_{t_n}^{t_{n+1}} \left(F(\varphi_1) - s\varphi_1 \right) dt - \frac{1}{s\Delta t} \int_0^{-s\Delta t} s\varphi^i + (\tilde{\mu} - \mu)\frac{dG}{d\omega}(\varphi^i)\, d\omega,$$

resulting in:

$$H_0^i = F(\varphi_1) - s\varphi_1 + \frac{\mu - \tilde{\mu}}{s\Delta t}(G(\varphi_s) - G(\varphi_0)) - \frac{1}{\Delta t} \int_0^{-s\Delta t} \varphi^i(\omega) d\omega, \tag{3.28}$$

with $\varphi_s = \varphi(-s\Delta t)$ and $\varphi_0 = \varphi(0)$. We have used travelling waves to approximate the exact solution, so φ_s and φ_0 approximate $u_s = u(x_j, t_{n+1})$ and $u_0 = u(x_j, t_n)$ respectively. It therefor holds that $v_s = s - \varphi_s$ and $v_0 = s - \varphi_0$. From Eq. (3.3) and Eq. (3.8), we obtain:

$$G(\varphi_s) - G(\varphi_0) = \frac{\gamma + 1}{2\gamma}(v_s - v_0) \begin{bmatrix} 0 \\ -1 \\ -s \end{bmatrix}.$$

To evaluate the flux integrals in Eq. (3.28), using Eq. (3.6a) and Eq. (3.8), it is only necessary to know the integral formulae for $\rho(\omega)$ and $v(\omega)$. From Eq. (3.10) and by using the definition $Q = \rho u$ we obtain:

$$\rho d\omega = \frac{\tilde{\mu}}{(v_1 - v)(v - v_2)}\, dv,$$

resulting in:

$$\frac{1}{\Delta t} \int_{\omega_a}^{\omega_b} \rho d\omega = \frac{1}{\Delta t} \int_{v_a}^{v_b} \frac{\tilde{\mu}}{(v_1 - v)(v - v_2)}\, dv$$
$$= \frac{\tilde{\mu}}{\Delta t(v_a - v_2)} \left(\ln\left(\left| \frac{v_b - v_2}{v_a - v_2} \right| \right) - \ln\left(\left| \frac{v_b - v_1}{v_a - v_1} \right| \right) \right).$$

Also from Eq. (3.10):

$$v d\omega = \frac{\tilde{\mu} v^2}{Q(v_1 - v)(v - v_2)}\, dv,$$

resulting in:

$$\frac{1}{\Delta t} \int_{\omega_a}^{\omega_b} v d\omega = \frac{1}{\Delta t} \int_{v_a}^{v_b} \frac{\tilde{\mu} v^2}{Q(v_1 - v)(v - v_2)}\, dv$$
$$= \frac{\tilde{\mu}}{Q\Delta t}(v_a - v_b) + \frac{\tilde{\mu}}{\Delta t Q(v_1 - v_2)} \left(v_2^2 \ln\left(\left| \frac{v_b - v_2}{v_a - v_2} \right| \right) - v_1^2 \ln\left(\left| \frac{v_b - v_1}{v_a - v_1} \right| \right) \right),$$

where ω_a and ω_b are arbitrary and $v_a = v(\omega_a)$ and $v_b = v(\omega_b)$.

If $\tilde{\mu}$ is negative, so $\tilde{\mu} = -\mu$, the characteristic speeds on the left and right of $\varphi(\omega)$ need to be checked to see whether the rarefaction is sonic. If $u_j - a_j < 0 < u_1^* - a_1^*$ on wave I or $u_2^* + a_2^* < 0 < u_{j+1} + a_{j+1}$ on wave III, then the respective rarefaction wave is sonic and a sonic entropy fix to the H_0^{TW} flux is made. As in the viscous Burgers case (see Section 2.2.3), we integrate Eq. (3.27) until the sonic point $\omega = \bar{\omega}$ is encountered, after which the profile of the travelling wave is kept stationary and the flux calculation is continued as if the wave speed were zero. From Eqs. (3.26) and (3.27), using $\omega = -s(t - t_n)$ at $x = x_j$ and employing the entropy fix, we obtain:

$$
H_0 = -\frac{1}{s\Delta t} \int_0^{\bar{\omega}} \left(F(\varphi_1) + s(\varphi - \varphi_1) - 2\mu \frac{dG}{d\omega}(\varphi) \right) d\omega
$$
$$
- \frac{1}{s\Delta t} \int_{\bar{\omega}}^{-s\Delta t} \left(F(\bar{\varphi}) - \mu \frac{dG}{d\omega}(\bar{\varphi}) \right) d\omega,
$$

which, after evaluating the integrals, results in:

$$
H_0^i = \frac{2\mu}{s\Delta t}(G(\bar{\varphi}) - G(\varphi_0)) - \frac{\bar{\omega}}{s\Delta t}(F(\varphi_1) - s\varphi_1) - \frac{1}{\Delta t} \int_0^{\bar{\omega}} \varphi(\omega) d\omega + \left(1 + \frac{\bar{\omega}}{s\Delta t} \right) \left(F(\bar{\varphi}) - \mu \frac{dG}{d\omega}(\bar{\varphi}) \right).
$$

The term $dG/d\omega$ is found as follows: by using Eqs. (3.3) and (3.8) we find:

$$
\frac{dG}{d\omega}(\varphi) = \frac{\gamma + 1}{2\gamma} \begin{bmatrix} 0 \\ \frac{du}{d\omega} \\ \frac{d}{d\omega}(H - \frac{1}{2}v^2 + \frac{1}{2}u^2) \end{bmatrix}.
$$

Using $u = s - v$ and $du/d\omega = -dv/d\omega$ we obtain:

$$
\frac{dG}{d\omega}(\varphi) = \frac{\gamma + 1}{2\gamma} \frac{dv}{d\omega} \begin{bmatrix} 0 \\ -1 \\ -s \end{bmatrix},
$$

The numerical flux with the entropy fix replaces Eq. (3.28) if the sonic point $\bar{\omega}$ lies between 0 and $-s\Delta t$. The sonic point is where $\bar{u} = \bar{a}$ for wave I and where $\bar{u} = -\bar{a}$ for wave III, where a is the speed of sound. For a polytropic gas, $a^2 = \frac{\gamma p}{\rho} = (\gamma - 1)h$, so we solve:

$$
\bar{u}^2 = \bar{a}^2 = (\gamma - 1)\bar{h} = (\gamma - 1)\left(H - \frac{1}{2}\bar{v}^2 \right)
$$
$$
\iff \frac{\gamma + 1}{2}\bar{u}^2 - s(\gamma - 1)\bar{u} - (\gamma - 1)\left(H - \frac{1}{2}s^2 \right) = 0,
$$

(3.29)

for $\bar{u} < 0$ for wave I and for $\bar{u} > 0$ for wave III. Having $\bar{u}$, the value of $\bar{\omega}$ is calculated from Eq. (3.14).

Next we look at the II wave. The velocity in the intermediate states is constant and equal to u_*. Therefor, define ω as: $\omega = x - x_{j+\frac{1}{2}} - u_*(t - t_n)$. Using this definition, so $d/dx = d/d\omega$, $d/dt = -u_* d/d\omega$ and $\omega = -u_*(t - t_n)$ in $x = x_{j+\frac{1}{2}}$, the integral in Eq. (3.26) is transformed to an integral over ω:

$$
\frac{1}{\Delta t} \int_{t_n}^{t_{n+1}} (F(\Phi^{II}) - \mu G(\Phi^{II})_x)(x_{j+\frac{1}{2}}, t) \, dt = \frac{-1}{u_*\Delta t} \int_0^{-u_*\Delta t} F(\varphi^{II}) - \mu \frac{d}{d\omega}G(\varphi^{II}) \, d\omega.
$$

Evaluating the integral over $\frac{d}{d\omega} G(\varphi^{II})$ we obtain the contribution of the contact field:

$$H_0^{II} = \frac{-1}{u_* \Delta t} \int_0^{-u_* \Delta t} F(\varphi^{II})(\omega) d\omega + \frac{\mu}{u_* \Delta t}(G(\varphi_s) - G(\varphi_0)),$$

where $\varphi_s = \varphi(-u_* \Delta t), \varphi_0 = \varphi(0)$. Across the contact, u_* is constant, so one need only calculate the integrals of ρ^{II} and p^{II} to obtain $\int F$.

The ODE, Eq. (3.10) gives the derivative of $v(\omega)$, and from Eq. (3.6a) and Eq. (3.8), the derivatives of the components of φ are computed as follows:

$$\frac{d\rho}{d\omega} = \frac{d}{d\omega}\left(\frac{Q}{v}\right) = -\frac{Q}{v^2}\frac{dv}{d\omega}. \tag{3.30}$$

The derivative $d(\rho u)/d\omega$ is determined as:

$$\frac{d(\rho u)}{d\omega} = u\frac{d\rho}{d\omega} + \rho\frac{du}{d\omega} = (s-v)\frac{d\rho}{d\omega} - \rho\frac{dv}{d\omega}.$$

Using Eq. (3.30) and the definition $Q = \rho v$:

$$(s-v)\frac{d\rho}{d\omega} - \rho\frac{dv}{d\omega} = \left(s - v + \frac{\rho v^2}{Q}\right)\frac{d\rho}{d\omega} = s\frac{d\rho}{d\omega},$$

so:

$$\frac{d(\rho u)}{d\omega} = s\frac{d\rho}{d\omega}, \tag{3.31}$$

The derivative $d(\rho E)/d\omega$ is determined as:

$$\frac{d(\rho E)}{d\omega} = \left(\frac{h}{\gamma} + \tfrac{1}{2}s^2\right)\frac{d\rho}{d\omega} + \left(\frac{\gamma+1}{2\gamma}Q\right)\frac{dv}{d\omega}. \tag{3.32}$$

3.3   The DG-TW scheme for 1D Navier-Stokes equations

In this section we will discuss the modifications that have to be made to the TW scheme by Weekes so that it can be applied in a DG context.

In a DG context, we only require finding the travelling waves φ^I, φ^{II} and φ^{III}. We do not need to determine integral terms as given in Section 3.2.4. The TW scheme by Weekes is developed for a finite volume scheme. In such a scheme the discontinuities do not arise on the vertices contrary to DG schemes. To make the scheme applicable to DG, we consider the vertex x_j in which the solution has a discontinuity due to the discontinuous nature of the approximations. Since in our DG approximation we use linear basis functions, we need to be careful as how to define the interpolation and conservation requirements. As explained in the scalar case, we do not use the traces at the face j, but the means of the approximation in each cell adjacent to face j. Defining ω as $\omega = x - x_j - s_j(t - t_n)$, we impose the following requirements:

For the I wave the interpolation requirement is:

$$\varphi^I\left(-\tfrac{1}{2}\Delta x\right) = \overline{U}_{j-1}, \qquad u^I\left(\tfrac{1}{2}\Delta x\right) = u_*,$$

and the conservation requirement:

$$\int_{-\frac{1}{2}\Delta x}^{\frac{1}{2}\Delta x} \rho^I(\omega)\, d\omega = \tfrac{1}{2}\Delta x(\bar{\rho}_{j-1} + \rho_1^*).$$

Similarly, over wave III, we require:

$$\varphi^{III}\left(\tfrac{1}{2}\Delta x\right) = \overline{U}_j, \qquad u^{III}\left(-\tfrac{1}{2}\Delta x\right) = u_*,$$

and:

$$\int_{-\frac{1}{2}\Delta x}^{\frac{1}{2}\Delta x} \rho^{III}(\omega)\, d\omega = \tfrac{1}{2}\Delta x(\rho_2^* + \bar{\rho}_j).$$

With these requirements we can solve a similar system as is done by Weekes, given a middle velocity $u_* = u_1^m = u_2^m$, to obtain the travelling waves φ^I and φ^{III}:
For the I-wave we need to solve the system consisting of Eq. (3.11) and:

$$\frac{\tilde{\mu}}{Q(u_2^I - u_1^I)}\left((s^I - u_2^I)\ln\left(\left|\frac{u_2^I - u_*}{u_2^I - \bar{u}_{j-1}}\right|\right) - (s^I - u_1^I)\ln\left(\left|\frac{u_1^I - u_*}{u_1^I - \bar{u}_{j-1}}\right|\right)\right) = \Delta x, \quad (3.33)$$

$$\frac{\tilde{\mu}}{(u_2^I - u_1^I)}\left(\ln\left(\left|\frac{u_2^I - u_*}{u_2^I - \bar{u}_{j-1}}\right|\right) - \ln\left(\left|\frac{u_1^I - u_*}{u_1^I - \bar{u}_{j-1}}\right|\right)\right) = \tfrac{1}{2}\Delta x(\bar{\rho}_{j-1} + \rho_1^*), \quad (3.34)$$

for u_1^I, u_2^I and s^I.
Similarly, for the III-wave the system consisting of Eq. (3.11) and:

$$\frac{\tilde{\mu}}{Q(u_2^{III} - u_1^{III})}\left((s^{III} - u_2^{III})\ln\left(\left|\frac{u_2^{III} - u_*}{u_2^{III} - \bar{u}_j}\right|\right) - (s^{III} - u_1^{III})\ln\left(\left|\frac{u_1^{III} - u_*}{u_1^{III} - \bar{u}_j}\right|\right)\right) = -\Delta x,$$
$$(3.35)$$

$$\frac{\tilde{\mu}}{(u_2^{III} - u_1^{III})}\left(\ln\left(\left|\frac{u_2^{III} - \bar{u}_j}{u_2^{III} - u_*}\right|\right) - \ln\left(\left|\frac{u_1^{III} - \bar{u}_j}{u_1^{III} - u_*}\right|\right)\right) = \tfrac{1}{2}\Delta x(\bar{\rho}_j + \rho_2^*). \quad (3.36)$$

needs to be solved for u_1^{III}, u_2^{III} and s^{III}. If u_* is such that $p_1^m = p^I(\tfrac{1}{2}\Delta x)$ and $p^{III}(-\tfrac{1}{2}\Delta x) = p_2^m$ are equal we define $U_1^m = \varphi^I(\tfrac{1}{2}\Delta x)$ and $U_2^m = \varphi^I(-\tfrac{1}{2}\Delta x)$. As in the previous section, there is no conservation of energy so we determine $Err1$ as in Eq. (3.21). The conservation error over the III-wave. $Err3$ follows from a similar equation.

For the flux calculation we seek a solution for U in $x = x_j$ at $t = t_n$. In the above, the domain has been scaled to $[-\Delta x/2, \Delta x/2]$ with $-\Delta x/2$ corresponding to $x_{j-\frac{1}{2}}$, $\Delta x/2$ to $x_{j+\frac{1}{2}}$ and 0 to x_j. With u_1, u_2 and s known for waves I and III we can determine $u^I(0) = s^I - \varphi^I(0)$ and $u^{III}(0) = s^{III} - \varphi^{III}(0)$ by solving (see also Eq. (3.14)):

$$\frac{\tilde{\mu}}{Q(u_2^I - u_1^I)}\left((s^I - u_2^I)\ln\left(\left|\frac{u_2^I - u^I(0)}{u_2^I - \bar{u}_{j-1}}\right|\right) - (s^I - u_1^I)\ln\left(\left|\frac{u_1^I - u^I(0)}{u_1^I - \bar{u}_{j-1}}\right|\right)\right) = \tfrac{1}{2}\Delta x, \quad (3.37)$$

$$\frac{\tilde{\mu}}{Q(u_2^{III} - u_1^{III})} \left((s^{III} - u_2^{III}) \ln \left(\left| \frac{u_2^{III} - u^{III}(0)}{u_2^{III} - \bar{u}_j} \right| \right) - (s^{III} - u_1^{III}) \ln \left(\left| \frac{u_1^{III} - u^{III}(0)}{u_1^{III} - \bar{u}_j} \right| \right) \right)$$
$$= -\tfrac{1}{2} \Delta x, \quad (3.38)$$

respectively. Knowing $u^I(0)$ and $u^{III}(0)$ the other variables, ρ, p and E, at $\omega = 0$ for each wave can be calculated using Eq. (3.6a), (3.8) and the definitions of internal- and total energy:

$$e = \frac{p}{\rho(\gamma - 1)}, \quad E = e + \tfrac{1}{2} u^2.$$

The travelling wave φ^{II} is similar to that found for the finite volume case, with the differences being that ω is defined as $\omega = x - x_j - s_j(t - t_n)$ and we use the means of the solutions instead of the traces. On the II-wave we know that the velocity is constant and equal to u_*. Using Eq. (3.22) and (3.23) and the definitions of internal- and total energy, $\rho^{II}(0)$, $u^{II}(0)$, $p^{II}(0)$, and $E^{II}(0)$ can be determined.

Derivatives of the components of U in $\omega = 0$ on each wave are computed analogously to the computation discussed in Section 3.2.4, but using the means of the solutions instead of the traces. We now have enough information to determine the flux in $\omega = 0$ for each wave:

$$H_k(U_L, U_R)(0) = F(U^k(0)) - \mu \frac{\gamma + 1}{2\gamma} \frac{dG}{d\omega}(U^k(0)), \quad \text{for } k = I, II, III. \qquad (3.39)$$

In [Wee98] the fluxes are calculated via a standard flux-difference splitting formulation. In our case this results in:

$$H(\overline{U}_{j-1}, \overline{U}_j) = F(\overline{U}_{j-1}) + \left(H_I(\overline{U}_{j-1}, U_1^*)(0) - F(\overline{U}_{j-1}) \right) + \left(H_{II}(U_1^*, U_2^*)(0) - F(U_1^*) \right)$$
$$+ \left(H_{III}(U_2^*, \overline{U}_j)(0) - F(U_2^*) \right). \quad (3.40)$$

If an entropy fix is needed we do not consider the solution at $\omega = 0$, but in the sonic point $\omega = \bar{\omega}$ (see Eq. 3.29). Summarizing, the algorithm for the flux computation is as follows:

1. Guess the middle velocity $u_* = u_1^m = u_2^m$.

2. Solve the system Eq. (3.11), (3.33) and (3.34) for u_1^I, u_2^I and s^I and the system Eq. (3.11), (3.35) and (3.36) for u_1^{III}, u_2^{III} and s^{III} using Newton's method (see also Appendix C).

3. If $P(u_*) = p_1^m - p_2^m \neq 0$, then use a bisection method for the equation $P(u_*) = 0$ (Eq. (3.20)) is used to obtain a new guess for u_* and return to step 2.

4. Solve Eq. (3.37) and Eq. (3.38) using a Newton method to obtain $u^I(0)$ and $u^{III}(0)$, respectively. $\rho^k(0)$, $p^k(0)$ and $E^k(0)$ with $k = I, III$ then can be computed.

5. Determine $Err1$ from Eq. (3.21). $Err3$ follows from a similar equation.

6. The variables on the II-wave in $\omega = 0$ can be determined using Eq. (3.22) and (3.23) and knowing that $u = u_*$ is constant.

7. Determine the derivatives of the variables in $\omega = 0$ using Eq.(3.30), (3.31) and (3.32).

8. Determine the fluxes in $\omega = 0$ on each wave using Eq. (3.39).

9. The travelling wave flux can be computed using Eq. (3.40).

3.4   Numerical results

3.4.1   Test case confirmation

In this section we consider a test cases described in [Wee98]. This test case has a very small viscosity coefficients, so the goal of this section is to show that viscosity plays a significant role in the solution. We use the method of Bassi and Rebay for the Navier-Stokes equations, Eq. (3.2), and compare with classic DG-FEM for the Euler equations using a stabilization operator to prevent oscillations around solutions with sharp gradients [vdVvdV02a] and the HLLC approximate Riemann solver. In the implementation we take the term $(\gamma + 1)/(2\gamma)$ in Eq. (3.2) equal to 4/3, so that Eq. (3.1) and Eq. (3.2) are the same. Furthermore, each element of the approximate solution vector are such that they belong to the space V_h (Eq. (2.4)).

We consider the following test case:

$x \in \Omega = [0,1]$, $\mu = 0.04$, $\Delta x = 0.02$ with initial data:

$$
\begin{aligned}
(\rho_L \ u_L \ p_L) &= (1 \quad 2.36643 \quad 1), & \text{for } x < 0.4 \\
(\rho_R \ u_R \ p_R) &= (2.66667 \quad 0.88741 \quad 4.5), & \text{for } x > 0.4
\end{aligned}
\tag{3.41}
$$

The solution of the density, $\rho(x,t)$, velocity, $u(x,t)$, and the total energy, $E(x,t)$, at time $t = 1.12$ are depicted in Figure 12.

For this test case, the following parameters are constant: CFL number $= 0.5$, diffusion number $= 0.02$, stabilization factor in the method of Bassi and Rebay $\eta = 3.5$ and a ratio of specific heats $\gamma = 1.4$. As can be seen in Figures 12, these test cases are suitable for the Navier-Stokes equations since the viscosity plays a significant part in the final solution.

3.4.2   Testing the DG-TW flux on the mass-equation

The travelling wave flux for DG-FEM as presented in Section 3.3 will be tested in this section for the Navier-Stokes equations. We do not consider entropy violating shocks. At this moment it is not possible to do more than four time steps using the DG-TW flux on all equations. Therefore, we only use the DG-TW flux for the mass equation. The method of Bassi and Rebay is used for the momentum and energy equation as well as for situations where an entropy violating shock occurs. It is also not possible yet to consider the test case from Section 3.4.1. Instead, we consider the following test case:

$x \in \Omega = [0,1]$, $\mu = 0.01$, $\Delta x = 0.02$ with initial data:

$$
\begin{aligned}
(\rho_L \ u_L \ p_L) &= (1.25 \quad 1.85 \quad 1.656875), & \text{for } x < 0.4 \\
(\rho_R \ u_R \ p_R) &= (1.45 \quad 1.65 \quad 2.046675), & \text{for } x > 0.4
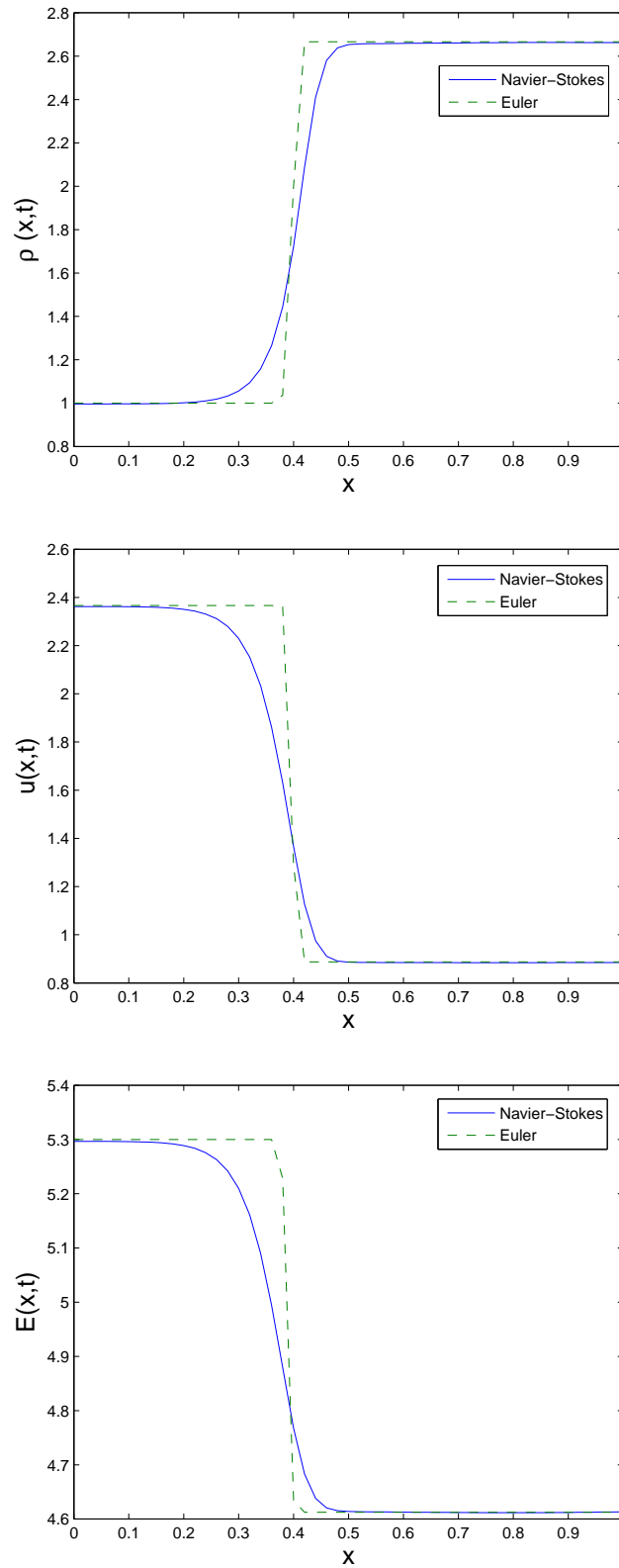\end{aligned}
\tag{3.42}
$$

Figure 12: Solutions of the Navier-Stokes equations and the Euler equations for test case Eq. (3.41). Used parameters: $\mu = 0.04$ and $\Delta x = 0.02$. The solution is depicted at time $t = 1.12$.

The solution of the density, $\rho(x,t)$, velocity, $u(x,t)$, and the total energy, $E(x,t)$, are depicted in Figures 13, 14 and 15 at time steps 5, 20, 40 and 60. It is not possible yet to do more than 60 time steps. For this test case, the following parameters are constant: CFL number CFL = 0.5, diffusion number DN = 0.02, stabilization factor in the method of Bassi and Rebay $\eta = 3.5$ and the ratio of specific heats $\gamma = 1.4$, where CFL, DN and η are found by trial and error. We see that the total energy starts to overshoot due to the small difference in the density solution between the DG-TW and Bassi and Rebay method. As mentioned in Section 3.3 various numbers of Newton iterations had to be performed. Although we know in which domain the solution has to lie, and so we can implement restrictions which the solution has to satisfy, the Newton iterations form the biggest problem in this method. It is possible that asymptotes are present in the domain in which we seek a solution resulting after a certain number of iterations in solutions which are not desired. The Newton iterations are also very costly since they have to be performed more than once (in step 3 of the summary of the algorithm in Section 3.3, u_* has to be such that the pressures p_1^m and p_2^m are equal) and are probably more expensive than the lifting operators and viscous contributions in the Bassi and Rebay method.

Remark. Since at time step 60 we are only at time $t = 0.022$, the solution of the Bassi and Rebay method still contains small peaks. These peaks dissappear as the number of time steps is increased.
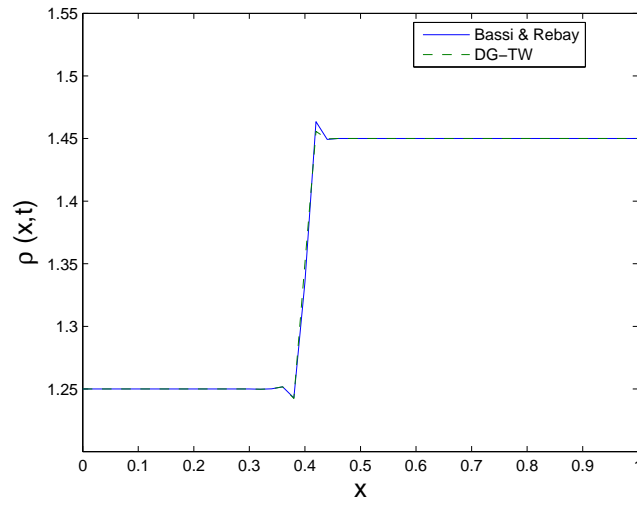
(a) 5th time step.
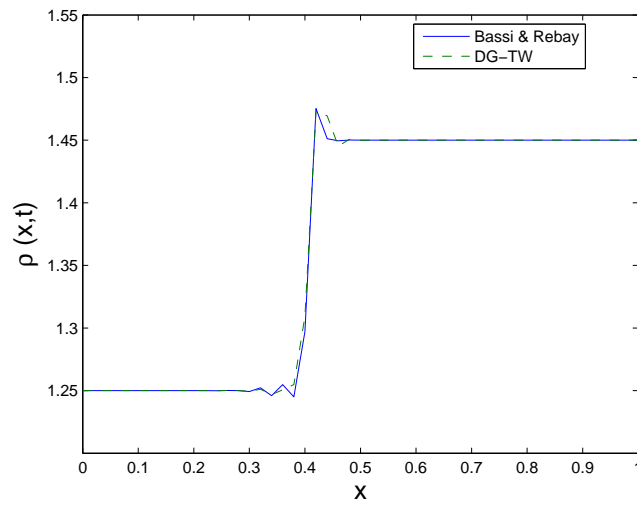
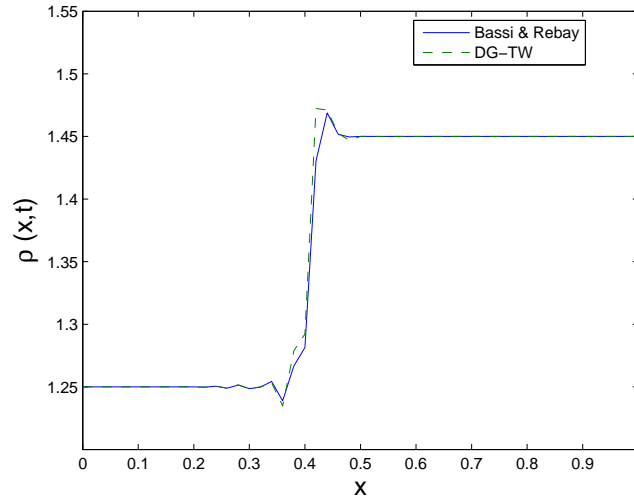(b) 20th time step.
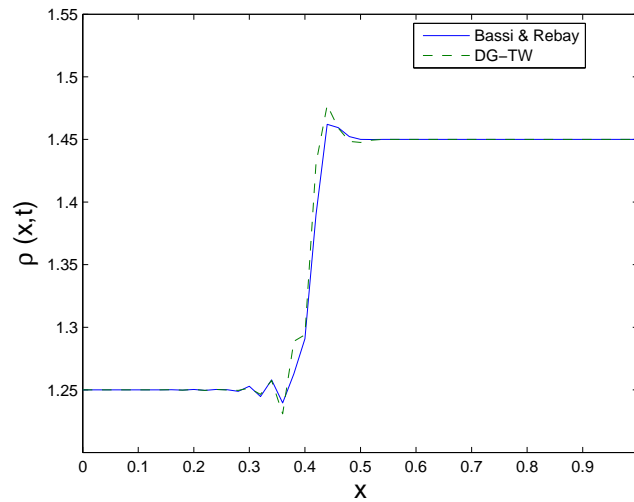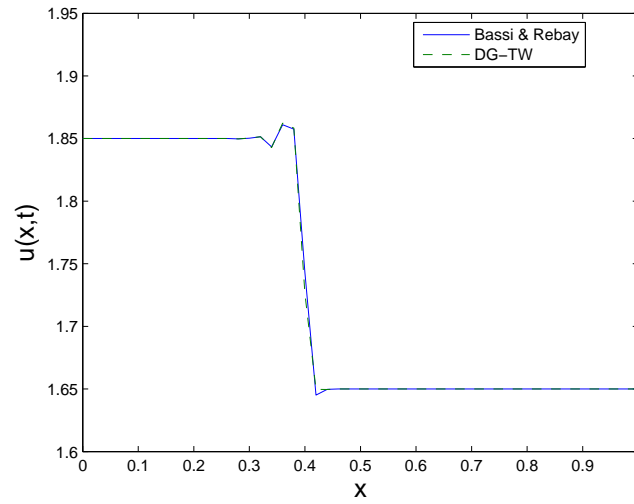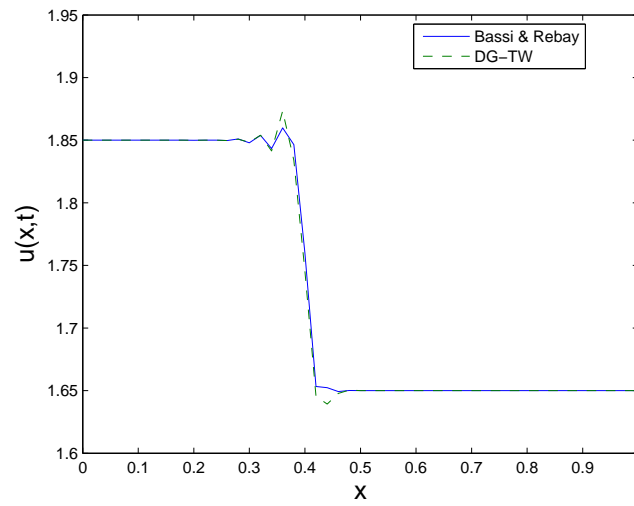
(c) 40$^{\text{th}}$ time step.

(d) 60$^{\text{th}}$ time step.

Figure 13: Results of the density solution determined with DG-TW compared to results determined with the method of Bassi and Rebay. The Weekes flux was only used for the mass equation. The method of Bassi and Rebay was used for the momentum and energy equation. Used parameters: CFL number = 0.5, diffusion number = 0.02, number of cells = 50, viscosity coefficient $\mu = 0.01$, stabilization factor for the method of Bassi and Rebay $\eta = 3.5$. Results determined for 5, 20, 40 and 60 time steps.

(a) 5th time step.

(b) 20th time step.

(c) 40$^{\text{th}}$ time step.

(d) 60$^{\text{th}}$ time step.

Figure 14: Results of the velocity solution determined with DG-TW compared to results determined with the method of Bassi and Rebay. The Weekes flux was only used for the mass equation. The method of Bassi and Rebay was used for the momentum and energy equation. Used parameters: CFL number = 0.5, diffusion number = 0.02, number of cells = 50, viscosity coefficient $\mu = 0.01$, stabilization factor for the method of Bassi and Rebay $\eta = 3.5$. Results determined for 5, 20, 40 and 60 time steps.
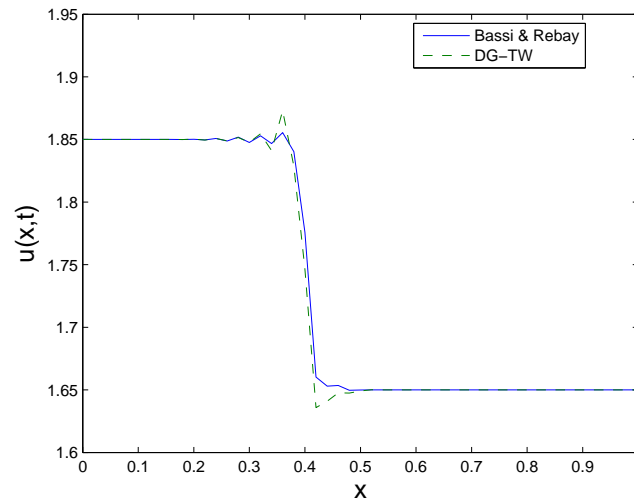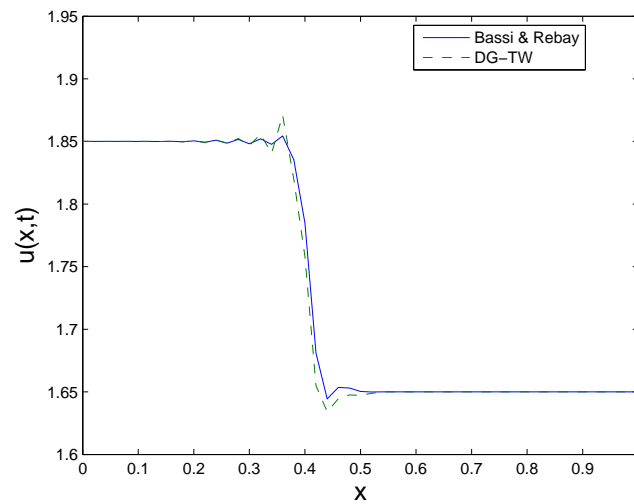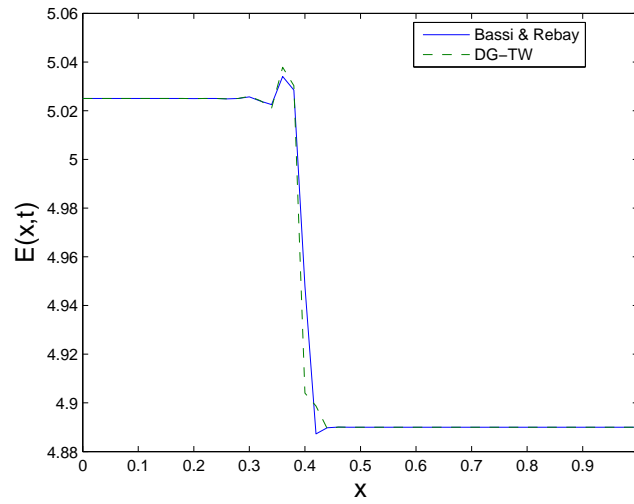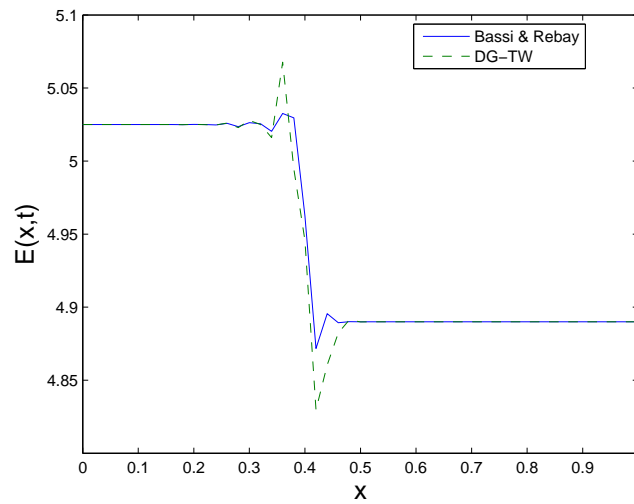
(a) 5th time step.

(b) 20th time step.

(c) 40$^{\text{th}}$ time step.

(d) 60$^{\text{th}}$ time step.

Figure 15: Results of the total energy solution determined with DG-TW compared to results determined with the method of Bassi and Rebay. The Weekes flux was only used for the mass equation. The method of Bassi and Rebay was used for the momentum and energy equation. Used parameters: CFL number = 0.5, diffusion number = 0.02, number of cells = 50, viscosity coefficient $\mu = 0.01$, stabilization factor for the method of Bassi and Rebay $\eta = 3.5$. Results determined for 5, 20, 40 and 60 time steps.
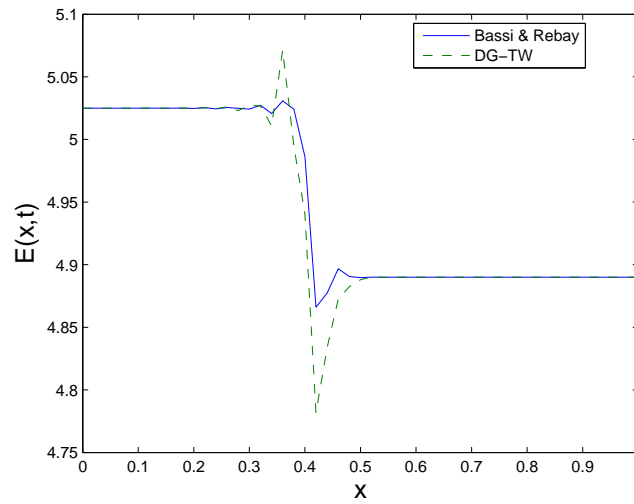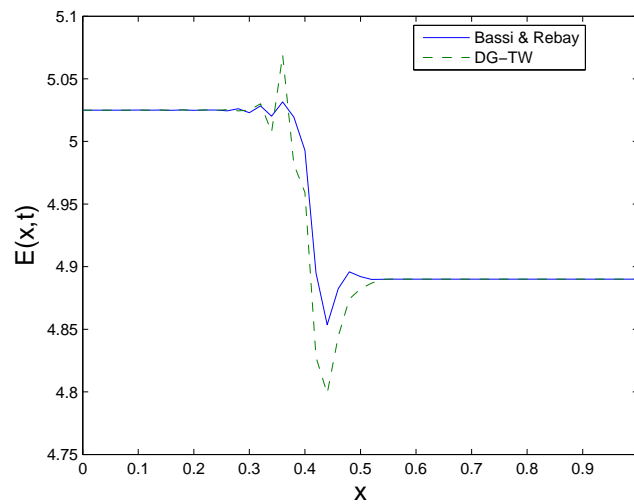
3.5 Simplifying the system

In the previous section we saw that it was not easy to obtain a solution to the 1D Navier-Stokes equations. The main problem is solving the system given by Eq. (3.11), (3.33) and (3.34) and the system given by Eq. (3.11), (3.35) and (3.36). In this Section we will simplify these equations in order to be able to solve them more efficiently.

3.5.1 Analysis of the shock speed s

In Appendix C we explain how to find the following expression for s by solving Eq. (3.11):

$$s_{\pm} = \frac{-b \pm \sqrt{b^2 - 4ac}}{2a},$$

where:

$$a = 1 - \tfrac{1}{2}\beta, \ b = -u_1 - u_2 + \beta\bar{u}_{j-1}, \ c = u_1 u_2 - \beta\gamma\overline{E}_{j-1} - \tfrac{1}{2}(1 - \gamma)\beta\bar{u}_{j-1}^2.$$

and:

$$\beta = \frac{2(\gamma - 1)}{\gamma + 1}.$$

Define the following small parameters:

$$\varepsilon_1 = u_1 - u_2, \ \varepsilon_2 = \bar{u}_{j-1} - u_2,$$

then:

$$\begin{aligned}
\sqrt{b^2 - 4ac} &= \sqrt{(u_1 - u_2)^2 + 2\beta(u_1 - \bar{u}_{j-1})(u_2 - \bar{u}_{j-1}) + 2\beta\gamma(2 - \beta)\left(\overline{E}_{j-1} - \tfrac{1}{2}\bar{u}_{j-1}^2\right)} \\
&= \sqrt{\varepsilon_1^2 - 2\beta(\varepsilon_1 - \varepsilon_2)\varepsilon_2 + 2\beta\gamma(2 - \beta)\left(\overline{E}_{j-1} - \tfrac{1}{2}\bar{u}_{j-1}^2\right)} \\
&\approx \sqrt{2\beta\gamma(2 - \beta)\left(\overline{E}_{j-1} - \tfrac{1}{2}\bar{u}_{j-1}^2\right)} + \mathcal{O}(\varepsilon).
\end{aligned}$$

We can therefore approximate the shock speed as:

$$s \approx \frac{(u_1 + u_2) - \beta\bar{u}_{j-1} \pm \sqrt{2\beta\gamma(2 - \beta)\left(\overline{E}_{j-1} - \tfrac{1}{2}\bar{u}_{j-1}^2\right)}}{2 - \beta},$$

which is an expression for the shock speed that is linear in u_1 and u_2. We continue by using the following expression for s:

$$s = \xi(u_1 + u_2) + A, \tag{3.43}$$

with:

$$\xi = \frac{1}{2 - \beta}, \quad A = \frac{-\beta\bar{u}_{j-1} \pm \sqrt{2\beta\gamma(2 - \beta)\left(\overline{E}_{j-1} - \tfrac{1}{2}\bar{u}_{j-1}^2\right)}}{2 - \beta}. \tag{3.44}$$

3.5.2   Simplifying Eq. (3.33) and (3.34)

We will simplify Eq. (3.33) and (3.34) using Taylor series expansions. Remember that $u_1 > \bar{u}_{j-1} > u_* > u_2$ in the case of a shock wave. We assume a smooth solution for the flow and therefore we take $|u_1 - u_2| \ll 1$ (this can always be achieved for smooth solutions by decreasing the mesh width, Δx). We introduce the following small parameter:

$$\varepsilon = u_2 - u_1. \tag{3.45}$$

Consider first Eq. (3.34). Substituting ε into Eq. (3.34) we can write Eq. (3.34) as :

$$\ln\left(\left|\frac{u_2 - u_*}{u_2 - \bar{u}_{j-1}}\right|\left|\frac{u_1 - \bar{u}_{j-1}}{u_1 - u_*}\right|\right) = \frac{\varepsilon\Delta x}{2\tilde{\mu}}(\bar{\rho}_{j-1} + \rho_1^*) \tag{3.46}$$

We know that $\rho_1^* = Q/(s - u_*)$ and $Q = \bar{\rho}_{j-1}(s - \bar{u}_{j-1})$ so, from Eq. (3.46):

$$\left|\frac{u_2 - u_*}{u_2 - \bar{u}_{j-1}}\right|\left|\frac{u_1 - \bar{u}_{j-1}}{u_1 - u_*}\right| = \exp\left(\frac{\varepsilon\Delta x}{2\tilde{\mu}}\bar{\rho}_{j-1}\left(1 + \frac{s - \bar{u}_{j-1}}{s - u_*}\right)\right).$$

Assume that $\varepsilon\Delta x/\tilde{\mu}$ is small, then, using Taylor series expansions, we find:

$$\left|\frac{u_2 - u_*}{u_2 - \bar{u}_{j-1}}\right|\left|\frac{u_1 - \bar{u}_{j-1}}{u_1 - u_*}\right| \approx 1 + \frac{\varepsilon\Delta x}{2\tilde{\mu}}\bar{\rho}_{j-1}\left(1 + \frac{s - \bar{u}_{j-1}}{s - u_*}\right). \tag{3.47}$$

We know that in the case of a shock $u_1 > \bar{u}_{j-1} > u_* > u_2$ (or in the case of a rarefaction $u_1 < \bar{u}_{j-1} < u_* < u_2$) so we can omit the absolute bars. By using the expression for s given by Eq. (3.43) and by introducing the constant κ defined as:

$$\kappa = \frac{\Delta x}{2\tilde{\mu}}\bar{\rho}_{j-1}, \tag{3.48}$$

we can write Eq. (3.47) as:

$$(u_2 - u_*)(u_1 - \bar{u}_{j-1}) = (u_2 - \bar{u}_{j-1})(u_1 - u_*)\left(1 + \kappa(u_2 - u_1)\left(1 + \frac{\xi(u_1 + u_2) + A - \bar{u}_{j-1}}{\xi(u_1 + u_2) + A - u_*}\right)\right),$$

or:

$$u_2\big(u_1 - \bar{u}_{j-1}\big) + \big(u_*(\bar{u}_{j-1} - u_1)\big) = \left(u_2\big(u_1 - u_*\big) + \big(\bar{u}_{j-1}(u_* - u_1)\big)\right)\cdot$$
$$\left(\frac{2\kappa\xi u_2^2 + \big(\xi + 2\kappa A - \kappa(u_* + \bar{u}_{j-1})\big)u_2 + \xi u_1 + A - u_* - 2\kappa\xi u_1^2 - 2\kappa A u_1 + \kappa u_1(u_* + \bar{u}_{j-1})}{\xi u_2 + \xi u_1 + A - u_*}\right), \tag{3.49}$$

where ξ and A are defined in Eq. (3.44). For notational purposes introduce the following parameters:

$$\begin{aligned}
\alpha_1 &= u_1 - \bar{u}_{j-1}, & \alpha_2 &= u_*(\bar{u}_{j-1} - u_1), \\
\alpha_3 &= u_1 - u_*, & \alpha_4 &= \bar{u}_{j-1}(u_* - u_1), \\
\alpha_5 &= \xi + 2\kappa A - \kappa(u_* + \bar{u}_{j-1}), & \alpha_6 &= \xi u_1 + A - u_* - 2\kappa\xi u_1^2 - 2\kappa A u_1 + \kappa u_1(u_* + \bar{u}_{j-1}), \\
\alpha_7 &= \xi u_1 + A - u_*,
\end{aligned}$$

then Eq. (3.49) is equivalent to:

$$u_2\alpha_1 + \alpha_2 = (u_2\alpha_3 + \alpha_4)\frac{2\kappa\xi u_2^2 + \alpha_5 u_2 + \alpha_6}{\xi u_2 + \alpha_7},$$

which can be written as the following cubic equation for u_2:

$$u_2^3(2\kappa\xi\alpha_3) + u_2^2(\alpha_3\alpha_5 + 2\kappa\xi\alpha_4 - \alpha_1\xi) + u_2(\alpha_3\alpha_6 + \alpha_4\alpha_5 - \alpha_1\alpha_7 - \xi\alpha_2) + (\alpha_4\alpha_6 - \alpha_2\alpha_7) = 0. \quad (3.50)$$

Using again the parameter given in Eq. (3.45), Eq. (3.33) can be rewritten as:

$$\ln\left(\left|\frac{u_2 - u_*}{u_2 - \bar{u}_{j-1}}\right|^{(s-u_2)}\left|\frac{u_1 - u_*}{u_1 - \bar{u}_{j-1}}\right|^{-(s-u_1)}\right) = \frac{Q\varepsilon\Delta x}{\tilde{\mu}}. \quad (3.51)$$

By again using $Q = \bar{\rho}_{j-1}(s - \bar{u}_{j-1})$ and κ as defined in Eq. (3.48), Eq. (3.51) can be written as:

$$\left(\frac{u_2 - u_*}{u_2 - \bar{u}_{j-1}}\right)^{(s-u_2)} = \left(\frac{u_1 - u_*}{u_1 - \bar{u}_{j-1}}\right)^{(s-u_1)}\exp\left(2\kappa(u_2 - u_1)(s - \bar{u}_{j-1})\right). \quad (3.52)$$

Assuming again that $\varepsilon\Delta x/\tilde{\mu}$ is small, so $\kappa(u_2 - u_1)$ is small, then using Taylor expansions and the expression for s given by Eq. (3.43), rewrite Eq.(3.52) as:

$$\left(\frac{u_2 - u_*}{u_2 - \bar{u}_{j-1}}\right)^{(\xi u_1 + u_2(\xi-1)+A)} = \left(\frac{u_1 - u_*}{u_1 - \bar{u}_{j-1}}\right)^{(u_1(\xi-1)+\xi u_2+A)}$$
$$\left(1 + 2\kappa(u_2 - u_1)(\xi(u_1 + u_2) + A - \bar{u}_{j-1})\right). \quad (3.53)$$

where ξ and A are defined in Eq. (3.44). Once u_2 has been determined from Eq. (3.50), Eq. (3.53) has just one unknown, namely u_1. Use a 1D Newton method or a bisection method to solve u_1 from Eq. (3.53).

3.5.3 Summarizing

Instead of solving the system given by Eq. (3.11), (3.33) and (3.34), we have obtained an easier system to solve. By using a shock speed given by:

$$s = \xi(u_1 + u_2) + A, \quad (3.54)$$

with:

$$\xi = \frac{1}{2 - \beta}, \quad A = \frac{-\beta\bar{u}_{j-1} \pm \sqrt{2\beta\gamma(2 - \beta)\left(\overline{E}_{j-1} - \frac{1}{2}\bar{u}_{j-1}^2\right)}}{2 - \beta},$$

we need to solve the following two equations for u_1 and u_2:
Eq. (3.33) has been simplified to:

$$\left(\frac{u_2 - u_*}{u_2 - \bar{u}_{j-1}}\right)^{(\xi u_1 + u_2(\xi-1)+A)} = \left(\frac{u_1 - u_*}{u_1 - \bar{u}_{j-1}}\right)^{(u_1(\xi-1)+\xi u_2+A)}$$
$$\left(1 + 2\kappa(u_2 - u_1)(\xi(u_1 + u_2) + A - \bar{u}_{j-1})\right), \quad (3.55)$$

Eq. (3.34) has simplified to:

$$u_2^3(2\kappa\xi\alpha_3)+u_2^2(\alpha_3\alpha_5+2\kappa\xi\alpha_4-\alpha_1\xi)+u_2(\alpha_3\alpha_6+\alpha_4\alpha_5-\alpha_1\alpha_7-\xi\alpha_2)+(\alpha_4\alpha_6-\alpha_2\alpha_7)=0, \quad (3.56)$$

with the α's given by:

$$
\begin{aligned}
\alpha_1 &= u_1-\bar{u}_{j-1}, & \alpha_2 &= u_*(\bar{u}_{j-1}-u_1), \\
\alpha_3 &= u_1-u_*, & \alpha_4 &= \bar{u}_{j-1}(u_*-u_1), \\
\alpha_5 &= \xi+2\kappa A-\kappa(u_*+\bar{u}_{j-1}), & \alpha_6 &= \xi u_1+A-u_*-2\kappa\xi u_1^2-2\kappa A u_1+\kappa u_1(u_*+\bar{u}_{j-1}), \\
\alpha_7 &= \xi u_1+A-u_*,
\end{aligned}
$$

First solve the cubic equation given by Eq. (3.56) for u_2. Substitution of this solution into Eq. (3.55) results in an equation that has to be solved for u_1. For this we can use a bisection or a 1D Newton method. There is no unique solution to these equations so we need requirements to obtain the physically correct solutions. One requirement is: $u_1 > \bar{u}_{j-1} > u_* > u_2$ (in the case of a shock wave) or $u_1 < \bar{u}_{j-1} < u_* < u_2$ (in the case of a rarefaction wave) . The big advantage of solving the system given by Eq. (3.55) and (3.56) instead of the system given by Eq. (3.11), (3.33) and (3.34) is that we do not need a two-dimensional Newton iteration process.

4   Conclusions and future work

Conclusions

In this thesis we present an approximate Riemann solver for viscous flows based on travelling waves. The purpose of the Riemann solver is to solve the local (viscous) Riemann problems occurring at the element faces due to the discontinuous nature of the polynomial representation in each element of the DG-FEM method. A standard way in DG-FEM to solve this problem is by splitting the viscous and inviscid contributions of the flux, solving an inviscid Riemann problem for the inviscid contributions and using the method of Bassi and Rebay for the viscous contributions of the flux. However, physically, there is no reason to split the flux. This method is based on mathematical properties. The DG-TW scheme presented in this thesis is a scheme based more directly on the physics of the problem in which the viscous and inviscid contributions are not split.

We tested the DG-TW scheme by solving the viscous Burgers equation. No significant differences are observed in the solution when comparing the DG-TW scheme to the method of Bassi and Rebay. We also obtained exactly the same order behavior with the DG-TW scheme as with the method of Bassi and Rebay. We also notice a great simplification in implementing the DG-TW scheme compared to Bassi and Rebay. Once the inviscid Burgers equation is implemented, we just need to modify the flux function and add a viscous volume term while, for the method of Bassi and Rebay, a number of viscous contributions have to be implemented.

We also attempted to develop a travelling wave scheme for the 1D Navier-Stokes equations, but we have not yet succeeded in doing so. The problems we have are the large number of non-linear equations that have to be solved. We made a first step in simplifying these equations, but no tests have been done so far.

Future work

We have shown that for the viscous Burgers equation it is possible to use travelling wave solutions to obtain a numerical flux in which viscous and inviscid contributions are not split. We tried taking the next step, namely applying travelling wave solutions in the 1D Navier-Stokes equations, but we have not yet succeeded. As mentioned above, this is due to the large number of non-linear equations that have to be solved. We made a first step in simplifying these equations. Future work will be to test these simplifications or to find other ways of solving the non-linear equations than using a 2D Newton iteration method. Once the 1D Navier-Stokes equations have been solved, the step to the 2D Navier-Stokes equations will have to be made.
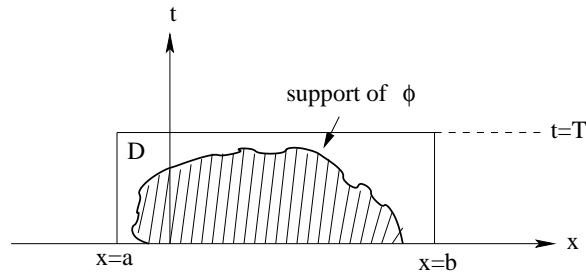
Figure 16: Definition of the support of the function ϕ, from [Smo94]

A   Rankine-Hugoniot relations

In this section we derive the Rankine-Hugoniot relations in viscous problems. In Section A.1 we do this for a general equation in which the shock is moving. In Section A.2 we derive the Rankine-Hugoniot relations for the 1D Navier-Stokes equations in a frame moving with the shock.

A.1   Rankine-Hugoniot conditions for viscous problems

In this section we will derive the Rankine-Hugoniot relations following [Smo94] and [vdVB03] for the following viscous problem:

$$U_t + F^e(U)_x = F^v(U, U_x)_x \qquad x \in \Omega, \ t \in \mathbb{R}^+, \tag{A.1}$$

with initial condition:

$$U(x, 0) = U_0(x). \tag{A.2}$$

We assume for now that the solution U of Eq. (A.1) is smooth. Later the problem will be extended to non-smooth solutions. We let ϕ be a continuously differentiable function, which vanishes outside of a compact subset in $t \geq 0$, i.e., (support ϕ) $\cap$ $(t \geq 0) \subseteq D$, where D is the rectangle $0 \leq t \leq T, a \leq x \leq b$, so chosen that $\phi = 0$ outside of D, and on the lines $t = T, x = a$ and $x = b$, see Figure 16. Hence, $\phi \in C_0^1$.
Multiplying Eq. (A.1) with ϕ and integrate over the domain $\mathbb{R} \times \mathbb{R}^+$ results in:

$$\int_a^b \int_0^T (U_t + F^e(U)_x - F^v(U, U_x)_x)\phi \, dx \, dt = 0.$$

Integrate by parts to obtain:

$$\int_a^b \int_0^T U_t \phi \, dx \, dt = \int_a^b U\phi \big|_{t=0}^{t=T} \, dx - \int_a^b \int_0^T U\phi_t \, dx \, dt$$

$$= -\int_a^b U_0(x)\phi(x, 0) \, dx - \int_a^b \int_0^T U\phi_t \, dx \, dt,$$

and:

$$\int_0^T \int_a^b (F^e(U) - F^v(U, U_x))_x \phi \, dx \, dt = -\int_0^T \int_a^b (F^e(U) - F^v(U, U_x))\phi_x \, dx \, dt.$$

Combining these terms, we can rewrite Eq. (A.1) as:

$$\iint_{t\geq 0} (U\phi_t + (F^e(U) - F^v(U, U_x))\phi_x)\, dx\, dt + \int_a^b U_0(x)\phi(x, 0)\, dx = 0. \tag{A.3}$$

If the solution $U(x, t)$ is a classical solution, $U \in C^1$, then both formulations, Eq. (A.1) and Eq. (A.3) are the same. If, however, U and U_0 are merely bounded and integrable, then Eq. (A.3) still makes sense as long as it is valid for all functions $\phi \in C^1$, even when discontinuities develop. The formulation of the conservation laws can therefore be generalized:

Definition A.1. A bounded integrable function $U(x, t)$ is called a weak solution of the initial value problem Eq. (A.1), with bounded and integrable initial data U_0, provided Eq. (A.3) holds for all $\phi \in C_0^1$.

The weak formulation is considerably more general than the formulation using the differential equation, but the weak formulation is non-unique. An additional requirement, the entropy condition, is imposed to obtain a unique, physically relevant solution.

Using the weak formulation, it is possible to solve problems with discontinuities, but not all discontinuities are permissible and the weak formulation imposes restrictions on the discontinuity. To analyze these conditions, a smooth curve Γ across which U has a jump discontinuity is considered. The solution U is smooth in the domain on both sides of the curve Γ and has a clear limit on both sides of Γ.

Let P be any point on Γ, and let D be a small sphere centered at P. Assume that in D the curve Γ is given by $x = x(t)$. The sphere around P can be split into two parts, D_1 and D_2, which are on either side of Γ, see Figure 17. Let $\phi \in C_0^1(D)$, hence ϕ is a continuously differentiable function in D and is zero at the boundary of D. The weak formulation, Eq. (A.3), is transformed into:

$$\iint_D (U\phi_t + (F^e(U) - F^v(U, U_x))\phi_x)\, dx\, dt = \iint_{D_1} (U\phi_t + (F^e(U) - F^v(U, U_x))\phi_x)\, dx\, dt$$
$$+ \iint_{D_2} (U\phi_t + (F^e(U) - F^v(U, U_x))\phi_x)\, dx\, dt,$$

where the integral of U_0 at initial time $t = 0$ in Eq. (A.3) disappears since ϕ is zero on the boundary of D. Using the fact that U is C^1 in D_i, $i = 1, 2$, the integral over each sub-domain can be further transformed into:

$$\iint_{D_i} (U\phi_t + (F^e(U) - F^v(U, U_x))\phi_x)\, dx\, dt = \iint_{D_i} \left((U\phi)_t + ((F^e(U) - F^v(U, U_x))\phi)_x\right) dx\, dt$$
$$- \iint_{D_i} \left(U_t + (F^e(U) - F^v(U, U_x))_x\right)\phi\, dx\, dt$$
$$= \iint_{D_i} \left((U\phi)_t + ((F^e(U) - F^v(U, U_x))\phi)_x\right) dx\, dt,$$

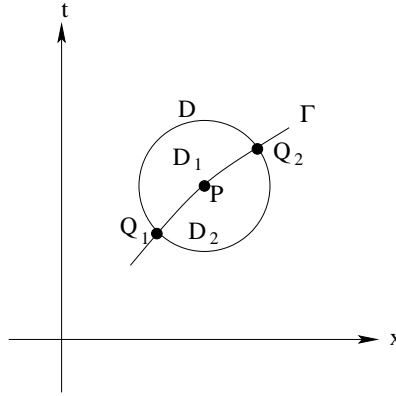since U satisfies the differential equation $U_t + (F^e(U) - F^v(U, U_x))_x = 0$ in D_i because the

Figure 17: Domains used in the derivation of the Rankine-Hugoniot relations, from [Smo94]

solution is smooth outside Γ. Applying the divergence theorem, we obtain:

$$\iint_{D_i} \left((U\phi)_t + ((F^e(U) - F^v(U, U_x))\phi)_x \right) dx \, dt = \int_{\partial D_i} \phi \left(-U \, dx + \left(F^e(U) - F^v(U, U_x) \right) dt \right)$$
$$= \int_{\Gamma} \phi \left(-U \, dx + \left(F^e(U) - F^v(U, U_x) \right) dt \right),$$

since $\phi = 0$ on all boundaries of D_i except along Γ.

By defining $U_L = \lim_{\varepsilon \downarrow 0} U(x(t) - \varepsilon, t)$, $U_R = \lim_{\varepsilon \downarrow 0} U(x(t) + \varepsilon, t)$, $U_x^L = \lim_{\varepsilon \downarrow 0} U_x(x(t) - \varepsilon, t)$ and $U_x^R = \lim_{\varepsilon \downarrow 0} U_x(x(t) + \varepsilon, t)$ we then find:

$$\int_{\partial D_1} \phi \left(-U \, dx + \left(F^e(U) - F^v(U, U_x) \right) dt \right) = \int_{Q_1}^{Q_2} \phi \left(-U_L \, dx + \left(F^e(U_L) - F^v(U_L, U_x^L) \right) dt \right),$$
$$(A.4)$$

$$\int_{\partial D_2} \phi \left(-U \, dx + \left(F^e(U) - F^v(U, U_x) \right) dt \right) = -\int_{Q_1}^{Q_2} \phi \left(-U_R \, dx + \left(F^e(U_R) - F^v(U_R, U_x^R) \right) dt \right),$$
$$(A.5)$$

where the minus sign in front of the integral on the righthand side in Eq. (A.5) is due to the fact that the integration path along Γ for domain D_2 is in opposite direction from the integration path along Γ for domain D_1. Combining Eq. (A.4) and Eq. (A.5), we find:

$$0 = \int_{\Gamma} \phi \left(-[\![U]\!] \, dx + [\![F^e(U) - F^v(U, U_x)]\!] \, dt \right),$$

where $[\![U]\!] = U_L - U_R$, the jump across Γ, and similarly, $[\![F^e(U) - F^v(U, U_x)]\!] = F^e(U_L) - F^v(U_L, U_x^L) - F^e(U_R) + F^v(U_R, U_x^R)$. Since ϕ was arbitrary, we conclude that:

$$S[\![U]\!] = [\![F^e(U) - F^v(U, U_x)]\!], \qquad\qquad\qquad\qquad (A.6)$$

at each point on Γ, where $S = dx/dt$ is the speed of the discontinuity. This relation is the Rankine-Hugoniot condition for viscous equations.

A.2   Rankine-Hugoniot derivation for 1D Navier-Stokes in a moving frame of reference

In this section, by following [Whi74], we shall derive the Rankine-Hugoniot relations for the 1D Navier-Stokes equations in a frame of reference moving with the shock.
Consider the following form of the Navier-Stokes equations:

$$
\begin{aligned}
\rho_t + (\rho u)_x &= 0, \\
(\rho u)_t + (\rho u^2 + p)_x &= \mu \frac{\gamma + 1}{2\gamma} u_{xx}, \\
(\rho E)_t + (\rho u(h + \tfrac{1}{2}u^2))_x &= \mu \frac{\gamma + 1}{2\gamma} (h + \tfrac{1}{2}u^2)_{xx}.
\end{aligned} \tag{A.7}
$$

The flow is steady relative to the shock, therefore all flow quantities are functions of $\omega = x - st$ alone. It holds that:

$$
\frac{\partial}{\partial t} = -s \frac{d}{d\omega}, \quad \frac{\partial}{\partial x} = \frac{d}{d\omega},
$$

so that Eq. (A.7) can be rewritten as:

$$
\begin{aligned}
-s \frac{d\rho}{d\omega} + \frac{d(\rho u)}{d\omega} &= 0, \\
-s \frac{d(\rho u)}{d\omega} + \frac{d}{d\omega}(\rho u^2 + p) &= \mu \frac{\gamma + 1}{2\gamma} \frac{d^2 u}{d\omega^2}, \\
-s \frac{d(\rho E)}{d\omega} + \frac{d}{d\omega}(\rho u(h + \tfrac{1}{2}u^2)) &= \mu \frac{\gamma + 1}{2\gamma} \frac{d^2}{d\omega^2}(h + \tfrac{1}{2}u^2),
\end{aligned}
$$

or, after integration:

$$
-s\rho + (\rho u) = A, \tag{A.8}
$$

$$
-s(\rho u) + (\rho u^2 + p) - \mu \frac{\gamma + 1}{2\gamma} \frac{du}{d\omega} = B, \tag{A.9}
$$

$$
-s(\rho E) + (\rho u(h + \tfrac{1}{2}u^2)) - \mu \frac{\gamma + 1}{2\gamma} \frac{d}{d\omega}(h + \tfrac{1}{2}u^2) = C, \tag{A.10}
$$

where A, B and C are constants of integration. Note that these relations can also be found by substituting U, $F^e(U)$ and $F^v(U, U_x)$, where

$$
U = \begin{bmatrix} \rho \\ \rho u \\ \rho E \end{bmatrix}, \quad F^e(U) = \begin{bmatrix} \rho u \\ \rho u^2 + p \\ \rho u(h + \tfrac{1}{2}u^2) \end{bmatrix}, \quad F^v(U, U_x) = \mu \frac{\gamma + 1}{2\gamma} \begin{bmatrix} 0 \\ u_x \\ \left(h + \tfrac{1}{2}u^2\right)_x \end{bmatrix},
$$

into Eq. (A.6).
Define the relative velocity $v = s - u$, then from Eq. (A.8):

$$
\rho v = Q, \quad \text{with } Q = -A. \tag{A.11}
$$

From Eq. (A.9), by noting that:

$$
\frac{du}{d\omega} = \frac{d}{d\omega}(s - v) = -\frac{dv}{d\omega},
$$

and:

$$\rho u(u - s) = -s\rho v + \rho v^2 = \rho v^2 - sQ,$$

we obtain:

$$\rho v^2 + p + \mu \frac{\gamma + 1}{2\gamma} \frac{dv}{d\omega} = P, \quad \text{with } P = B + sQ. \tag{A.12}$$

By noting that:

$$(\tfrac{1}{2}u^2 + e)\rho u + pu = (\tfrac{1}{2}u^2 + h)\rho u,$$

and that $E = e + \tfrac{1}{2}u^2$, Eq. (A.10) can be written as:

$$-v\rho(\tfrac{1}{2}u^2 + e) + (s - v)p - \mu\frac{\gamma + 1}{2\gamma}\left(\frac{dh}{d\omega} + u\frac{du}{d\omega}\right) = C.$$

Since $p = (\gamma - 1)e\rho$ and $u = s - v$ it follows that:

$$-v\rho(\tfrac{1}{2}(s - v)^2 + \gamma e) + sp - \mu\frac{\gamma + 1}{2\gamma}\left(\frac{dh}{d\omega} + \frac{d}{d\omega}(\tfrac{1}{2}v^2) - s\frac{dv}{d\omega}\right) = C.$$

Using $h = \gamma e$:

$$v\rho(h + \tfrac{1}{2}v^2) + \mu\frac{\gamma + 1}{2\gamma}\frac{d}{d\omega}(h + \tfrac{1}{2}v^2) + v\rho(\tfrac{1}{2}s^2 - sv) - sp - s\mu\frac{\gamma + 1}{2\gamma}\frac{dv}{d\omega} = -C. \tag{A.13}$$

From Eq. (A.12) we obtain:

$$s\mu\frac{\gamma + 1}{2\gamma}\frac{dv}{d\omega} = sP - s\rho v^2 - ps.$$

Substituting into Eq. (A.13):

$$v\rho(h + \tfrac{1}{2}v^2) + \mu\frac{\gamma + 1}{2\gamma}\frac{d}{d\omega}(h + \tfrac{1}{2}v^2) = \mathcal{E}, \quad \text{with } \mathcal{E} = -C + sP - \tfrac{1}{2}s^2Q. \tag{A.14}$$

From Eq. (A.11), (A.12) and (A.14) we obtain the following form of the Rankine-Hugoniot relations for the 1D Navier-Stokes equations:

$$Q = \rho v,$$

$$P = \rho v^2 + p + \mu\frac{\gamma + 1}{2\gamma}\frac{dv}{d\omega},$$

$$\mathcal{E} = v\rho(h + \tfrac{1}{2}v^2) + \mu\frac{\gamma + 1}{2\gamma}\frac{d}{d\omega}(h + \tfrac{1}{2}v^2),$$

where P, Q and $\mathcal{E}$ are constants.

B   Approximate viscous Riemann solvers

In this section we will introduce some ideas for an approximate viscous Riemann solver. We will present a scheme and test it on the viscous isothermal equations. We use the viscous isothermal equations since in these equations only two waves occur, each wave separating a constant state. This makes it possible to apply the HLL flux.

Deriving the approximate viscous Riemann solver we will consider conservation laws given by:

$$U_t + F^e(U)_x = F^v(U, U_x)_x \qquad x \in \Omega, \ t \in \mathbb{R}^+, \tag{B.1}$$

with initial condition:

$$U(x, 0) = U_0(x). \tag{B.2}$$

Let the inviscid part of the equation admit two real and distinct eigenvalues so that the inviscid part of the equation is hyperbolic. Physically, the eigenvalues represent the speeds of propagation of information.

B.1   An approximate viscous Riemann solver

In this section an approximate viscous Riemann solver will be presented using the Rankine-Hugoniot conditions as derived in Section A.1 and transformations as in [vdVK03].

As in Section A.1, we consider the following equation:

$$U_t + F^e(U)_x - F^v(U, U_x)_x = 0,$$

but now in a control volume $\Omega = [x_L, x_R] \times [0, T]$. On the domain $\Omega_2 \cup \Omega_3$, where the open domain Ω_2 is bounded by waves S_L and S_M, and the open domain Ω_3 by S_M and S_R respectively, see Figure 18, the solution is smooth, so in this region we can express the weak formulation as:

$$\int_{\Omega_2 \cup \Omega_3} \left(U_t + F^e(U)_x - F^v(U, U_x)_x \right) dx \, dt = 0. \tag{B.3}$$

Using the transformations as in [vdVK03], we can rewrite Eq. (B.3):

$$
\begin{aligned}
\iint_{\Omega_2} U_t \, dx \, dt &= \int_{t=0}^{T} \int_{x=tS_L}^{tS_M} U_t \, dx \, dt \\
&= -\int_{t=0}^{T} \int_{\xi=S_L}^{S_M} U_\xi \frac{x}{t^2} t \, d\xi \, dt \\
&= -\int_{t=0}^{T} \int_{\xi=S_L}^{S_M} U_\xi \xi \, d\xi \, dt \\
&= -T \int_{s=0}^{1} \int_{\xi=S_L}^{S_M} U_\xi \xi \, d\xi \, ds \\
&= -T \int_{s=0}^{1} \left(U\xi \Big|_{S_L}^{S_R} - \int_{S_L}^{S_R} U \, d\xi \right) ds \\
&= -T \int_{s=0}^{1} \left(S_M U_M^{*-} - S_L U_L^* \right) ds + T \int_{s=0}^{1} \int_{\xi=S_L}^{S_M} U(\xi) \, d\xi \, ds,
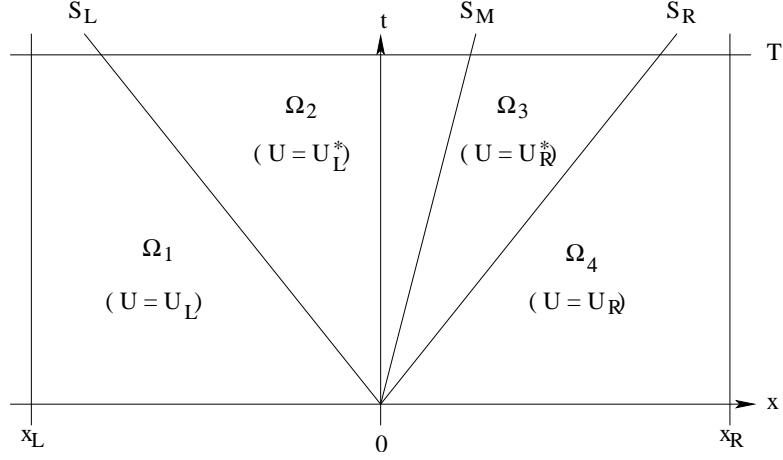\end{aligned}
\tag{B.4}
$$

Figure 18: Wave pattern used in the definition of the HLLC flux function. Here S_L and S_R are the fastest left and right moving signal velocities. The solution in the star region U^* is divided by the wave with velocity S_M.

where U_L^* and $U_M^{*^-}$ denote the trace of U in Ω_2 at S_L and S_M, respectively. Similarly we find over the domain Ω_3:

$$\iint_{\Omega_3} U_t \, dx \, dt = -T \int_{s=0}^1 \left(S_R U_R^* - S_M U_M^{*^+} \right) ds + T \int_{s=0}^1 \int_{\xi=S_M}^{S_R} U(\xi) \, d\xi \, ds, \qquad (B.5)$$

where $U_M^{*^+}$ and U_R^* denote the trace of U in Ω_3 at S_M and S_R, respectively.
Define the averaged star state $\bar{U}^*$ as:

$$\bar{U}^* = \frac{1}{T(S_R - S_L)} \int_{TS_L}^{TS_R} U(x,T) \, dx.$$

Using the self similarity of $U(x,t)$ in the star region, the average of the exact solution $\bar{U}^*$ can also be expressed as:

$$\bar{U}^* = \frac{1}{(S_R - S_L)} \int_{S_L}^{S_R} U^*(\xi) \, d\xi. \qquad (B.6)$$

Using Eq. (B.6) we can combine Eq. (B.4) and Eq. (B.5) to:

$$\iint_{\Omega_2 \cup \Omega_3} U_t \, dx \, dt = -T \int_{s=0}^1 \left(S_M U_M^{*^-} - S_L U_L^* + S_R U_R^* - S_M U_M^{*^+} \right) ds + T \int_{s=0}^1 \int_{S_L}^{S_R} U^*(\xi) \, d\xi \, ds$$

$$= -T \int_{s=0}^1 \left(S_M U_M^{*^-} - S_L U_L^* + S_R U_R^* - S_M U_M^{*^+} \right) ds + T \int_{s=0}^1 (S_R - S_L) \bar{U}^* \, ds.$$

$$(B.7)$$

Analogously to the above relations we can find expressions for the integral over the domain

$\Omega_2 \cup \Omega_3$ for the inviscid and viscous fluxes:

$$\iint_{\Omega_2} \left(F^e(U)_x - F^v(U,U_x)_x \right) dx\, dt = \int_{t=0}^{T} \int_{x=tS_L}^{tS_M} \left(F^e(U)_x - F^v(U,U_x)_x \right) dx\, dt$$
$$= T \int_{s=0}^{1} \left(\left(F^e(U) - F^v(U,U_x) \right) \Big|_{tS_L}^{tS_M} \right) ds. \tag{B.8}$$

Similarly, over Ω_3 we find:

$$\iint_{\Omega_3} \left(F^e(U)_x - F^v(U,U_x)_x \right) dx\, dt = T \int_{s=0}^{1} \left(\left(F^e(U) - F^v(U,U_x) \right) \Big|_{tS_M}^{tS_R} \right) ds. \tag{B.9}$$

Combining Eq. (B.7), Eq. (B.8) and Eq. (B.9), we find the following expression for the average of the exact solution:

$$\bar{U}^* = \frac{1}{S_R - S_L} \Big(F^e(U_L^*) - F^v(U_L^*, U_x^{L^*}) + F^e(U_M^{*+}) - F^v(U_M^{*+}, U_x^{M^{*+}}) - F^e(U_R^*) + F^v(U_R^*, U_x^{R^*})$$
$$- F^e(U_M^{*-}) - F^v(U_M^{*-}, U_x^{M^{*-}}) - S_L U_L^* + S_M(U_M^{*-} - U_M^{*+}) + S_R U_R^* \Big). \tag{B.10}$$

Using the Rankine-Hugoniot relations as given in Section A.1, this expression can be transformed into an expression of only known variables. Over the S_L-wave we have the Rankine-Hugoniot expression:

$$F^e(U_L) - S_L U_L - F^v(U_L, U_x^L) = F^e(U_L^*) - S_L U_L^* - F^v(U_L^*, U_x^{L^*}),$$

over the S_R-wave:

$$-F^e(U_R) + S_R U_R + F^v(U_R, U_x^R) = -F^e(U_R^*) + S_R U_R^* + F^v(U_R^*, U_x^{R^*}),$$

and over the S_M-wave:

$$-F^e(U_M^{*-}) + S_M(U_M^{*-} - U_M^{*+}) + F^v(U_M^{*-}, U_x^{M^{*-}}) + F^e(U_M^{*+}) - F^v(U_M^{*+}, U_x^{M^{*+}}) = 0.$$

Expression Eq. (B.10) becomes:

$$\bar{U}^* = \frac{1}{S_R - S_L} \Big(S_R U_R - S_L U_L + F^e(U_L) - F^v(U_L, U_x^L) - F^e(U_R) + F^v(U_R, U_x^R) \Big). \tag{B.11}$$

The flux along the t-axis is obtained by integrating Eq. (A.1) over part of Ω_2:

$$\int_{t=0}^{T} \int_{x=tS_L}^{0} (U_t + F^e(U)_x - F^v(U,U_x)_x)\, dx\, dt.$$

Analogously to the above relations we find:

$$\int_{t=0}^{T} \int_{x=tS_L}^{0} U_t\, dx\, dt = T \int_{s=0}^{1} S_L U_L^*\, ds + T \int_{s=0}^{1} \int_{\xi=S_L}^{0} U(\xi)\, d\xi\, ds,$$

and:

$$\int_{t=0}^{T} \int_{x=tS_L}^{0} F^e(U)_x - F^v(U, U_x)_x \, dx \, dt = T \int_{s=0}^{1} \left(F^e(U_0) - F^v(U_0, U_x^0) - F^e(U_L^*) + F^v(U_L^*, U_x^{L^*}) \right) ds.$$

Combining these two expressions and using the Rankine-Hugoniot relation across the S_L-wave, we obtain:

$$F^e(U_0) - F^v(U_0, U_x^0) = F^e(U_L) - F^v(U_L, U_x^L) - S_L U_L - \int_{\xi=S_L}^{0} U(\xi) \, d\xi.$$

By replacing $U(\xi)$ in the integral term by the average of the exact solution in the star state, Eq. (B.11), we obtain:

$$F^e(U_0) - F^v(U_0, U_x^0) = \frac{S_R(F^e(U_L) - F^v(U_L, U_x^L)) - S_L(F^e(U_R) - F^v(U_R, U_x^R)) + S_L S_R(U_R - R_L)}{S_R - S_L},$$
$$\text{(B.12)}$$

which is the flux along the t-axis without considering contact waves.

B.2   Testing the viscous HLL-flux and conclusions

Consider the viscous isothermal equations:

$$U_t + F^e(U)_x - F^v(U, \nabla U)_x = 0, \tag{B.13}$$

with:

$$U = \begin{bmatrix} \rho \\ \rho u \end{bmatrix}, \quad F^e(U) = \begin{bmatrix} \rho \\ \rho(u^2 + a^2) \end{bmatrix}, \quad F^v(U, \nabla U) = \begin{bmatrix} 0 \\ \mu u_x \end{bmatrix}.$$

In general, the weak formulation for Eq. (B.13) is given by:
Find a $U \in W_h$ *such that* $B(U, V) = 0, \forall V \in W_h$ *with:*

$$B(U, V) = \int_{\Omega_h} V U_t \, dx - \int_{\Omega_h} V_x F^e(U) \, dx + \int_{\Omega_h} V_x F^v(U, \nabla U) \, dx + \sum_{k=1}^{N} \int_{\partial K_k} \widehat{H}(U_L, U_R) V \, ds,$$

where $\widehat{H}$ is the numerical flux from Eq. (B.12) ensuring continuous fluxes at each face and W_h is the discrete discontinuous finite element space given by:

$$W_h = \{V \in L^2(\Omega_h) : V|_{K_k} \in P^1(K_k), k = 1, ..., N\},$$

in which $P^1(K_k)$ denotes the space of linear polynomials, and $L^2(\Omega_h)$ the space of Lebesque square integrable functions.
We tested the numerical flux for a test case with the following initial condition:

$$\rho(x, 0) = \begin{cases} 10, & \text{for } x \leq \frac{1}{2} \\ 8, & \text{for } x > \frac{1}{2} \end{cases} \quad , \quad \rho u(x, 0) = 0,$$
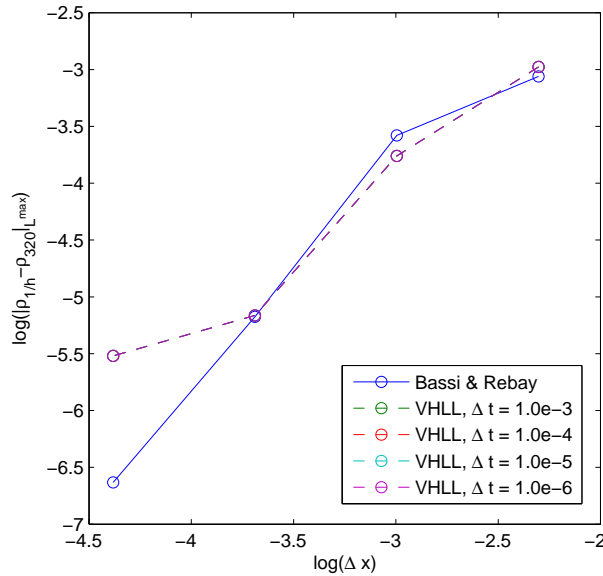
Figure 19: Order behavior of the density variable ρ. The method of Bassi and Rebay and the viscous Riemann solver as given by Eq. (B.12) were used. As reference, an "exact" solution was calculated with the method of Bassi and Rebay on a grid with 320 cells. Depicted are the results at $t = 0.2$ time units using a viscosity coefficient of $\mu = 0.1$.

and different values of the viscosity coefficient. For small values of the viscosity coefficient the flux seems to work without any problems, however, increasing the viscosity coefficient to a value of $\mu = 0.1$, the order behavior of the scheme deteriorates. In Figure 19 the order behavior of the solution determined with the method of Bassi and Rebay and with the viscous Riemann solver is depicted. We see that as the cell size decreases the order behavior of the viscous Riemann solver deteriorates. For small values of the viscosity coefficient the viscous terms in the numerical flux are insignificant explaining the good order behavior for these cases. Increasing the viscosity coefficient, the viscous terms in the numerical flux become more important. In our case, increasing the viscosity coefficient resulted in a deteriorating order behavior, meaning that something is wrong with the viscous terms in our flux. We also tested the numerical flux in a 2D-Navier Stokes code. We did a Couette test case and the results were bad.

A reason why this viscous flux does not work for large viscosity coefficients: In Eq. (B.12) we need, among other terms, the following: $F^v(U_L, U_x^L)$ and $F^v(U_R, U_x^R)$. Since we are working with linear approximations to the exact solution, we have values for U_x^L, the derivative of U in the left state and U_x^R, the derivative of U in the right state. We therefore use these slopes in $F^v(U_L, U_x^L)$ and $F^v(U_R, U_x^R)$. This is, however, not consistent with the way the original HLL flux is derived, since here it is assumed that all states are constant states, which in our case results in $F^v(U_L, U_x^L) = F^v(U_L, 0)$ and $F^v(U_R, U_x^R) = F^v(U_R, 0)$. This has proven to be a problem in many attempts to derive an approximate viscous Riemann solver. Taking all

states constant results in the removal of the viscous terms and taking U linear in all regions can result in introducing new unknown terms which are absent if U is constant.

C   Newton's method for a system of two equations

In this section we will explain how we implemented Newton's method for solving the system given by Eq. (3.33) and (3.34) for u_1^I and u_2^I. The system given by Eq. (3.35) and (3.36) is solved similarly for u_1^{III} and u_2^{III}.

First we determine s^I from Eq. (3.11):

$$v_1 v_2 = \frac{2(\gamma - 1)}{\gamma + 1} H. \tag{C.1}$$

From Eq. (3.8):

$$\begin{aligned} H &= h + \tfrac{1}{2}v^2 \\ &= e + \frac{p}{\rho} + \tfrac{1}{2}v^2 \\ &= \gamma e + \tfrac{1}{2}v^2 \\ &= \gamma E + \tfrac{1}{2}v^2 - \tfrac{1}{2}\gamma(s - v)^2. \end{aligned}$$

We know the means of E and u in cell $j - 1$ and we know that H is constant so:

$$H = \gamma \overline{E}_{j-1} + \tfrac{1}{2}(s - \bar{u}_{j-1})^2 - \tfrac{1}{2}\gamma \bar{u}_{j-1}^2. \tag{C.2}$$

Define the following constant:

$$\beta = \frac{2(\gamma - 1)}{\gamma + 1},$$

then, substituting $v_1 = s - u_1$, $v_2 = s - u_2$ and Eq. (C.2) into Eq. (C.1) we obtain:

$$(s - u_1)(s - u_2) = \beta\big(\gamma \overline{E}_{j-1} + \tfrac{1}{2}(s - \bar{u}_{j-1})^2 - \tfrac{1}{2}\gamma \bar{u}_{j-1}^2\big),$$

which can be rewritten as:

$$as^2 + bs + c = 0,$$

where:

$$a = 1 - \tfrac{1}{2}\beta, \;\; b = -u_1 - u_2 + \beta \bar{u}_{j-1}, \;\; c = u_1 u_2 - \beta\gamma \overline{E}_{j-1} - \tfrac{1}{2}(1 - \gamma)\beta \bar{u}_{j-1}^2.$$

It follows that:

$$s_\pm = \frac{-b \pm \sqrt{b^2 - 4ac}}{2a}.$$

We do not know which s to take since in certain test cases both speeds, s_- and s_+ both agreed to the entropy shock conditions. In the implementation we took $s = s_-$ for the I-wave and $s = s_+$ for the III-wave. This is based on trial and error. This choice proved to be the most successful. A good condition still needs to be found for obtaining the wave-speed s.

Write Eq. (3.33) as:

$$f_1(u_1, u_2) = \frac{\tilde{\mu}}{\bar{\rho}_{j-1}(s(u_1, u_2) - \bar{u}_{j-1})(u_2 - u_1)} \left((s(u_1, u_2) - u_2) \ln\left(\left| \frac{u_2 - u_*}{u_2 - \bar{u}_{j-1}} \right| \right) \right.$$
$$\left. - (s(u_1, u_2) - u_1) \ln\left(\left| \frac{u_1 - u_*}{u_1 - \bar{u}_{j-1}} \right| \right) \right) - \Delta x, \quad \text{(C.3)}$$

and write Eq. (3.34) as:

$$f_2(u_1, u_2) = \frac{\tilde{\mu}}{(u_2 - u_1)} \left(\ln\left(\left| \frac{u_2 - u_*}{u_2 - \bar{u}_{j-1}} \right| \right) - \ln\left(\left| \frac{u_1 - u_*}{u_1 - \bar{u}_{j-1}} \right| \right) \right) - \tfrac{1}{2}\Delta x \left(\bar{\rho}_{j-1} + \bar{\rho}_{j-1} \frac{s(u_1, u_2) - \bar{u}_{j-1}}{s(u_1, u_2) - u_1^*} \right).$$
$$\text{(C.4)}$$

In these equations we used $\rho_1^* = Q/(s - u_1^*)$ and $Q = \bar{\rho}_{j-1}(s - \bar{u}_{j-1})$, since the means of u and ρ are known in cell $j - 1$ and Q is constant. We are now able to solve the system consisting of Eq. (C.3) and (C.4) for u_1 and u_2 using Newton's method.

Consider the system:

$$F(U) = 0, \quad F = \begin{bmatrix} f_1 \\ f_2 \end{bmatrix}, \quad U = \begin{bmatrix} u_1 \\ u_2 \end{bmatrix}.$$

This system is solved using Newton's method as follows:

$$U^{(k+1)} = U^{(k)} - \left(\frac{\partial F}{\partial U}(U^{(k)}) \right)^{-1} \cdot F(U^{(k)}),$$

where $\partial F/\partial U$ is the Jacobian of $F(U)$. We note that $u_1 > \bar{u}_{j-1} > u_* > u_2$. Therefore, as initial guess, we take $u_1 = \bar{u}_{j-1} + \varepsilon$ and $u_2 = u_* - \varepsilon$ with $\varepsilon = 0.0001$. We did not use the exact Jacobian but an approximation:

$$\frac{\partial F}{\partial U} \approx \begin{bmatrix} \frac{f_1(u_1+\delta,u_2) - f_1(u_1,u_2)}{\delta} & \frac{f_1(u_1,u_2+\delta) - f_1(u_1,u_2)}{\delta} \\ \frac{f_2(u_1+\delta,u_2) - f_2(u_1,u_2)}{\delta} & \frac{f_2(u_1,u_2+\delta) - f_2(u_1,u_2)}{\delta} \end{bmatrix},$$

with $\delta = 10^{-6}$. As stated before, u_1^{III} and u_2^{III} are determined similarly.

References

[ABCM02] D. Arnold, F. Brezzi, B. Cockburn, and D. Marini. Unified analysis of discontinuous Galerkin methods for elliptic problems. *SIAM J. Numer. Anal.*, 39:1749–1779, 2002.

[BMM+00] F. Brezzi, G. Manzini, D. Marini, P. Pietra, and A. Russo. Discontinuous Galerkin approximations for elliptic problems. *Numer. Meth. Part. Diff. Eq.*, 16(4):365–378, 2000.

[BO99] C.E. Baumann and J.T. Oden. A discontinuous *hp* finite element method for the Euler and Navier-Stokes equations. Tenth International Conference on Finite Elements in Fluids (Tucson, AZ, 1998). *Internal. J. Numer. Methods Fluids*, 31(1):79–95, 1999.

[BR97] F. Bassi and S. Rebay. A high-order accurate discontinuous finite element method for the numerical solution of the compressible Navier-Stokes equations. *J. Comput. Phys.*, 131:267–279, 1997.

[BRM+] F. Bassi, S. Rebay, G. Mariotti, S. Pedinotti, and M. Savini. *A high-order accurate discontinuous finite element method for inviscid and viscous turbomachinery flow. In R. Decypere and G. Dibelius, editors.*

[CS98] B. Cockburn and C.-W. Shu. The local discontinuous Galerkin method for time-dependent method for convection-diffusion systems. *SIAM J. Numer. Anal.*, 35:2240–2463, 1998.

[CS01] B. Cockburn and C.-W. Shu. Runge-Kutta discontinuous Galerkin methods for convection-dominated problems. *J. Sci. Comput.*, 16(3):173–261, 2001.

[Har90] E.H. Harabetian. A numerical method for viscous perturbations of hyperbolic conservation laws. *SIAM J. Numer. Analysis*, 27:870–884, 1990.

[Kla04] C.M. Klaij. Space-time DGFEM for the compressible Navier-Stokes equations. *Internal report*, 2004.

[KvdVvdV] C.M. Klaij, J.J.W. van der Vegt, and H. van der Ven. Space-time discontinuous Galerkin method for the compressible Navier-Stokes equations. *Preprint submitted to J. Comput. Phys.*

[Liu86] T.-P. Liu. Shock Waves for Compressible Navier-Stokes Equations are Stable. *Commun. on Pure and Applied Math.*, 39:565–594, 1986.

[Rhe05] S. Rhebergen. Literature report, Master's thesis Part I. *Internal report*, 2005.

[Smo94] J. Smoller. *Shock Waves and Reaction-Diffusion Equations.* Springer-Verlag, 1994.

[Tor97]   E.F. Toro.   *Riemann Solvers and Numerical Methods for Fluid dynamics.* Springer, 1997.

[vDDS⁺01]   R. van Damme, D. Dijkstra, G. Still, C. Traas, and G. Zwier. *Dictaat: Numerieke Wiskunde, Universiteit Twente.* 2001.

[vdVB03]   J.J.W. van der Vegt and O. Bokhove. Upwind discretizations for Conservation Laws. *Lecture notes, Reader 2002-2003 / Version 2.0*, 2003.

[vdVK03]   J.J.W. van der Vegt and C.M. Klaij. Extending the HLLC Riemann solver to low Mach number gas dynamics. 2003.

[vdVvdV02a]   J.J.W. van der Vegt and H. van der Ven. Space-time discontinuous Galerkin finite element method with dynamic grid motion for inviscid compressible flows. I. General formulation. *J. Comput. Phys*, 182:546–585, 2002.

[vdVvdV02b]   J.J.W. van der Vegt and H. van der Ven. Space-time discontinuous Galerkin finite element method with dynamic grid motion for inviscid compressible flows. II. Efficient flux quadrature. *Comput. Meth. Appl. Mech. Engrg.*, 191:4747–4780, 2002.

[Wee98]   S.L. Weekes. The travelling wave scheme for the Navier-Stokes equations. *SIAM J. Numer. Analysis*, 35:1249–1270, 1998.

[Whi74]   G.B. Whitham. *Linear and Non-Linear Waves.* Wiley-Interscience, New York, 1974.